University of Alberta
Department of Civil &
Environmental Engineering

Characteristics of Concrete Containing Fly Ash with Hg-Adsorbent

by

Mehrdad Mahoutian

Vivek S. Bindiganavile

and

Adam S. Lubell

December, 2011

CHARACTERISTICS OF CONCRETE CONTAINING

FLY ASH WITH Hg-ADSORBENT

by

Mehrdad Mahoutian

Vivek S. Bindiganavile

and

Adam S. Lubell

Structural Engineering Report #293

Department of Civil and Environmental Engineering

University of Alberta, Edmonton, Alberta

December 2011

ABSTRACT

The present study has focused on the effects of Powdered Activated Carbon (PAC) in fly ash on the air-entraining admixture demand and consequent properties of concrete. An extensive laboratory test program was completed during this investigation. Three series of mixes were designed to evaluate the effect of PAC as an Hg-adsorbent on the fresh and hardened properties of concrete containing class F fly ash. In addition to concrete with normal volume fly ash (less than 50% replacement by weight of cement), concrete with high volume fly ash was also cast. Fresh properties including the air void content and density were evaluated. Permeable air voids and compressive strength of hardened concrete at four different ages were also measured. Finally, the air void content, specific surface area, spacing factor and shape factor of hardened concrete were determined using the image analysis technique. The results of this study show that the fly ash if injected with PAC in front of the precipitator has insignificant effect on the mechanical properties and air-void network which affect durability (specifically freeze and thaw resistance) of concrete.

Keywords: concrete, air-void characteristics, powdered activated carbon, fly ash, high volume fly ash, permeable voids, image analysis, durability

ACKNOWLEDGMENTS

Table of Contents

List of Tables

List of Figures

List of Symbols

A   Air void content

di   Void diameter

g   Surface tension

g_1 Bulk density, dry

g_2 Apparent density

L   Spacing factor

M_s Saturated mass

M_r Dry mass

M_a Mass of oven-dried sample in air

M_b Mass of surface-dry sample in air after immersion

M_c Mass of surface-dry sample in air after immersion and boiling

M_d Apparent mass of sample in water after immersion and boiling

n_i Number of voids

P   Volume of paste

q   Contact angle of pressure

r   Pore entry radius

SHF   Shape factor

V   Volume of selected zone

V_h Volume of air voids

W   Water uptake

τ PAC content in fly ash

ξ PAC injection rate

α Specific surface area

ψ Area of voids

ρ Density of water

Ω Applied mercury pressure

χ Perimeter of voids

CHAPTER 1- INTRODUCTION

1-1 INTRODUCTION

Fly ash has been successfully used as a supplementary cementing admixture in concrete for decades as it is economic, environmentally advantageous and improves the concrete mechanical properties and durability (Montgomery et al. 1981; Idorn and Thaulow 1985; Naik 2005; Laskar and Talukdar 2008). According to the American Coal Ash Association, over 15 million tons of fly ash was consumed as cement replacement in the United States in 2005 which shows a 15% increase compared with 2003 (Stencel et al. 2009). In Canada, 4.7 million tons of fly ash is produced annually, but only 31% of this quantity is used in construction (CIRCA 2006). However, this value shows a relative increase in the usage of fly ash when compared to the 21% used in 2002 (CIRCA 2006).

It is well known that during the production of Portland cement, approximately one ton of CO_2 is emitted for each ton of clinker produced through the calcinations of the raw materials and the burning of the fuel (Naik 2005). Filtering fly ash from the flue gases emitted from coal-fired thermal power plants results in a significant reduction in particulates released into the atmosphere. Due to its composition (mostly amorphous SiO_2) and its fineness, fly ash has been used in lieu of Portland cement to impart superior rheological properties, strength and durability to concrete, while also decreasing the equivalent CO_2 emissions per ton of concrete.

Recent concerns about air pollution control at coal-fired thermal power stations and the wider use of co-firing with secondary fuels have changed fly ash in terms of its characteristics. In Canada, the regulations governing reduced mercury (Hg) emissions came into effect in 2011 (Beusse 2005). Some of the more popular methods to check mercury emissions from the coal-

fired power plants involve the injection of Powdered Activated Carbon (PAC) into the flue gases to adsorb mercury vapour which then settles along with the fly ash in the electrostatic precipitator (Gong et al. 2007). Powdered activated carbon is a form of carbon that has been processed to make it extremely porous and thus to have a very large surface area available for adsorption of chemical components such as mercury. PAC has extensive applications in different industrial fields, especially in gas purification, gold purification, metal extraction, water purification, filters in gas masks and compressed air supply (Aizpuru et al. 2003).

The increased carbon level in the resulting fly ash can interfere with surface active chemical admixtures typically used in concrete production and may potentially affect both fresh and hardened properties. Concerns regarding the adverse performance of concrete incorporating fly ash that contains mercury adsorbents must be addressed immediately if the concrete industry is to continue using fly ash as a cement replacement at current (or higher) dosage rates. Thus, while the changes to mercury emission regulations are intended to improve the environment, the substantial corresponding impact on the cement and concrete industries must also be addressed. Meanwhile, no published report is available explaining the effect of PAC on the air-void characteristics of concrete. In this study, the effect of powdered activated carbon on the air-void characteristics of concrete is investigated.

In recent years, advanced techniques such as image analysis have been employed to determine the air-void characteristics of concrete (Laurencot et al. 1992; Elsen 2001; Zhang et al. 2005; Yun et al. 2007; Peterson 2009). The image analysis method has been chosen as one of the most reliable tools for measuring the microstructure of concrete (Pleau et al. 1990). Image analysis is a technique to capture valuable information from images by means of digital image processing techniques. Complicated and time-consuming methods (such as ASTM C457, 2010

standard test method) can be substituted by this quick method to capture size distribution, air void content, specific surface, shape factor and spacing factor. For example, the traditional ASTM C457 method demands a highly trained expert for conducting the time consuming counting procedure that makes the analysis too tedious. Other techniques including the standard ASTM C642 (2006) test method is also used to assess the air-void characteristics of cementitious materials. This simple test can provide some basic and useful information on the density, absorption and voids of hardened concrete. Due to its ease of use, the application of this test has been growing in recent years. However, it remains an indirect assessment of the air-void network. Both discussed techniques were implemented in this study to determine the air void characteristics of concrete.

1-2 STRUCTURE OF THE REPORT

This report consists of 7 chapters in addition to the list of references and appendices. In the first chapter, a general description of the entire thesis is provided as an introduction. In the second chapter, the aim and scope of this research project are clarified. A comprehensive literature review on the importance of using fly ash in concrete, the effect of carbon on the air void structure and different air void analysis techniques was performed. In particular, a literature review was performed on measuring the air-void characteristics using the image analysis technique and all of these are reported in Chapter 3. The mix design, specimen preparation and test procedures are explained in Chapter 4. In Chapter 5, the results of the tests performed on all mixes (including mixes without AEA, with AEA and with different types and percentages of fly ash and PAC) are reported and discussed. The summary of the thesis is stated in Chapter 6. In

Chapter 7, some recommendations are expressed for future studies. Finally, the list of references

and appendices are provided at the end of this thesis.

CHAPTER 2- SCOPE AND OBJECTIVES

2-1 SCOPE AND OBJECTIVE

In Canada, the regulations (Canadian Council of Ministers of the Environment 2006) governing reduced mercury emissions from coal-fired power plants came into effect in January 2011. Clearly, concerns regarding the adverse performance of concrete incorporating fly ash that contains mercury adsorbents must be addressed immediately if the concrete industry should continue to blend fly ash at current dosage rates in Portland cement concrete. Prior research has focused mainly on the effects of unburnt carbon in fly ash on air-void characteristics (Gao et al. 1997, Hill et al. 1997, Kulatos et al. 1998). Very few reports (Zhou 2007) address the effect of mercury adsorbents, such as PAC, on the air entrained admixture (AEA) demand and consequent properties of concrete. Crucially, there is no North American standard to govern the use of fly ash containing mercury-adsorbents so that all the blended cement and ready-mix concrete produced in Canada are based on design guidelines developed for conventional fly ash. Having no information on durability and mechanical properties of concrete containing mercury-adsorbents prevents accurate predictability of material response. As a result, severe structural damages in the long term as well as economic losses may happen. Investigation of the concrete microstructure leading to an air-void assessment helps to determine the feasibility of blending fly ash containing mercury adsorbents.

In this study the effect of mercury adsorbents on the air entrained admixture demand and the consequent properties of concrete has been investigated. An extensive laboratory test program was provided. Mixes were designed to evaluate the effect of powdered activated carbon (PAC) on the fresh and hardened properties of concrete. In addition to mixes with normal

volume fly ash (taken here as <50% concrete replacement by weight), concrete with high volume fly ash was also cast. Fresh properties including the air void content and density of fresh concrete are reported. The volume of permeable void and compressive strength of hardened concrete at four different ages were also measured. Finally, the air void content, the specific surface area, spacing factor and shape factor of voids within hardened concrete were determined using the image analysis technique.

The short term goal of this research program is to resolve the Alberta cement industry's concerns about the continued use of fly ash which will contain PAC after the 2011 legislative changes regarding emissions control. The long term goal of the project is to enhance the quality and sustainability of concrete produced in Alberta and Canada over the next decade. Use of high volume fly ash in concrete can enable production of concrete with enhanced properties at a lower cost compared to conventional concrete.

2-2 DETAILED TASKS

Three phases were designed for this study. The first phase of the research project studied the effect on concrete from incorporating Class F fly ash that has been intentionally charged with different weight fractions of Powdered Activated Carbon (PAC). PAC will soon be commonly used as a mercury adsorption agent in coal-fired power generating stations in Western Canada. The mechanical properties and the air-void network of this concrete are investigated. Since the permeability of cementitious materials is widely considered as the most important indicator of concrete durability (Xing et al. 2009), it is investigated through an inspection of porosity and pore structure. The permeability was indirectly assessed as the traditional methods are time-

consuming. In the second phase, the effect of PAC on the air-void characteristics of concrete containing 20% fly ash by the weight of cement was investigated. In this phase, PAC up to 10% by weight of fly ash was employed. In the third phase, the study investigated the air void characteristics and mechanical properties of concrete containing fly ash already treated with PAC in the power plant. On top of that, the development of mix designs to allow the use of fly ash at higher dosages than is common practice, at up to 80% by weight of cement was targeted. Although several reports have been published on the properties of various High volume fly ash (HVFA) concrete types which incorporate normal fly ash (Yang et al. 2007; Kumar et al. 2007) no study has examined the mechanical or rheological properties of HVFA where the fly ash contains mercury adsorbents. The tasks completed in each phase are as follows:

1- In the first phase, nineteen mixes were cast, designated as Series #1. Aside from the reference mix containing no fly ash, the remaining 18 mixes included fly ash at 10%, 20% and 30% replacement of cement by weight. For each fly ash dosage, PAC was introduced at 0, 1, 2, 3, 4 and 5 % of the fly ash by weight. Noting that PAC may physically adsorb other admixtures and cause changes to the properties of concrete, in Series #1, no superplastisizer or air entraining admixture was used so that the results reflect the effect of PAC alone on the fresh and hardened properties. The density and slump were measured for the fresh concrete. The volume of permeable voids (in accordance with ASTM C642) and compressive strength tests were performed on the hardened samples. For finding the pore structure of mixes, image analysis was employed using two different sample preparation techniques namely, epoxy-impregnation and inked preparation.

2- In the second phase, four mixes were cast and designated as Series #2, where the fly ash (from Lafarge) was kept constant at 20% by weight of cement. Powdered activated carbon at 0%, 2%, 5% and 10% of fly ash by weight were added to mixes containing an air-entraining admixture (AEA). The tests performed on this series were similar to those on Series #1, so that the fresh density, slump, volume of permeable voids (in accordance with ASTM C642) and compressive strength were evaluated. In addition, the image analysis technique was also implemented to assess the spacing factor, the specific surface area and the shape factor of the air voids within concrete. Again, two sample preparation techniques namely, epoxy-impregnated and inked preparation were applied on the samples.

3- In the last phase, nine mixes were cast and designated as Series #3. Fly ash was sourced from the Genesee plant, Alberta/Canada, produced in such a way that PAC is injected into the flue gas ahead of the electrostatic precipitator. Series #3 was designed to demonstrate the effect of fly ash already containing PAC (PAC injected at power plant) on the air void parameters of concrete and to compare these results to the previous series is which PAC was added during the casting of concrete. In this series, cement was replaced by the Genesee fly ash at up to 80% of the cement weight in increments of 10% substitution (0, 10, 20, 30, 40, 50, 60, 70 and 80% by weight of cement). Four mixes (50, 60, 70 and 80% by weight of cement) in this series were classified as high volume fly ash concrete as they incorporated greater than 50% fly ash by weight of cement. All tests including fresh density, slump, volume of permeable voids (in accordance with ASTM C642), compressive and image analysis were performed on the samples. Only the inked preparation technique was used for image analysis in Series #3 since the results of

previous series showed greater consistency for inked preparation sample compared to the

ones prepared with epoxy ones.

CHAPTER 3- LITERATURE REVIEW

3-1 IMPORTANCE, BENEFITS AND APPLICATION OF FLY ASH IN CONCRETE

Fly ash is a by-product of coal combustion in power plant operations. Here, the different steps of fly ash production are briefly explained, see Figure 3-1. Before coal is consumed in a power plant, it is first ground into powder (Xu 2008). Then, this pulverized coal is injected into the power plant's boiler that consumes the carbon, leaving molten particles rich in silica, alumina, and calcium (Headwaters Resources 2009). These particles crystallize as microscopic, glassy spheres which are collected from the power plant's exhaust through use of an electro static precipitator. An image taken of fly ash with high magnification and physical appearance of fly ash are shown in Figures 3-2a and 3-2b, respectively. Chemically, fly ash is classified as a pozzolanic material due to its high content of amorphous siliceous oxide (ASTM C618 2008). This pozzolanic material shows cementitious properties when combined with calcium hydroxide (Idorn and Thaolow 1985; ASTM C618-2008). Such pozzolans are commonly used as supplementary cementing materials in Portland cement concrete mixtures to improve both the short-term and long-term properties.

Concrete containing fly ash can be stronger, more durable, and more resistant to chemical attack than concrete without fly ash (Malhotra 1990; Ahmaruzzaman 2010). A reduction in the material cost has been reported as one of the major reasons to justify the usage of fly ash in some reports (Ahmaruzzaman 2010).
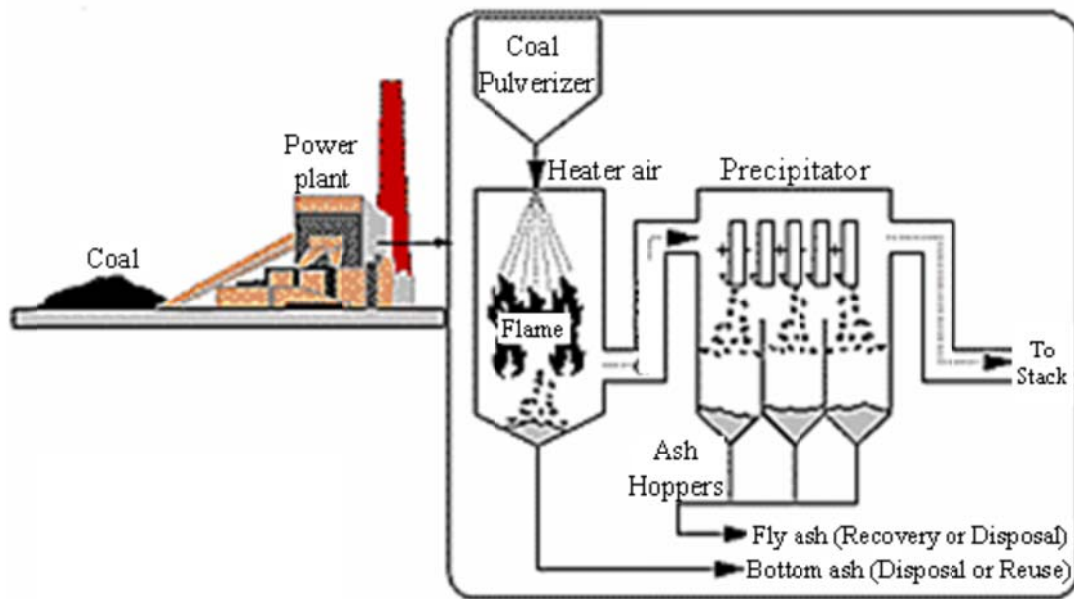
Fig. 3-1 Fly ash production process (Xu 2008)
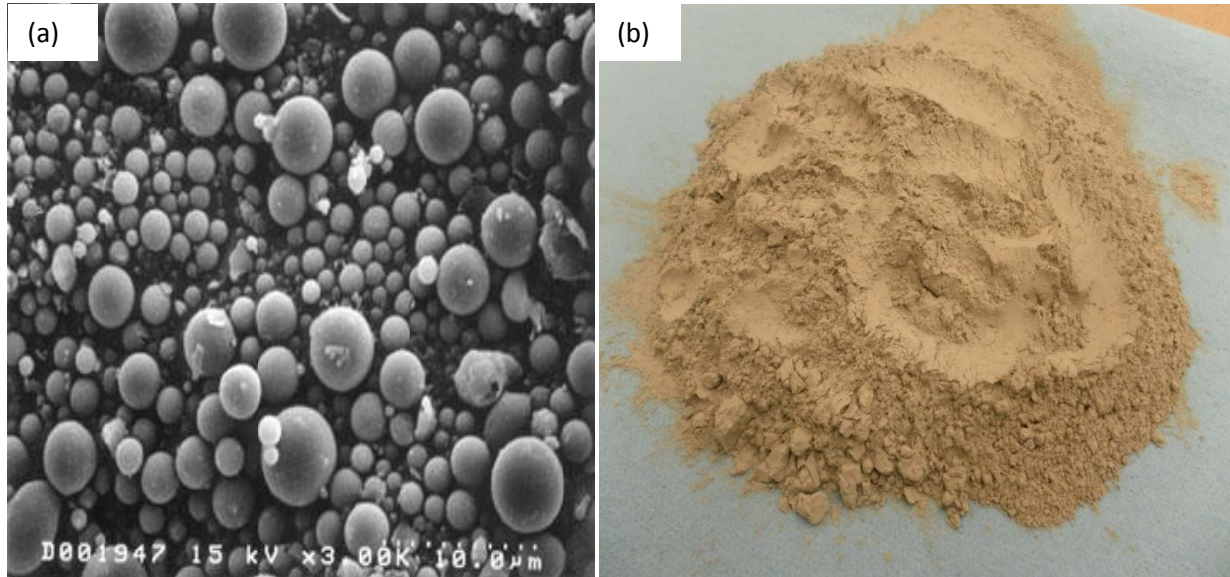
Fig. 3-2 a) Scanning electron microscope of fly ash particles (Xu 2008); b) fly ash (from

Lafarge) used in Series #1 and #2 in this study

As fly ash is made of particles equal, or finer than cement particles, it effectively fills voids and pores inside the concrete matrix. Being spherical, fly ash particles reduce the water demand for the specific workability due to a ball-bearing effect. The ball-bearing effect of fly ash particles leads to lubrication when concrete exists in its early fresh state (Xu 2008). Therefore, the rheological advantages achieved by use of fly ash in a concrete mix (Laskar and Talukdar 2008; Ahmaruzzaman 2010) include:

1) Improved workability: Concrete is easier to consolidate with less work, responding better to vibration to fill forms more completely.

2) Ease of pumping: Pumping requires less energy and longer pumping distances are possible.

3) Improved finishing: Smooth architectural surfaces are easier to achieve as is often required for exposed elements.

4) Reduced mix segregation: Segregation and bleeding decrease due to improvement in the cohesiveness of the material. Segregation leads to a non-homogenous concrete. As a result, different properties in different parts of the concrete occur, while excessive bleeding can result a weak layer at the concrete surface.

Finally, the usage of fly ash creates significant benefits for the environment. Saving natural resources and avoiding landfill disposal of ash products can be achieved by replacing cement with fly ash in concrete mixes (Ahmaruzzaman 2010). In addition, by increasing the durability of the concrete, life cycle costs of structures can be significantly reduced. Furthermore, significant energy savings and reductions in greenhouse gas emissions occur by partially replacing the Portland cement with fly ash.

3-1-1 Formation and Classification of Fly Ash

The formation process of fly ash contributes to the structure and composition of fly ash particles (Xu 2008). As mentioned in Section 3-1, the main constituents of fly ash particles include amorphous alumina and silica, which are formed during combustion from the melting of the inorganic constituents in the individual coal particles. According to the American Society for Testing Materials (ASTM C618 2008), two classes of fly ash can be distinguished based on the type of coal used. Class F fly ash is mostly produced from anthracite or bituminous coals. Class C fly ash is produced by burning lignite or sub-bituminous coals (ASTM C618 2008). Both classes of fly ash exhibit pozzolanic properties. Class C fly ash also exhibits some cementitious properties and can react with water without the presence of cement particles.

Class F fly ash (which is used in the current study) is mainly siliceous, and it has a constant fineness and carbon content. Class C of fly ash also has a high lime content of up to 25%. Compared with Class F fly ash, Class C fly ash has a lower carbon content, higher fineness, and lighter colour (Neville 1995). Table 3-1 provides the chemical requirements of both Class C and Class F fly ash according to ASTM C 618 (2008).

3-1-2 Use of Fly Ash in Concrete

As mentioned earlier, fly ash has been successfully used as a mineral admixture in Portland cement concrete for nearly 70 years. According to the American Coal Ash Association, 15 million tons of fly ash was consumed as cement replacement in the United States in 2005, which shows a 15% increase compared with 2003 (Stencel et al. 2009, American Coal Ash Association 2004). In Canada, 4.7 million tons of fly ash are produced annually, but only 31% of this quantity is used in construction (Berndt 2009). However, this value shows an increase in the

usage of fly ash when compared to the 21% in 2002. It should be noted that the consumption of fly ash in concrete can increase to 57% of total ash production if the Canadian fly ash is incorporated without any major processing, i.e., if no further carbon removal is required (Smith 2005).

Table 3-1 Chemical requirements for fly ash (ASTM C618 2008)

Oxide	Class F (%)	Class C (%)
$Fe_2O_3+Al_2O_3+SiO_2$, min, %	70.0	50.0
SO_3, max, %	5.0	5.0
Moisture content, max, %	3.0	3.0
Loss in ignition, max, %	6.0	6.0

3-1-3 Benefits

The benefits of using fly ash in concrete were briefly listed in Section 3-1. In this section some of the mechanisms of these advantages are explained in more detail. As discussed earlier, the environmental advantages of using fly ash in the construction industry include reduction of cost of fly ash disposal, efficient land use, and an equivalent decrease in CO_2 emissions associated with a reduction in production of Portland cement (Naik 2005). It is well known that during the production of Portland cement, a large amount of CO_2 is emitted from calcination of the raw materials (for instance limestone) as well as the burning fuel (Smith 2005). By using fly ash in concrete, the required cement content to achieve a specified strength can be decreased. As a result the equivalent CO_2 emissions decrease. The second environmental benefit refers to the

reduction of fly ash disposal in landfills (Xu 2008). Landfill space is a big issue especially in countries with limited dry-land areas.

Concrete made with fly ash exhibits improved transport properties, a more homogenous interfacial transition zone, improved rheological behaviour and workability, reduced bleeding and less water demand, higher ultimate strength, reduced permeability and chloride ion penetration, lower heat of hydration, greater resistance to sulfate attack, greater resistance to alkali-aggregate reactivity, a reduction in drying shrinkage, and higher electrical resistivity (Poon et al. 2001; Lee et al. 2003; Miranda et al. 2005). Figure 3-3 shows the increase of the compressive strength in concrete containing fly ash. The figure shows that concrete containing fly ash continues to gain strength up to 365 days.
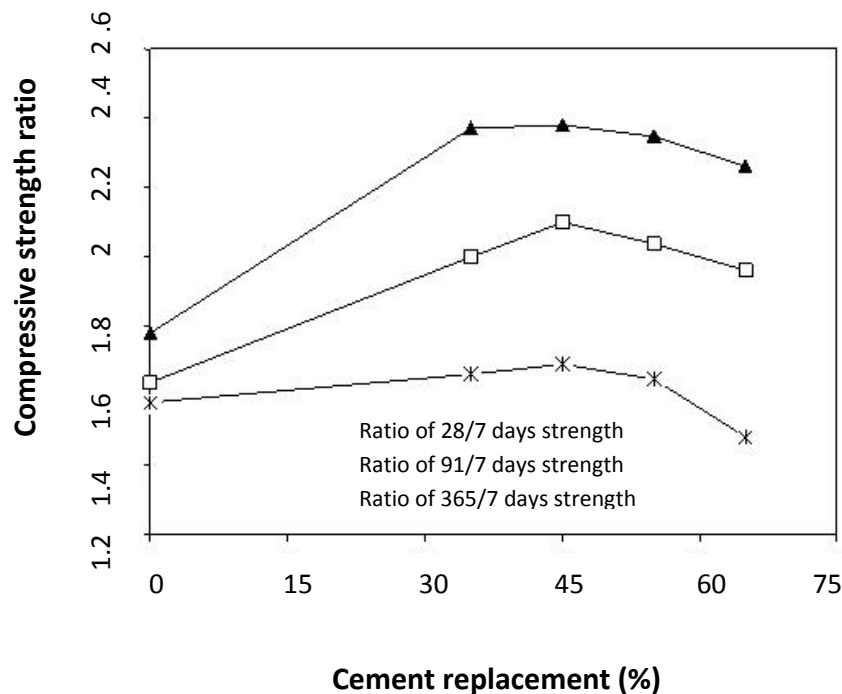
Fig. 3-3 Improvement of compressive strength with amount of fly ash in

binder (Siddique et al. 2007)

15

There are two justifications for the improved workability of concrete containing fly ash (Zain et al. 1999; Yucel 2006). First, fly ash reduces the amount of water required to produce a specific slump. The smooth spherical shape of fly ash particles provides water-reducing characteristics similar to a water-reducing admixture. The water demand of a concrete mix with fly ash is typically reduced by up to 10%, depending on other factors which include the volume, class and the fineness of fly ash.

Second, fly ash reduces the amount of sand needed in the mix to achieve a specified workability because it creates more paste (Ahmaruzzaman 2010). Since the surface area to volume of sand particles is higher than coarse aggregates, sand requires more paste. Therefore, reducing the sand content leaves more paste available to coat the surface of remaining aggregates.

In the case of improved durability and transport properties, not only does fly ash reduce the amount of water needed to produce a given slump, but through pozzolanic activity it also creates more solid Calcium Silicate Hydrate (CSH) components which fill the capillary pores and disconnects them (Poon et al. 2001; Boel et al. 2007; Elahi et al. 2010). Fly ash can also reduce the corrosion rate of steel embedded in the concrete. By reducing the concrete permeability though use of fly ash, the penetration rate of aggressive ions, including water, corrosive chemicals and oxygen reduces significantly. Figure 3-4 shows the effect of fly ash on the reduction of concrete permeability. It can be seen in Figure 3-4 that chloride permeability (accordance with ASTM C1202-2005) of concrete cured for 365 days decreased with an increase in the fly ash content.
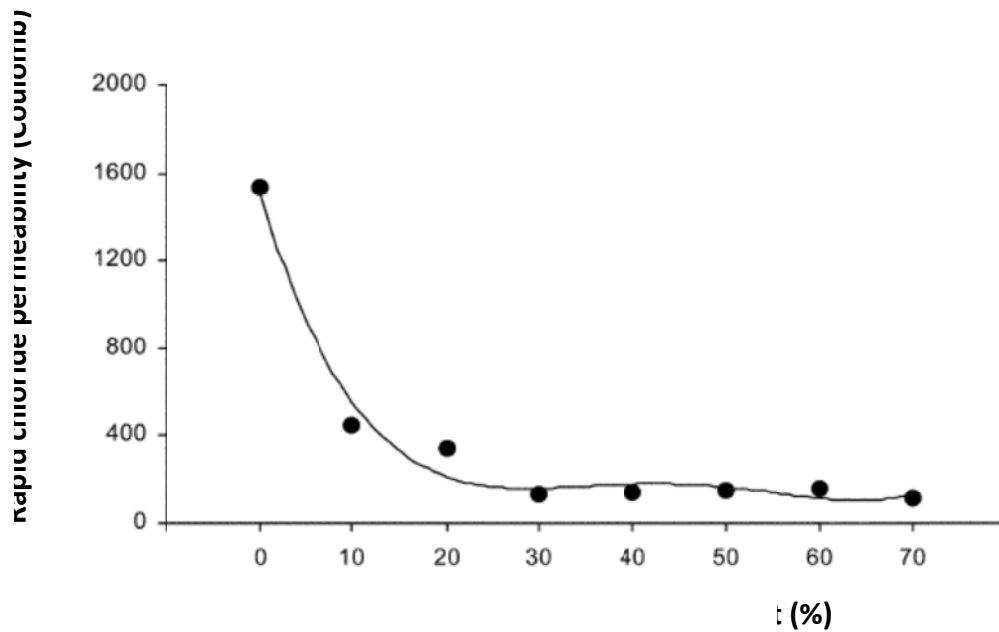
Fig. 3-4 Decrease of permeability in concrete containing fly ash (Sengul et al. 2005)

Fly ash also increases resistance from sulphate attack and reduces the possibility of alkali-silica reaction (ASR). Fly ash in concrete reduces sulphate attack in two ways (Plowman and Cabrera 1996; Sahmaran 2007). First, fly ash as a Portland cement replacement reduces the total calcium hydroxide content available to combine with sulphates to produce gypsum. The gypsum reacts with the monosulphoaluminate to form ettringite. Although the volume expansion of gypsum is higher compared to ettringite, the latter is more damaging to the concrete. Figure 3-5 shows how fly ash can reduce sulphate attack. It can be seen that using fly ash at 50% of the total binder weight led to decreased expansion of the mortar prisms by 85%. Second, aluminates available in cement also combine with sulphates to create expansive compounds. By replacing Portland cement and reducing its total volume in a concrete mix, the amount of free aluminates reduces. Therefore, the potential for expansive reaction and developing internal cracks drops.
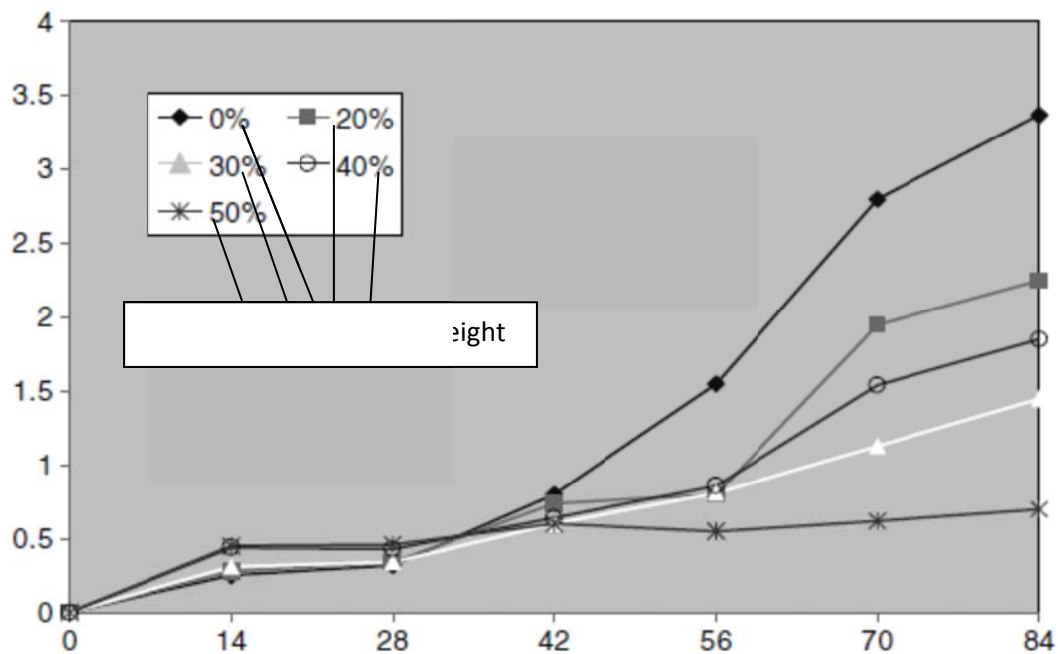
Fig. 3-5 Reduction of sulphate attack through use of fly ash (Mulenga et al. 2003)

In the case of an alkali-silica reaction (ASR), fly ash reacts with the alkali hydroxides in Portland cement paste to make them unavailable for reaction with reactive silica in certain aggregates. As a result, the potential of ASR decreases in concrete containing fly ash (Shehata and Thomas 2000; Shon et al. 2007).

3-2 GROWING CONCERN ON USING FLY ASH

In Section 3-1, the importance of fly ash as an admixture for concrete's properties was explained. However, there is growing concern with regard to the continued usage of fly ash in concrete due to the potentially high carbon content arising from two sources. Across North America the coal-fired thermal power plants will soon be required to take action towards reducing mercury emissions. The U.S. Environmental Protection Agency announced in 2000 that

it would regulate all coal-fired electric utility steam generating units for mercury emissions (Beusse 2005). In Canada, similar legislation requires a significant drop in mercury emissions (Canadian Council of Ministers of the Environment 2006). For the majority of coal-fired thermal power plants, the easiest and most economical technique to comply with these regulations is to inject Powdered Activated Carbon (PAC) into the flue gas ahead of the electrostatic precipitator. As a result, the generated fly ash is rich in its concentration of PAC (Liu et al. 2011). On the other hand, prompted by clean-air legislation imposed by local governments, several utilities have changed their conventional burners to low-NO_x burners (Nkinamubanzi et al. 2003). As a result, while the flue gases are low in SO_2 and NO_x, the resulting fly ash is known to be higher in its carbon content (Pederson et al. 2008). Unfortunately, carbon in fly ash (especially powdered activated carbon) is suspected to adsorb the surface active admixtures in concrete, in particular the air-entraining admixtures (AEA).

Activated carbon consists of pores enclosed by carbon atoms, so that these pores are of the size of molecules (Marsh and Reinoso 2006). Activated carbon has been used since the times of ancient Egyptians, who employed it to purify oils and for medicinal purposes. After the First World War, an increase in the manufacture and applications of activated carbon has been seen (Cameron Carbon Incorporated 2006). This material is made from hardwoods, coconut shell, fruit stones, coals, and synthetic macromolecular systems. According to Cameron Carbon Incorporated (2006), two methods of manufacturing activated carbon are available, namely, steam activation and chemical activation. The former is achieved by removing volatiles and then oxidising the structure's carbon atoms, while the latter is achieved by degradation or dehydration of the cellulosic raw material structure. High temperatures, 800-1000° C, are needed for both methods. According to Bansal and Goyal (2005), activated carbon can be used in various forms

including the granulated form, the powdered form, and the recently developed fibrous form. The Granulated Activated Carbon (GAC) has granules that are 0.6 to 4.0 mm in diameter and it is generally hard, abrasion-resistant, and dense. It can be formulated into a module that can be removed after saturation to be regenerated and re-used again. Meanwhile, GAC is more expensive compared to PAC which makes its application limited to specific industrial applications. On the other hand, Powdered Activated Carbon (PAC) is smaller in diameter compared to GAC with an average diameter of 0.15 and 0.25 mm. The small particle size of PAC helps to adsorb more material (Xu 2008).

It is worth noting that besides the injection of PAC as described above, there are at least two alternative methods to achieve a reduction in the mercury emissions at coal-fired generating stations without causing any negative consequence to the concrete (Derenne et al. 2009). These methods include: a) injecting PAC after the fly ash has been removed from the flue gas stream and then removing the activated carbon particles through an additional precipitator and b) using alternative adsorbents that are physically and chemically inert when accompanying fly ash in concrete (Derenne et al. 2009). Investigations performed by Zhou et al. (2007) and Lockert et al. (2005) confirmed that using alternative adsorbents can cause no negative consequences on concrete. Figure 3-6 shows the diagram of the proposed method by Toxecon (Derenne et al. 2009).
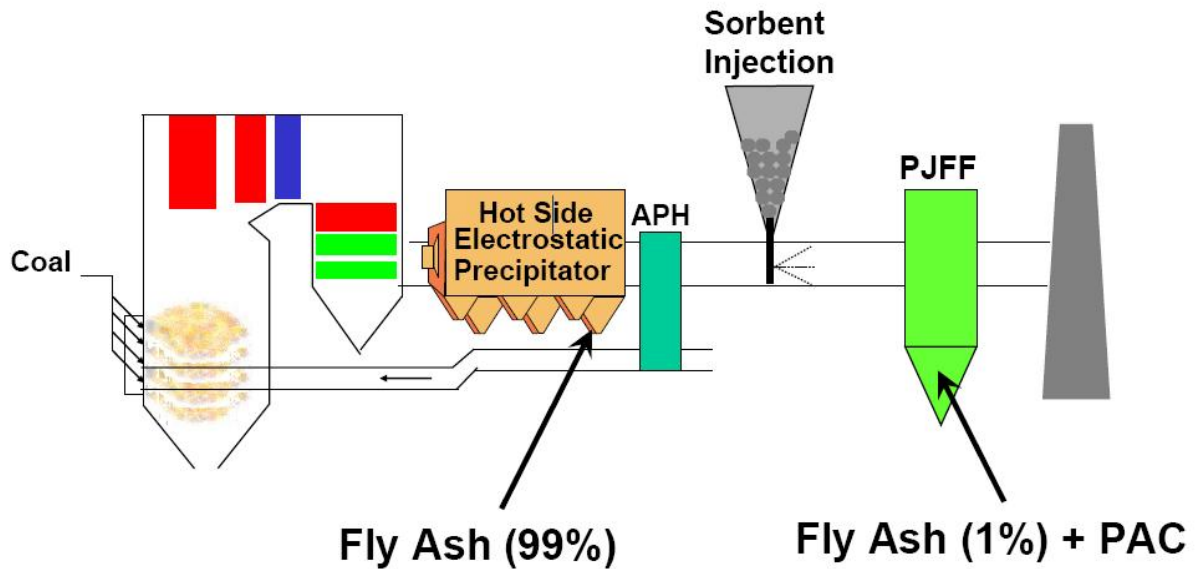
Fig. 3-6 New method proposed by Toxecon to obtain fly ash without PAC (Derenne et al. 2009)

Nonetheless, these techniques are at present either too expensive or at the investigative stage so that they have not been used as the industrial scale (Landreth et al. 2007, Lockert et al. 2005).

3-3 EFFECT OF CARBON ON AIR VOID STRUCTURE

In this section, the previous studies performed to investigate the effect of unburnt carbon on the air-void structures are explained. It is worth to remind that the unburnt carbon can be evaluated by Loss of Ignition (LOI). Although the effect of unburnt carbon and PAC on concrete may be different the following sentences list the effect of unburnt carbon as there is little published information (Liu et al. 2011) on PAC's effect on concrete.

Osbaeck and Smith (1985) believed that fly ash affects the air void network through a direct contribution from its porous particles and by adsorbing the AEA. Many researchers opine

21

that the amount of unburnt carbon in fly ash, usually measured by the loss on ignition (LOI), is related to the rate of adsorbtion of surfactants like AEA. However, others have shown that there are numerous parameters related to fly ash that affect the efficiency of AEA. Suuberg et al. (1998) found that the porosity and surface area of carbon particles and their electrical polarity are important factors affecting the adsorption of AEA. Similar conclusions were reached by Kulaots et al. (1998), who studied the effect of polarity and accessible surface porosity of carbon particles in fly ash on the adsorption of AEA. Gao et al. (1997) indicated that the accessible, hydrophobic and carbonaceous surface area of carbon in fly ash is primarily responsible for increasing the AEA demand. In addition to the unburnt carbon (LOI), Gelber and Klieger (2005) showed that the SO_3 content and the specific gravity of fly ash influence the air void content of concrete. Again, the reader should be aware of the existing difference between unburnt carbon and PAC. Hill et al. (1997) showed that different samples of fly ash with the same unburnt carbon content may demand different amounts of AEA for the same efficiency. They found that the surface chemistry and structure of smaller particles and the random orientation of the optically isotropic carbon impart a greater active surface area for polar agents such as AEA's. Sporel et al. (2009) indicated that the specific surface area of the porous unburnt carbon in the fly ash is the single most important parameter that affects the demand of AEA for a certain range of air void contents in the fresh concrete. It is therefore clear from these investigations that the air-void structure of concrete containing fly ash is intimately connected to the unburnt carbon that accompanies it. However, there is limited information on how PAC, an externally introduced carbon additive to the flue gases in thermal power plants, affects the AEA demand, the air-void network, and the consequent rheological and time-dependent mechanical performance of concrete.

3-4 REVIEW OF DIFFERENT AIR VOID ANALYSIS TECHNIQUES

Over the years, concrete technology experts have introduced different ways to estimate the microstructure and pore structure of concrete. Some of these methods have been widely used by researchers due to their reliability. In this section some of the common tests related to pore structure of concrete are described.

3-4-1 Mercury Intrusion Porosimetry (MIP)

The pore structure characteristics of cementitious materials can be evaluated by Mercury Intrusion Porosimetry (MIP) (Laskar et al. 1997; Kumar and Bhattacharjee 2003a; Cnudde et al. 2009). Figure 3-7 shows the principles of the MIP technique. The usual model is that of a system of cylindrical pores each of which is completely accessible to the outer surface of the specimen, and thus to the surrounding mercury (Diamond 2000; Care 2008; Stroeven et al. 2010). For porous material like concrete that conform to such a model, the well-known Washburn equation may be properly applied to assess the diameter of cylindrical pores intruded at each pressuring step (Diamond 2000). The Washburn equation proposes the pore diameter as r =2gcos q/Ω, where r is the pore entry radius in which mercury is being intruded, g is surface tension, q and Ω are contact angles of mercury with solid and applied pressure, respectively (Abell et al. 1999). As mentioned earlier, the Washburn model has been based on two major assumptions namely, that 1) pores are cylindrical and 2) the pores are accessible from the outer surface of the specimen. These simple assumptions were criticized by researchers where they especially doubt if the pores are perfectly cylindrical (Ilavsky et al. 1997). In order to overcome this criticism, shape factor corrections can be applied to the original Washburn equation (Ilavsky et al. 1997).

Meanwhile, the results of shape factor that are reported later in this text show values close to unity. This can help confirm the first assumption of the Washburn model.

Mercury Intrusion Porosimetry

Principle:

Evacuate   Fill with mercury   Apply pressure

$p_0 = 0$ < p_1 < p_2

The relation between the applied pressure and the smallest filled pores is:

$$p = \frac{2\,\sigma\,\cos\theta}{r} \quad \text{(Washburn)}$$

σ = Surface tension (0.48 N/m)   p = Pressure
θ = Wetting angle (140°)   r = Pore radius
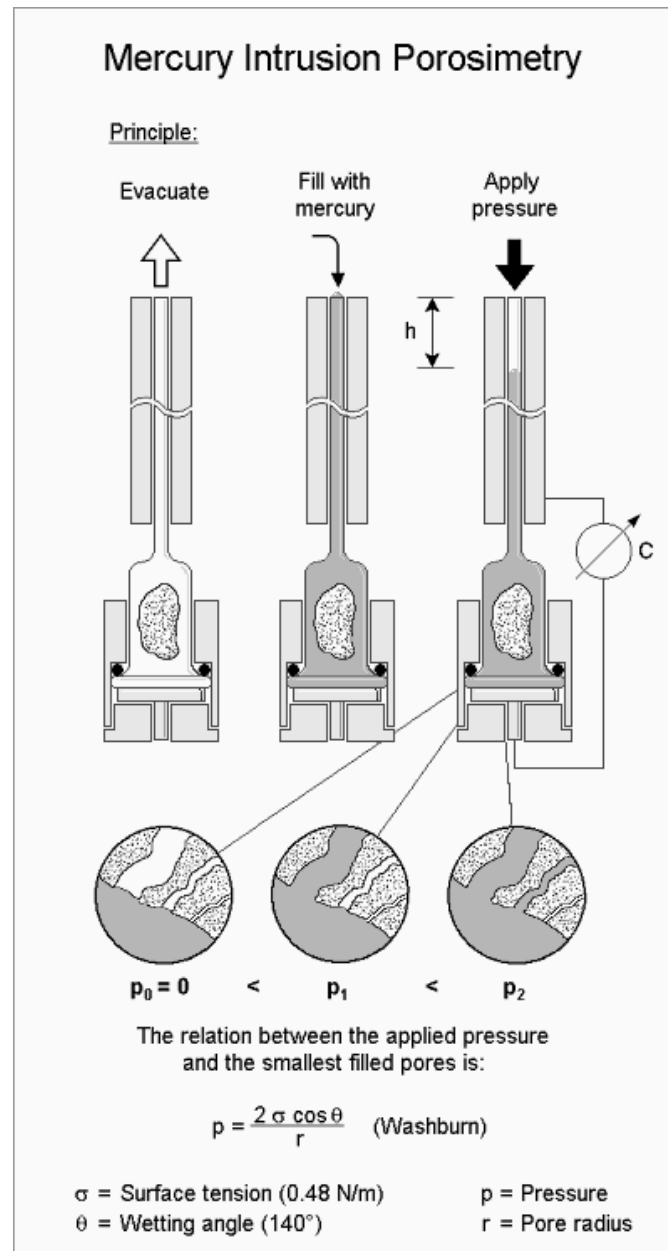
Fig. 3-7 Principles of the MIP technique (Fraunhofer as of September 15th 2011)

Despite the MIP method being the most common technique to find the pore size distribution, mercury porosimetry results are affected by a number of experimental factors including the contact angle and surface tension of mercury, sample preparation, forms and types of sample, sample drying technique, and rate of pressure application (Cook and Hover 1991; Hearn and Hooton 1992; Bourdtte et al. 1995; Feldman and Beaudoin 1997; Laskar et al. 2003). According to a literature review of porosimetry for cement-based materials, commonly adopted values of contact angles are typically 117 for oven-dried sample, 130 for chemical dried samples using magnesium perchlorate hydrate, and 140 for all other techniques (Winslow and Diamond 1970; Schneider and Diederichs 1983; Kaufmann et al. 2009). For cement-based materials, the adopted values for surface tension of mercury vary between 0.473 and 0.485 N/m.

It has been observed that for cement-based materials, other factors including solid compressibility and mercury compression may also affect the pore size distribution curve but only for pore diameters less than 50 nm (Kumar and Bhattacharjee 2003b). The error due to solid compressibility and mercury compression is not more than 3% (Allen 1975).

According to the Patil and Bhattacharjee (2008) study, MIP has some drawbacks in measuring the pore distribution of concrete. They state that "the measured radius is only the pore entry radius and volume of pore registered against a pore size may be misrepresented as many large pores in the cementitious system are surrounded by smaller gel pores."

Several researchers have conducted extensive investigation on the MIP method to determine pore size distribution of cementitious material. Various models have been proposed making a relationship between air void size and its distribution for concrete with different water/cement ratios and curing conditions (Khan et al. 2000; Herman and Yajun 2003). It should be noted that MIP technique was not executed in this study.

3-4-2 Nitrogen Sorption

Nitrogen sorption is a widely established method to analyze the pore structure of concrete. Researchers believe that "adsorption of nitrogen is independent from network effects as filling of the pores is from small to large, whereas desorption may be significantly influenced by metastable nitrogen located in pores that are accessible by smaller ones only" (Kaufmann et al. 2009). Large pores cannot be analyzed as the pressure of nitrogen gas does not reach to the saturation level (Kaufmann et al. 2009). Therefore, condensation of nitrogen does not occur in these pores.

In this technique, the equilibrium of the internal and external nitrogen pressure is achieved only approximately. Since the dynamics of the nitrogen filling are not investigated, no information about the tortuosity or the connectivity of a pore to an external surface is achieved (Kaufmann et al. 2009). Figure 3-8 shows a typical result of a nitrogen sorption test. The X-axis, P and P_0 denote the relative pressure, nitrogen pressure and atmospheric pressure, respectively.
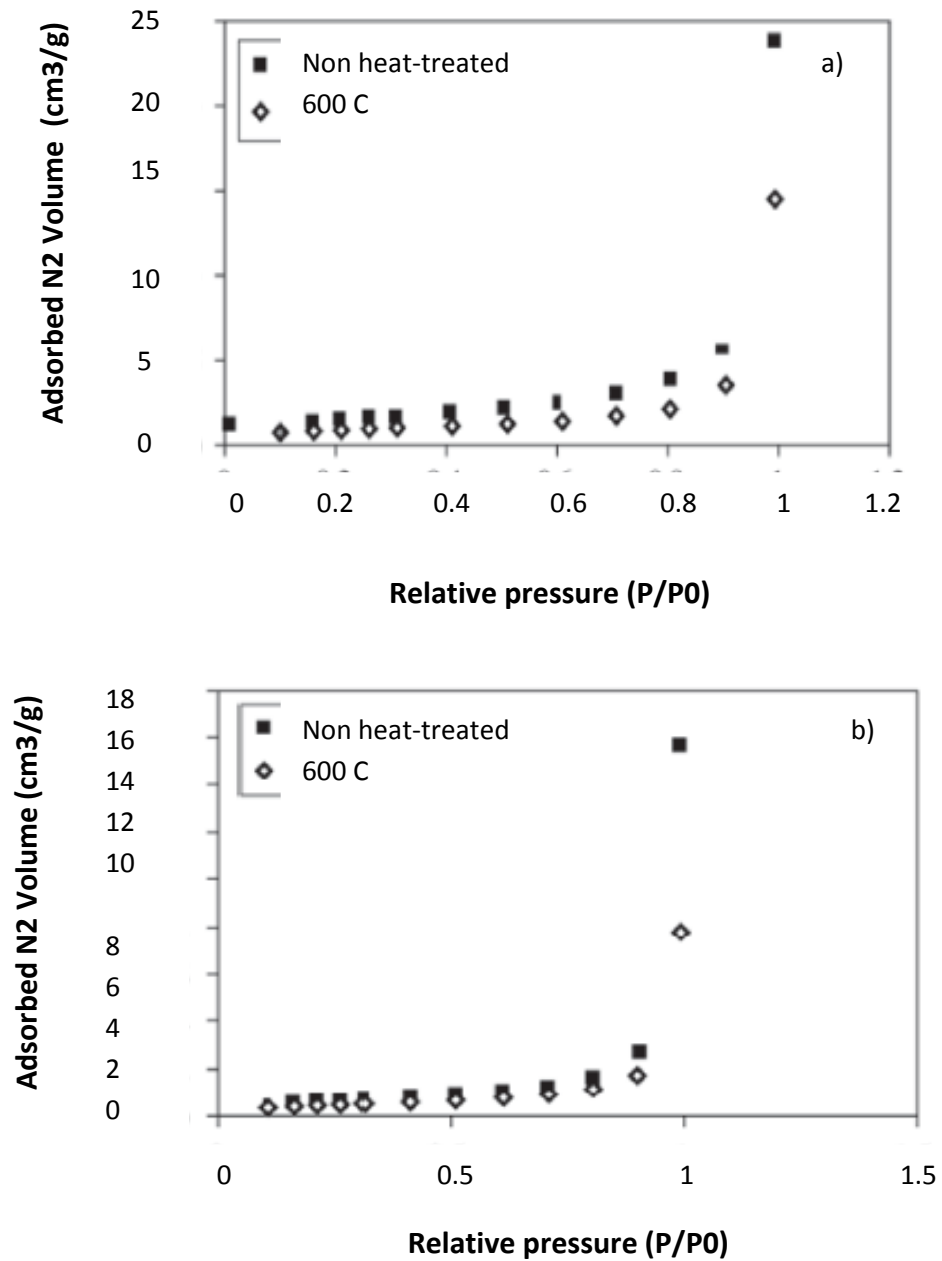
Fig. 3-8 Sample result of the nitrogen sorption test for a) normal strength concrete; b) high

strength concrete (Tolentino et al. 2002)

3-4-3 Permeability

Concrete permeability relates to the ease of fluids or gases (water, carbon dioxide, chloride ion, and oxygen) to migrate through the hardened concrete body. The permeation characteristics of concrete are one of the most important parameters impacting the durability of concrete structures (Sanjuan and Martilaty 1995). Up to 60 years ago it was an accepted theory that the total air void content is the major factor affecting the permeability and durability of concrete. Later, this idea was changed by a theory proposed by Powers (1949). He introduced the spacing factor as a parameter to describe the effect of void spacing on the durability of concrete. The spacing factor is an index presenting the maximum distance of any point in a cement paste from an air void. Powers (1949) concluded that the spacing of voids compared to the total air voids controls the resistance of concrete against freeze and thaw cycles. He showed that lower spacing factors correlated with more durable concrete. This factor is the basis of protecting the paste from freeze and thaw cycles (Lawrence et al. 2002). Many researchers also reported the importance of spacing factor on the durability of concrete. Pigeon and Lachance (1981) showed that the spacing factor affects the durability of concrete against freeze and thaw cycles. Pigeon et al. (1985) also showed the importance of spacing factor on the durability of concrete. They confirmed the critical value of spacing factor obtained from Powers (1949) as per the hydraulic pressure theory.

Permeability can be indirectly used to predict the pore structure of concrete paste, especially its interconnected voids. There are several proposed relationships between permeability and porosity in the literature (Powers et al. 1954; Felix and Munoz 2006). One should notice that several parameters may affect the result of permeability, including moisture content, degree of saturation, and the preconditioning process that make the results uncertain.

28

Meanwhile, the most common permeability tests are the water, gas and chloride permeability tests (Boel et al. 2007). However, the gas permeability test slowly dominates against the others due to its high speed and its inert reaction role with concrete. Figure 3-9 shows typical devices used for gas and water permeability tests.
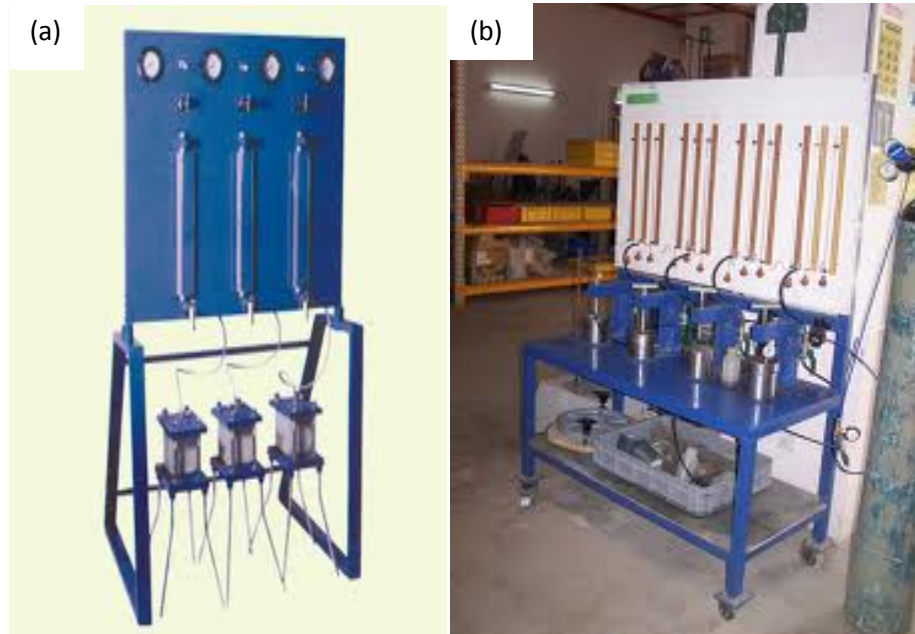
Fig. 3-9 Devices for a) water permeability; b) gas tests

(Universiti Teknologi Mara as of September 15th 2011,

M.K. Instruments as of September 15th 2011)

3-4-4 Absorption and Sorptivity

In many countries, water absorption is widely used as a practical compliance criterion with regard to concrete durability (Schutter and Audenaert 2004). Maximum water absorption values can form part of technique specifications for concrete products. Water absorption tests can

be performed in the laboratory using specimens dried and saturated in a standard way. The water absorption (*W*) is expressed as the water uptake relative to the dry mass:

$W=(M_s-M_r)/M_r$ *Eq. 3-1*

where M_s and M_r denote the saturated and dry mass of concrete, respectively.

The rate of water absorbed into concrete through the pores gives important information about the microstructure and permeability characteristics of concrete (Kumar and Bhattacharjee 2003b). Experimental results show that the depth of water absorbed into concrete increases linearly with respect to the square root of wetting time (Parrott 1992). In terminology, the sorptivity is the change in volume of water absorbed per unit area against the square root of time (Claisse et al. 1997). Water absorption and sorptivity can suggest useful data regarding the pore structure of the cement paste.

3-4-5 Image Analysis

Image analysis is a relatively new way to determine the pore structure of hardened concrete giving valuable information in this field. Both manual and automated analysis methods can be used to assess the pore distribution of concrete paste. Standard ASTM C457 (2010) is one of the accepted methods which measures the chords intercepted in the air voids along a series of regularly spaced lines of traverse (Hover and Phares 1996). In the automated methods, images captured through a scanning electron microscope (SEM), optical microscope, or micro tomography device are analyzed by a suitable image analysis software. The air-void percentage, the spacing factor, shape factor, and surface area can be obtained when the automated technique

is employed. Figure 3-10 shows an apparatus developed for the image analysis technique. The

image analysis technique is explained in more detail in Sections 3-5 and 4-2-5.
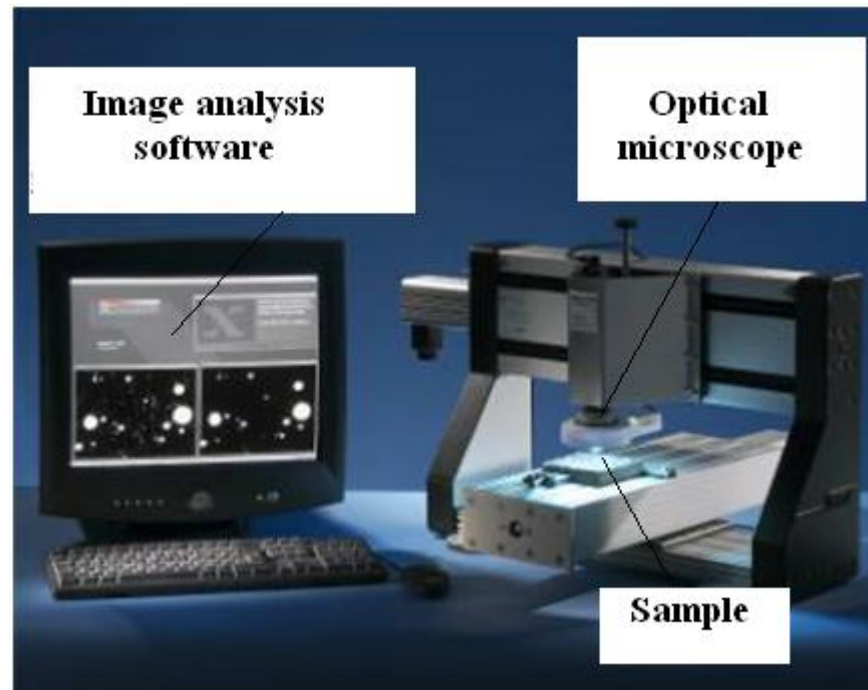
Fig. 3-10 Image analysis technique employed for determining the structure of concrete (CXI

Corporate as of September 15th 2011)

3-5 EVALUATION OF AIR-VOID STRUCTURE USING IMAGE ANALYSIS

In the previous section, investigation of the air void parameters of concrete by using

traditional methods including absorption and sorptivity, mercury intrusion porosimetry, nitrogen

sorption, and measuring the permeability was discussed. However, in recent years advanced

techniques such as image analysis have been employed to determine the air-void characteristics

of concrete. Several researchers have chosen image analysis method as one of the reliable tools

for measuring the microstructure of concrete. It is a method of capturing valuable information

from images by means of digital image processing techniques. Complicated and time-consuming methods can be substituted by this quick method to capture size distribution, air void content, specific surface area, shape factor, and spacing factor. For example, the ASTM C457 method demands a highly trained expert to conduct the time-consuming counting procedure that makes the analysis too tedious.

Pleau et al. (1990) believe that the image analysis method eliminates drawbacks of the manual ASTM C457 method. They state that the image analysis method gives more reliable results compared to ASTM C457 and believe that this technique yields a better assessment of the real spacing of the air void in concrete by providing a simple and easy way to record the size distribution. According to the Pleau et al. (1990) study, preparation of the concrete surface prior to microscopic examination is an important factor influencing the accuracy of the results. Elsen (2001) compared the air void parameters of concrete with different range of air void using manual point count, manual linear traverse, and automated linear traverse methods. He found that application of different methods causes no significant change in the results. Nevertheless, sampling is the major cause of variation in air void results (CTRE 2008). Elsen also concluded that automated methods are fast but can be problematic when a high amount of porous sand grains exist in concrete. Yun et al. (2007) measured the micro air void system of concrete using the image analysis method. They applied this technique to acquire a better understanding of chloride permeability. They showed that the use of latex polymer can significantly lower the value of the air void spacing factor. Peterson et al. (2009) employed the minimum deviation from the unity method and maximum Kappa statistic method (as two methods to determine the optimum threshold value) to calculate the air-void parameters using flatbed scanner images. They found that the optimum threshold level according to the minimum deviation from unity and

maximum Kappa methods were 149 and 153, respectively. They determined the spacing factor of 0.637 mm for the non-air entrained concrete.

One of the earliest studies on the air-void network of concrete using image analysis was done by Lange et al. (1994). They applied the image analysis method and compared its results with the mercury intrusion porosimetry method. According to their observations, both methods generated pore size distribution curves of similar shape, although their magnitudes were distinctively different. They showed that using the image analysis technique results in measurement of larger pores at 100-time order of magnitude compared to the MIP. They also found that the image-based pore-size distribution curve can better describe the large porosity of matrix in concrete. Zhang et al. (2006) developed a new automated system for microscopic determination of air-void parameters in hardened concrete involving a new sample preparation technique. This automated linear traverse method needs additional preparation treatment besides the normal sample preparation. They compared the results of the air-void network of concrete samples obtained from both normal and automated linear traverse methods. They summarized that the automated linear traverse method yields an acceptable range of air-void parameters. In another study performed by Zalocha et al. (2005), a new automated image analysis method using a flatbed scanner was introduced. They believe that this technique possesses some advantages, including the need for less preparation, lower cost and a very steady source of light. One should notice that unsteady light may cause trouble in microscopic observations.

Comparison between the manual linear traverse and automated image analysis methods to measure air-void characteristic has been done by various researchers (Roberts and Scali 1984; Laurencot et al. 1992; Pleau et al. 2001). Some believe that both methods result in the same air

void content and spacing factor, while others disagree. There is general agreement among the researchers that sample preparation plays an important role in image analysis results.

Image analysis has also been employed to determine the air-void characteristic of concrete containing supplementary admixtures. Glinicki and Zielinski (2008) performed an investigation on the air-void network of concrete containing a new type of fly ash by using the image analysis method. They found that fly ash with a higher LOI (recall that higher LOI is not necessarily equivalent to higher PAC) leads to a higher spacing factor. In addition, they showed that the air-void diameter of concrete with fly ash is higher than that of concrete without fly ash. Another study was performed by Giergiczny et al. (2009) to investigate the influence of slag-blended cement on the air-void structure. Using automated image analysis they found that increasing slag percentages resulted in a decrease of the total air volume in hardened concrete and consequently corruption of the air-void system. Generally, it should be noted that the easy, quick, and low-cost automated image analysis method in some cases may cause different air void content results in respect to actuality, reminding us that improvement of its accuracy is necessary.

3-6 SUMMARY

The literature reviewed narrates the influence of fly ash on the mechanical and chemical properties of concrete. It is seen that due to the new rules imposed by the government, the carbon content of fly ash has increased. The increase of the carbon content raises concern with regard to the continued usage of fly ash in concrete. The effect of carbon on the air-void network of concrete is discussed in the current chapter. Different available methods regarding to prediction

of the air-void characteristics are also described in this chapter. Finally, the advantages of using the image analysis technique to determine the air-void network are described. It is shown that the image analysis method is a reliable tool to measure the microstructure of concrete. In the next chapter, the experimental program is explained in details.

CHAPTER 4: EXPERIMENTAL PROGRAM

This chapter describes the details of the experimental program including material properties, concrete mixture designs and test procedures that were used in this study to investigate the air-void characteristic of concrete.

4-1 MIX DESIGN AND SPECIMEN PREPARATION

4-1-1 Material Properties

The chemical properties of Class F fly ash (from Lafarge), Genesee fly ash (Class F), Type GU cement, silica fume and limestone that were provided by the suppliers are listed in Table 4-1. The particle size distribution for fly ash and limestone is shown in Figure 4-1. It has to be clarified that in this study, only one batch of fly ash from the Genesee power plant was received and all samples in Series #3 were made from that particular batch.

Table 4-1 Chemical analysis of fly ash, cement, silica fume and limestone

Compound	SiO_2	Al_2O_3	Fe_2O_3	CaO	MgO	SO_3	Na_2O	K_2O	TiO_2	P_2O_5	LOI
Class F fly ash	55.53	23.24	3.62	10.9	1.22	0.24	2.83	0.76	0.68	0.1	0.54
Genesee fly ash	59.40	22.40	3.91	5.91	-	0.11	2.75	1.62	-	-	0.33
Type GU Cement	19.87	4.14	2.84	62.2	0.21	2.52	0.21	0.62	0.20	0.07	3.20
Silica fume	92.40	0.50	4.00	0.6	0.4	0.90	0.20	1.00	-	-	-
Limestone	1.36	0.10	0.20	50.96	2.60	-	0.11	0.40	-	-	-
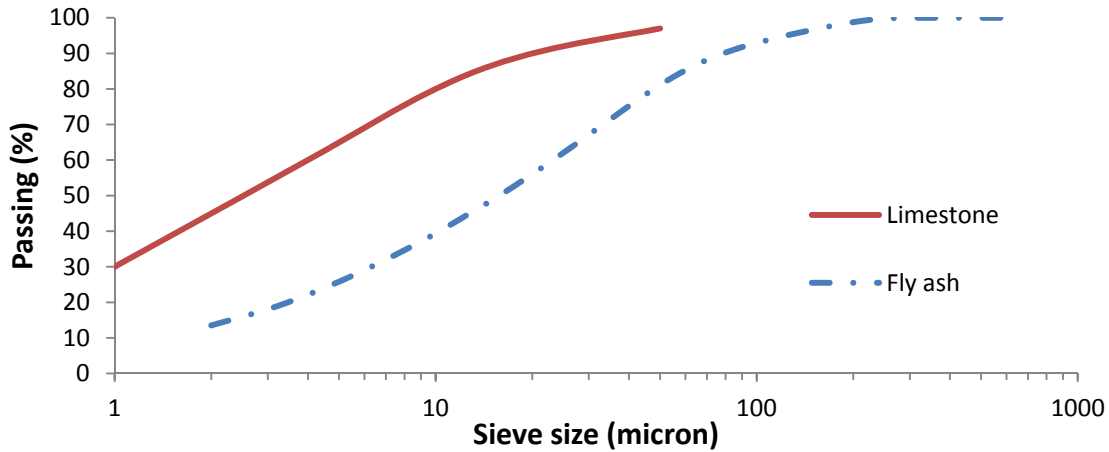
Fig. 4-1 Particle size distribution of Class F fly ash and limestone used in this study

A Powdered Activated Carbon (PAC) that is commonly used as the mercury adsorbent in thermal power plants was sourced locally for this study. The moisture content, Iodine number, apparent density, and the ash content of the PAC were presented by the manufacturer as 8%, 750 mg/g, 0.65 g/cc, and 15%, respectively. The particle size distribution of the PAC that was tested by the supplier is shown in Figure 4-2. Figure 4-3 shows images from a scanning electron microscope at two different magnifications that reveal the high specific surface area of the PAC. The specific surface area was specified by the supplier as 500 m^2/g. Another PAC, sourced from a different supplier, was used in the Genesee Plant during the production of fly ash and it showed similar properties (moisture content, apparent density and specific surface area) as the PAC used in this study. The moisture content, apparent density, specific surface area and particle size of the PAC used in the Genesee Plant were presented by the manufacturer as 12%, 0.5-0.7 g/cc, 500 m^2/g and 15-25 microns, respectively. It is worth restating that although these two powdered activated carbons are not identical, they show similar properties.
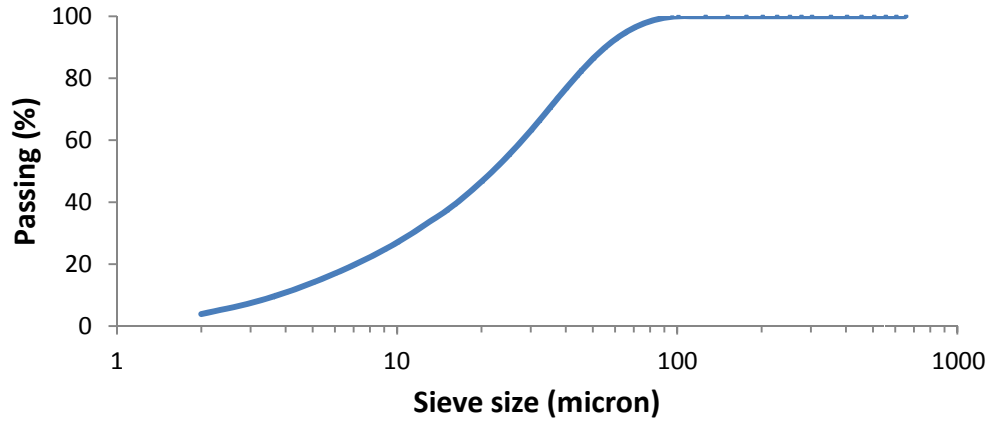
Fig. 4-2 Particle size distribution of powdered activated carbon used in

Series #1 and 2 of this study
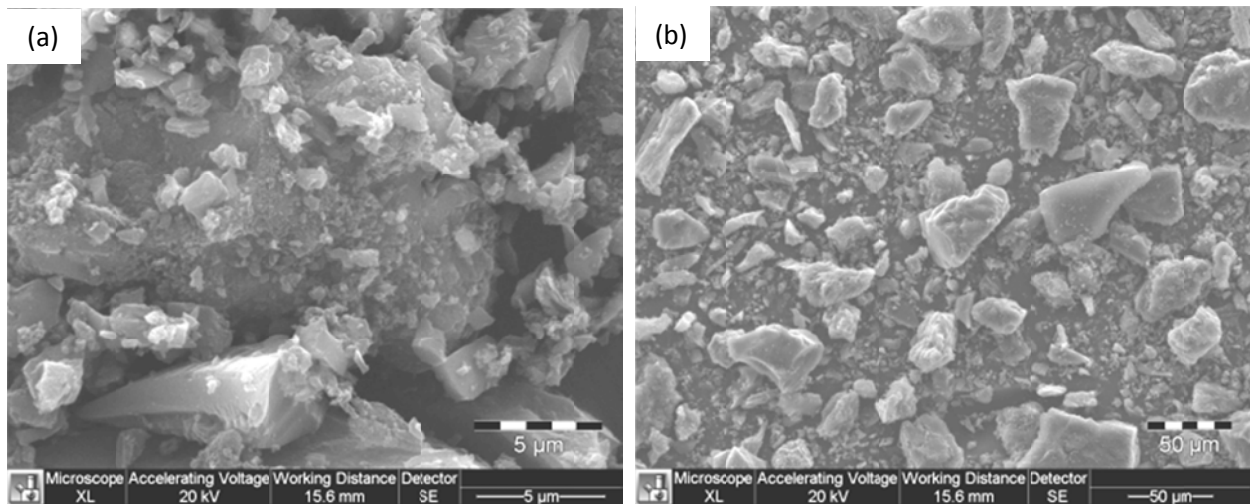
Fig. 4-3 SEM images of PAC used in Series #1 and 2 of this study at

a) magnification = 12,000 X; b) magnification = 800 X

The fine and coarse aggregate were siliceous, angular and of normal weight. Their respective particle size distribution is shown in Figure 4-4. The water absorption of the fine and coarse aggregate was measured as 1.0% and 1.2%, respectively. The relative density of aggregates was measured as 2.65 per ASTM C128 (2007).
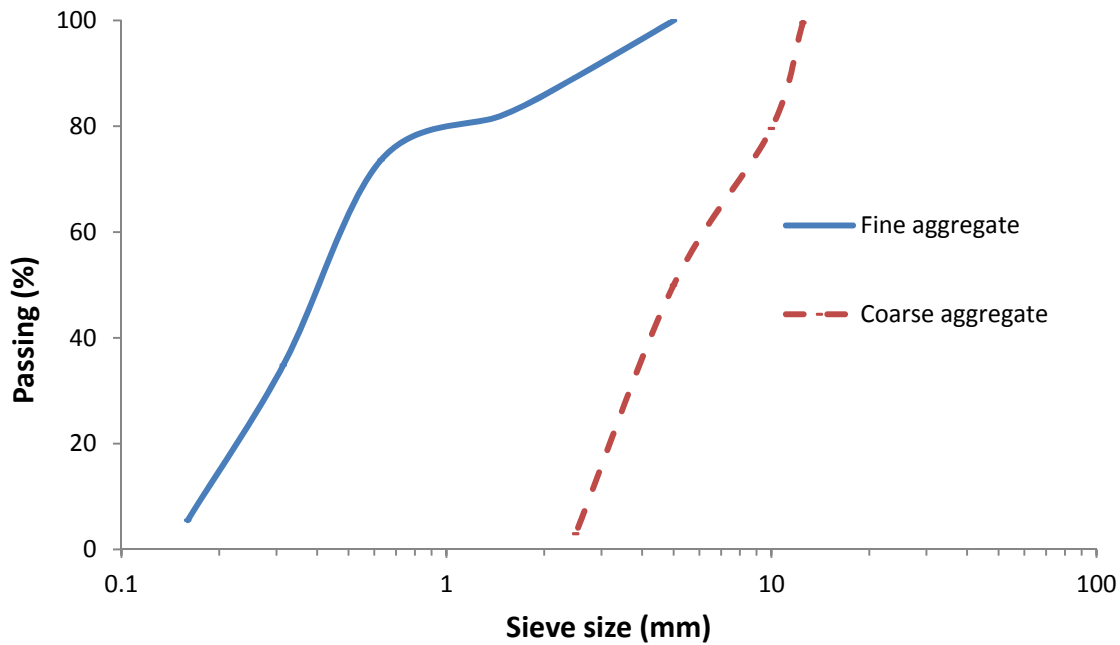
Fig. 4-4 Sieve analysis of the aggregates

4-1-2 Mix Proportions

The concrete mixture designs have been divided into three series that are explained in the following paragraphs. In the first series, Series #1, nineteen mixes were cast according to the mix compositions shown in Table 4-2 using Type GU Portland cement and Class F fly ash. Aside from the reference mix (0F0P: i.e. 0% fly ash and 0% PAC) containing no fly ash, the remaining 18 mixes included fly ash at 10%, 20%, and 30% replacement of cement by weight. In all mixes, the water to binder (cement plus fly ash) ratio was kept constant at 0.5 and 900, 900, and 185 kg/m^3 of fine aggregate, coarse aggregate, and water were used, respectively. In practice, PAC is injected into the flue gases in the range of 0-15 lb/MMacf (Nelson et al. 2004, Dombrowski 2007, Lockert et al. 2005) which is equivalent to 0-5% of PAC by weight in the fly ash.

Therefore, in this research program, PAC was introduced at 0, 1, 2, 3, 4, 5 and 10 % of fly ash by weight for Series #1 and 2 where Portland cement was partially replaced with fly ash. The Genesee fly ash in Series #3 included PAC as described below. Noting that PAC may physically adsorb other admixtures and cause changes to the properties of concrete, in Series #1 no superplastisizer or air entraining admixture was used so that the results would reflect the effect of PAC alone on the fresh and hardened properties. The mix designation is explained as follows: For example, mix 10F4P refers to the mixture that had 10% fly ash by weight of binder, and further, the fly ash contained PAC at 4% by weight.

In the second series, Series #2, four mixes were cast. The quantity of fly ash was kept constant at 20% replacement of cement by weight. The water to binder (cement plus fly ash) ratio was kept constant at 0.5. The fine aggregate, coarse aggregate, and water content were used at 900, 900, and 185 kg/m^3, respectively. PAC at 0, 2, 5 and 10% was added to mixes containing the air-entraining admixture (AEA) to determine the effect of PAC on air-entrained concrete. The cementitious content and air-entraining admixture were kept constant at 370 kg/m^3 and 0.5% of the total binder weight, respectively. MB-AE 90 (BASF 2007), which meets the requirements of ASTM C 260 (2010), was used as the air-entraining admixture. The mixture design is shown in Table 4-3. The mix designation is explained as follows: For example, mix A20F5P refers to the mixture containing an air-entraining admixture as designated by the capital letter A. This mixture had 20% fly ash by weight of binder and PAC at 5% by weight of fly ash.

Table 4-2 Mix composition and proportions for Series #1

Number	ID	Cement (kg/m^3)	Fly ash (kg/m^3)	PAC (kg/m^3)
1	0F0P	370	0	0
2	10F0P	333	37	0
3	10F1P	333	37	0.37
4	10F2P	333	37	0.74
5	10F3P	333	37	1.11
6	10F4P	333	37	1.48
7	10F5P	333	37	1.85
8	20F0P	296	74	0
9	20F1P	296	74	0.74
10	20F2P	296	74	1.48
11	20F3P	296	74	2.22
12	20F4P	296	74	2.96
13	20F5P	296	74	3.7
14	30F0P	259	111	0
15	30F1P	259	111	1.11
16	30F2P	259	111	2.22
17	30F3P	259	111	3.33
18	30F4P	259	111	4.44
19	30F5P	259	111	5.55

Series #3 includes 9 mixes. In this series no added PAC was used. Instead, fly ash obtained from the Genesee Power Plant replaced the ordinary fly ash used in the previous series. The Genesee Plant injects PAC into the flue gas ahead of the electrostatic precipitator at 5-10 lb/MMacf. A linear fit to Figure 4-5 gave Equation 4-1. Subbituminous coal was chosen from Figure 4-5 for developing the equation as the Genesee power plant uses Subbituminous coal

(AAD Document Control 2006). Subbituminous coal is a type of coal that varies from black to brown and mostly formed by lignite. Bituminous coal is an organic sedimentary rock formed by Anthracite. It is worth stating that the Genesee power plant used subbituminous and as a result, it produced Class F fly ash.

$\tau\ (\%) = 0.273x\xi\ \ (lb/MMacf)$ Eq. 4-1

where, τ and ξ denote the PAC content in fly ash and PAC injection rate, respectively. In this equation, the PAC injection rate is in as the lb/MMacf, where it results in the percent of PAC content in fly ash.
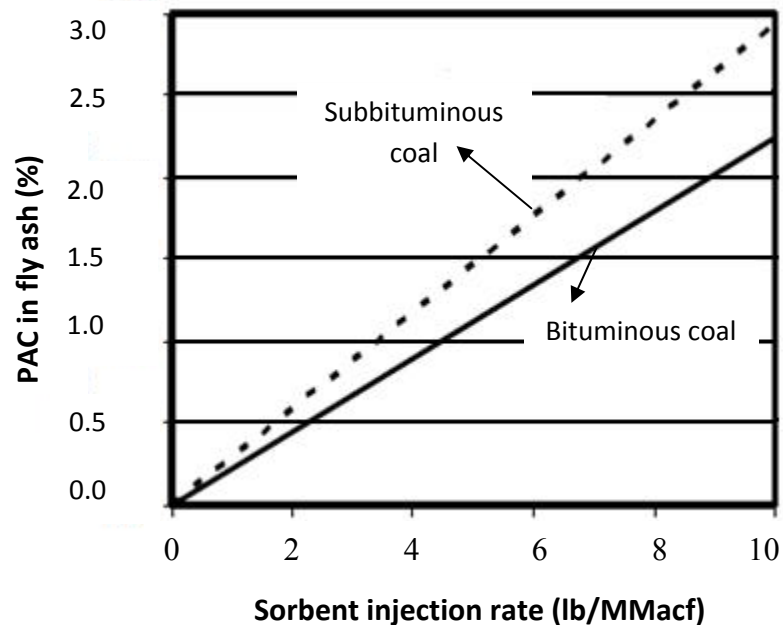
Fig. 4-5 Relationship between the PAC injection rate and percentage of PAC in concrete

(Lockert et al. 2005)

It is worth nothing that the lb/MMacf unit means pounds/million actual cubic foot and describes that the rate measured under actual conditions. One lb/MMacf is equivalent to 16.02

milligrams/cubic meter. As discussed, based on the volume of the flue gas, the required powdered activated carbon is injected in front of the gas precipitator. For instance, the PAC injection rate of 5 lb/MMacf shows that for each million cubic feet of flue gas, 5 pounds of PAC should be used. Inputting the injection rate at 5 and 10 lb/MMacf as the injection rate (AAD Document Control 2006) into this equation yields 1.4-2.7 percent of PAC in fly ash. In this study, the median of this range (2%) was assumed as the PAC content of the Genesee fly ash. The Genesee fly ash used in this study was sampled in 2009 where the injection rate was reported in 2006. However, it can be concluded that the injection rate has not changed over those years (Hoffmann and Brown 2003, CCME 2008). It is worth restating that throughout this study, the PAC content of the Genesee fly ash was assumed to be 2% as there is no available technique or equipment to measure the actual PAC content of fly ash. This assumption was the best approximate which could be made when there was no alternative way to determine the PAC content of the Genesee fly ash.

Table 4-3 Mix composition and proportions for Series #2

Number	ID	Cement (kg/m^3)	Fly ash (kg/m^3)	PAC (kg/m^3)	AEA (kg/m^3)
1	A20F0P	296	74	0	1.85
2	A20F2P	296	74	1.48	1.85
3	A20F5P	296	74	3.70	1.85
4	A20F10P	296	74	7.40	1.85

Recall that the total PAC content inclusion in the concrete containing high volume Genesee fly ash (A50F-G, A60F-G, A70F-G and A80F-G) is higher than those mixes containing 2% or 5% PAC (A20F2P and A20F5P). Series #3 was designed to examine the effect of the fly

43

ash containing carbon on the air void parameters of concrete and to compare these results to the previous series in which PAC was added during the casting of concrete. In Series #3 mixes, the water to binder (cement plus fly ash) ratio was kept constant at 0.5. The amount of fine aggregate, coarse aggregate and water per cubic meter of concrete was 900 kg/m^3, 900 kg/m^3, and 185 kg/m^3, respectively. No superplastisizer was used in the mixes. In the third series, the cementitious content and air-entraining admixture were kept constant at 370 kg/m^3 and 0.5% of the total binder weight, respectively. MB-AE 90 (BASF 2007) and Type GU Portland cement were used as the air-entraining admixture and cement, respectively. In this series, high volume fly ash concrete was also cast. Genesee fly ash replaced up to 80% of the cement weight. It should be noted that making concrete with a high volume of fly ash poses difficulties in industrial practice since the initial and final set times increase substantially (Bentz and Ferraris 2010). Silica fume and limestone were added to the mixes at 5% of the binder (cement+fly ash) content for those mixes with 70 and 80% of fly ash by weight of concrete to compensate this delay. The mixture design of Series #3 is shown in Table 4-4. The mix designation is explained as follows: For example, mix A10F-G refers to the mixture which had 10% Genesee fly ash by weight of binder. The capital letters G and A stand for Genesee fly ash and AEA, respectively. Mixes A70F-G and A80F-G containing silica fume and limestone also follow the same designation as others.

4-1-3 Specimen Preparation

For each designated mix, twelve cylinders of dimension 100 x 200 mm and twelve cylinders of dimension 75 x 150 mm were cast. The larger specimens were used to determine

the compressive strength of concrete after 7, 14, 28 and 60 days while the smaller specimens were used to determine the volume of permeable voids in hardened concrete in accordance with ASTM C642 (2006) at the same age as the compression tests. All specimens were cured in a controlled temperature (25±2 °C) and humidity (95% ± 5% RH) room before the tests.

Table 4-4 Mix composition and proportions for Series #3

Number	ID	Cement (kg/m^3)	Fly ash (kg/m^3)	PAC inclusion* (kg/m^3)	AEA (kg/m^3)	Silica fume (kg/m^3)	Limestone (kg/m^3)
1	A0F-G	370	0	0	1.85	0.0	0.0
2	A10F-G	333	37	0.74	1.85	0.0	0.0
3	A20F-G	296	74	1.48	1.85	0.0	0.0
4	A30F-G	259	111	2.22	1.85	0.0	0.0
5	A40F-G	222	148	2.96	1.85	0.0	0.0
6	A50F-G	185	185	3.7	1.85	0.0	0.0
7	A60F-G	148	222	4.44	1.85	0.0	0.0
8	A70F-G	111	259	5.18	1.85	18.5	18.5
9	A80F-G	74	296	5.92	1.85	18.5	18.5

* The equivalent PAC based on 2% by weight of fly ash assumption for Genesee ash

4-2 TEST PROCEDURE

In this section the details of the tests that were performed in this investigation are described. These tests include the foam index test, measurement of air void content in the fresh

concrete, fresh density, compressive strength, fresh density, absorption, voids in hardened concrete, and image analysis to evaluate the air void parameters.

4-2-1 Foam Index Test

The foam index test is considered the most common test used for determining if a particular fly ash can be employed as a concrete additive (Kulaots et al. 2003). The test is widely used because it can be performed with simple equipment and simple training of technicians. The purpose of the foam index test is to determine the relative levels of AEA needed for concrete containing fly ash and other materials that affect air entrainment in concrete (GRACE 2002). Generally, if a higher dosage of admixture is needed for getting a stable condition at the endpoint of the foam index test, it means that the fly ash will have poor performance in the field (Kulaots et al. 2003). Unfortunately, different AEAs can give different values of foam index, which makes it difficult to develop a truly standard test. Also, since it has not been recognized as a standard test, it is carried out in different ways by different research groups. Therefore, it cannot be used as a reliable test in the concrete area. Nonetheless, in general, this test is performed to allow industrial companies to compare their products.

The test method used in this study is described in the following lines (GRACE 2002):

1. Twenty grams of fly ash are placed in a bowl.

2. In the next step, 50 mL of water is added to the bowl, then it is capped and mixed. Mixing continues for 1 minute. Here, a 250-watt one blade mixer is used to mix the contents.

3. AEA solution is added in small increments of 5 drops at a time. Each drop equals to 0.05 ml. After each addition, the contents are vigorously mixed for 15 seconds. The stability of the foam is observed.

4. Until the foam remains stable on the surface for at least 45 seconds, the step 3 is repeated. This step is subjective and depends on the judgment of the technician. The volume of AEA in which the foam is judged stable is quantified as the foam index.

By repeating the test and gaining more experience, more reliable results can be achieved. All foam index tests were replicated at least twice, and the reported values are the averages of the two results. The foam index test setup and bubbles created on the surface of the mix are shown in Figures 4-6a and 4-6b, respectively.
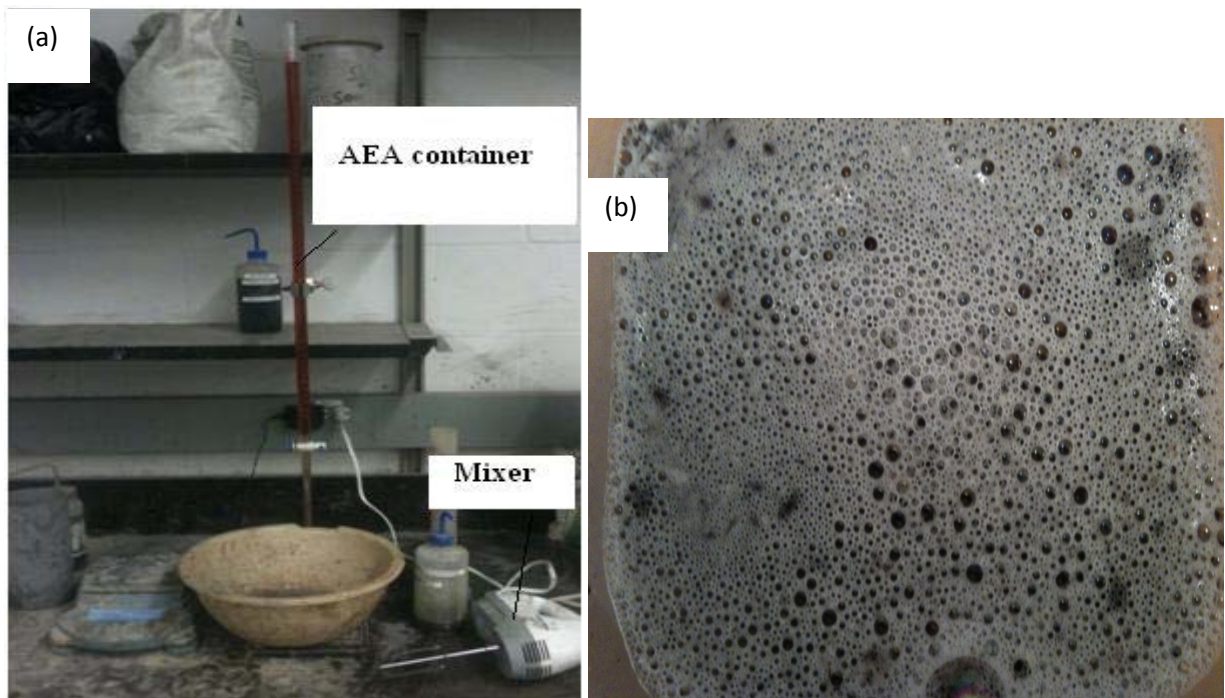
Fig. 4-6 a) Foam index test setup; b) stable foam

The foam index test was performed for the fly ash used in this study. In addition to the plain fly ash, the foam index test was also performed for fly ash with two different percentages (2.5% and 5%) of PAC.

4-2-2 Fresh Air Void Content and Fresh Density

The air void content of fresh concrete was obtained in accordance with ASTM C231 (2009) which addresses the pressure method. For each mix, the air void content was obtained three times. The density of fresh concrete was also measured by implementing the same container used for the air-content test. The volume of the container was 7 liters. The density of fresh concrete was determined by dividing the weight of concrete by its volume. The fresh density was measured three times for each mix.

4-2-3 Compressive Strength

The compression tests were performed in accordance with ASTM C39 (2010) to investigate compressive strength under quasi-static loading using the Forney machine (FX-700) with the capacity of 3600 kN available at the concrete materials laboratory of the University of Alberta. The compressive strength test was performed at four different ages to monitor the strength gain trend versus time. The test arrangement is shown in Figure 4-7. The loading rate was kept constant for all samples at 2 MPa/s. Three specimens were tested for each mix design and the average of the three results was used in later discussions.

Fig. 4-7 Compressive strength test machine

4-2-4 Density, Absorption, and Voids in Hardened Concrete (ASTM C642)

For measuring the voids and absorption of the hardened concrete samples, the ASTM C642 (2006) standard test method was used. A balance, water bath, and container suitable for immersing the specimen are needed for performing the test. Figure 4-8 shows the equipment required for this test.

Fig. 4-8 Equipments for the ASTM C642 standard test

This paragraph explains the steps of the test procedure. After the cylindrical 75mm x 150mm samples were cured in the curing room for the required time (for each mix, three different ages were chosen for the ASTM C642 test), three samples were removed from the curing room and put into an oven at 100° C for 24 hours. The dried samples were taken from the oven and put on the cabinet to cool for about 30 minutes. The samples were then weighed (M_a) using a balance with an accuracy within 0.01 grams. The samples were submerged in the water tank for 24 hours. It should be noted that if warm samples were put in the tank, they might crack, so they were allowed to cool first for 4 hours. After 24 hours, the samples were removed from the water tank and their surface was dried with a paper towel to obtain a saturated surface dry (SSD) condition. The weight (M_b) of the SSD samples was measured. In the next step, the samples were put into a water bath with boiling water for 5 hours. The total time that the samples were in the water bath was about six and half hours, including 90 minutes for heating up the

water (inside the water bath) and five hours for warming the samples in the boiling water. The samples were removed from the boiling water and left in the laboratory environment (on the cabinet) for 12 hours. The weight of the samples was measured (M_c). On the same day, the apparent weight of each sample (M_d) was measured by immersing the samples in the water using a basket that had been installed to the balance with a rod. Using the measured weights (M_a to M_d) and the equations from the ASTM C642 standard test method (2006), the absorption after immersion, the absorption after immersion and boiling, the bulk density, the bulk density after immersion, the bulk density after immersion and boiling, the apparent density, and the volume of permeable voids can be calculated. Following equations were used for measuring these parameters.

$$\text{Absorption after immersion} = \frac{M_b - M_a}{M_a} \times 100 \qquad \text{Eq. 4-2}$$

$$\text{Absroption after immersion and boiling} = \frac{M_c - M_a}{M_a} \times 100 \qquad \text{Eq. 4-3}$$

$$\text{Bulk density} = \frac{M_a}{M_c - M_d} \rho = g_1 \qquad \text{Eq. 4-4}$$

$$\text{Bulk density after immersion} = \frac{M_b}{M_c - M_d} \rho \qquad \text{Eq. 4-5}$$

$$\text{Bulk density after immersion and boilng} = \frac{M_c}{M_c - M_d} \rho \qquad \text{Eq. 4-6}$$

$$\text{Apparent density} = \frac{M_a}{M_a - M_d} \rho = g_2 \qquad \text{Eq. 4-7}$$

$$\text{Volume of permeable voids} = \frac{g_2 - g_1}{g_2} \times 100 \qquad \text{Eq. 4-8}$$

where:

M_a = mass of oven-dried sample in air, g

M_b = mass of surface-dry sample in air after immersion, g

M_c = mass of surface-dry sample in air after immersion and boiling, g

M_d = apparent mass of sample in water after immersion and boiling, g

g_1 = bulk density, dry (Mg/m^3) and

g_2 = apparent density (Mg/m^3)

ρ= density of water (1Mg/m^3)

4-2-5 Image Analysis of Cementitious Materials

The image analysis technique requires several steps which are described in the following paragraphs. However, sample preparation is considered to be one of the most important tasks in the image analysis process. Any lack of stringency in this step may drastically affect the results of image analysis. Different sample preparation methods have been developed over the years. The most common sample preparation methods for the image analysis technique are summarized here:

Kunhanandan Nambiar and Ramamurthy (2007)

1- Polish the specimens to attain a surface on which the boundaries of the air voids and matrix are sharp and easily distinguishable

2- Place the specimens in the oven (50° C) until the surface moisture evaporates

3- Cover the specimens with black ink using a permanent marker

4- Spread white talc powder on the surface

5- Wipe away excess powder leaving only the powder worked into the air void

Zhang et al. (2005)

1- Saw the samples using a diamond blade

2- Polish the samples with silicon carbide and aluminum oxide abrasives with successive use of finer grits through the process

3- Paint surface black with a water-based washable paint and dry in oven (150° C) for five minutes

4- Fill surface voids with white zinc oxide paste by pressing the paste across the surface of the specimen

5- Place the specimen in a refrigerator for a period of 10 min to solidify the zinc oxide paste

6- Wipe off the excess solidified paste from the surface using a flat wood ruler and delicate task wipe

Pleau et al. (2001)

1- Use silicon carbide to polish the specimens

2- Fill void with white ink under vacuum in the vacuum chamber

3- Clean surfaces with an alcohol impregnated soft cloth so that the voids remain white and will return to its original condition.

Zalocha and Kasperkieiwicz (2005)

1- Cut, grind and polish the specimen with help of SiC polishing powders

2- Colour the surface with a blue water-resistant marker

3- Fill voids with zinc paste

4- Clean surplus paste using paraffin oil

In this study, the traditional resin epoxy-impregnated method (Sahu et al. 2004) and an inked method (Toumi and Resheidat 2010) were used to prepare the samples for the image analysis method. The common applications of the epoxy-impregnated method can be listed as study of microstructure of cement-based materials, evaluation of crack system and determining the water-cement ratio of the hardened concrete (Badger et al. 2001). The inked method is commonly used to evaluate the air-void characteristics of cement-based materials. The epoxy-impregnated method is explained first: After the concrete was cast, it was cured in a humid room for 60 days followed by curing in the laboratory environment for another 60 days. In the next step, a 20 mm thick disk was cut from each sample and a cube of 20 mm side was extracted from the disk using a diamond saw. The cube was put into an oven at 105° C for 24 hours. For damage protection of any voids inside the concrete during the subsequent grinding, a resin epoxy-impregnated process was carefully performed. Running a vacuum vessel device for 15 minutes, the epoxy resin that was made by mixing a resin (specific gravity of 1.04 and viscosity of 500 mPas) and a hardener penetrated to the whole cube body. After keeping the impregnated cube in the laboratory environment for another 24 hours, the specimens were polished with 600# silicon carbide with the wheel grinder. More polishing was performed with 50 and 10 micron aluminum powder on a glass plate. The sample preparation equipment and steps including concrete in a container containing epoxy, vacuum vessel, grinding with silicon carbide, polishing with aluminum powder and final prepared sample are shown in Figures 4-9a, 4-9b, 4-9c, 4-9d and 4-9e, respectively.
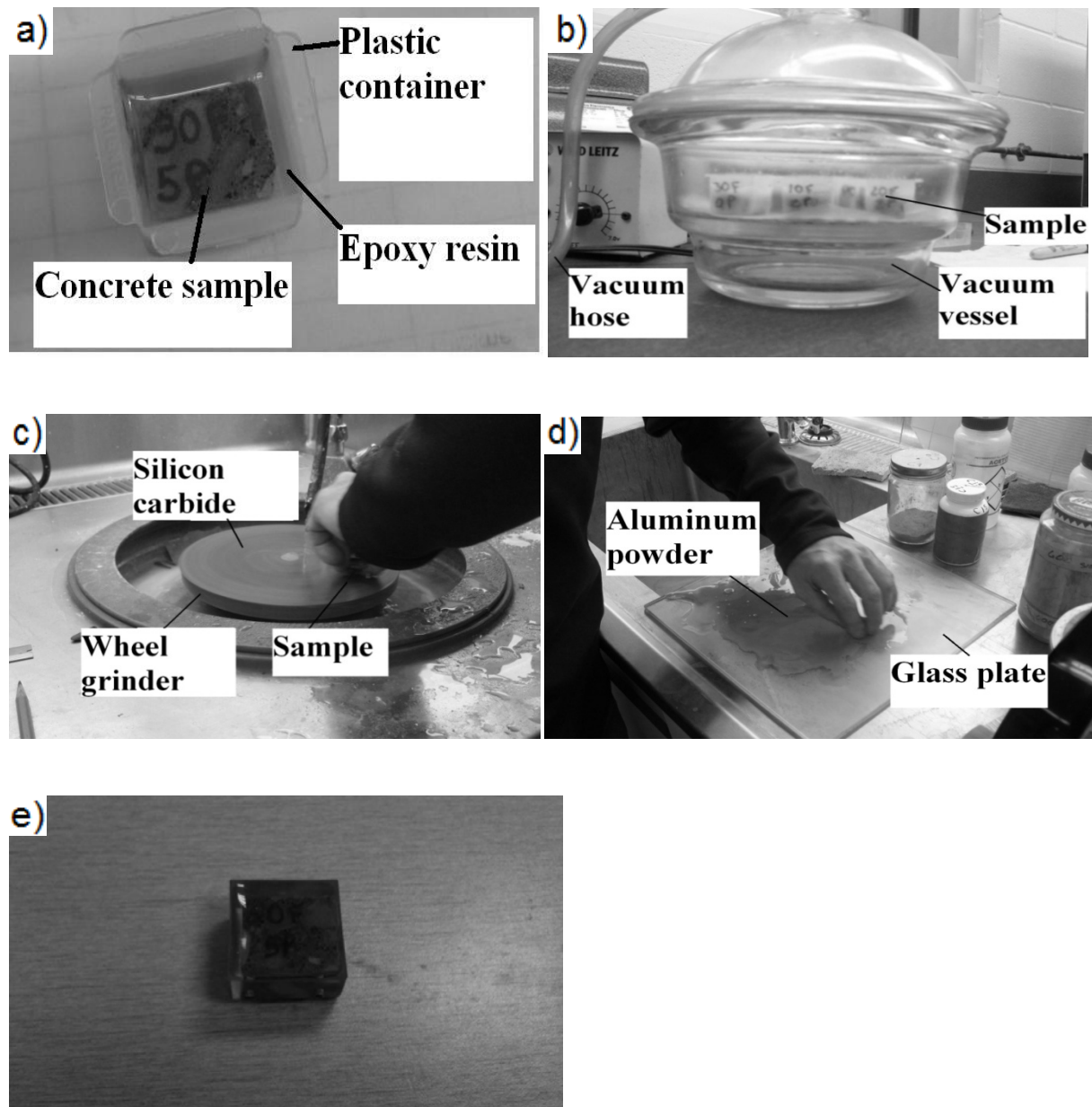
Fig. 4-9 Image analysis sample preparation a) concrete in a container containing epoxy; b) vacuum vessel; c) grinding with silicon carbide; d) polishing with aluminum powder; e) final prepared sample

In the inked preparation method, after the concrete was cast, it was cured in a humid room for 60 days followed by curing in the laboratory environment for another 60 days. In the next step, a 20 mm thick disk was cut from each 75mm-diameter sample and a cube of 20 mm

side was extracted from the disk using a diamond saw. The cube was put into an oven at 105° C for 24 hours. These steps are exactly the same as the epoxy-impregnated method. In the next step, instead of injecting epoxy inside the samples, the surface of the samples was covered with an oil-based black colour. This step could be done by either a thick permanent marker or a spray colour (Figure 4-10a). Then, the coloured samples were allowed to dry for 30 minutes. After 30 minutes, a zinc oxide cream was gently applied on the surface of the concrete by the pressure of a finger. The excess material was removed with a soft fabric. The white cream penetrated the holes and voids. Since the background of the surface was black, the white holes were easily distinguishable with an optical microscope. The samples prepared with inked method are shown in Figure 4-10b.
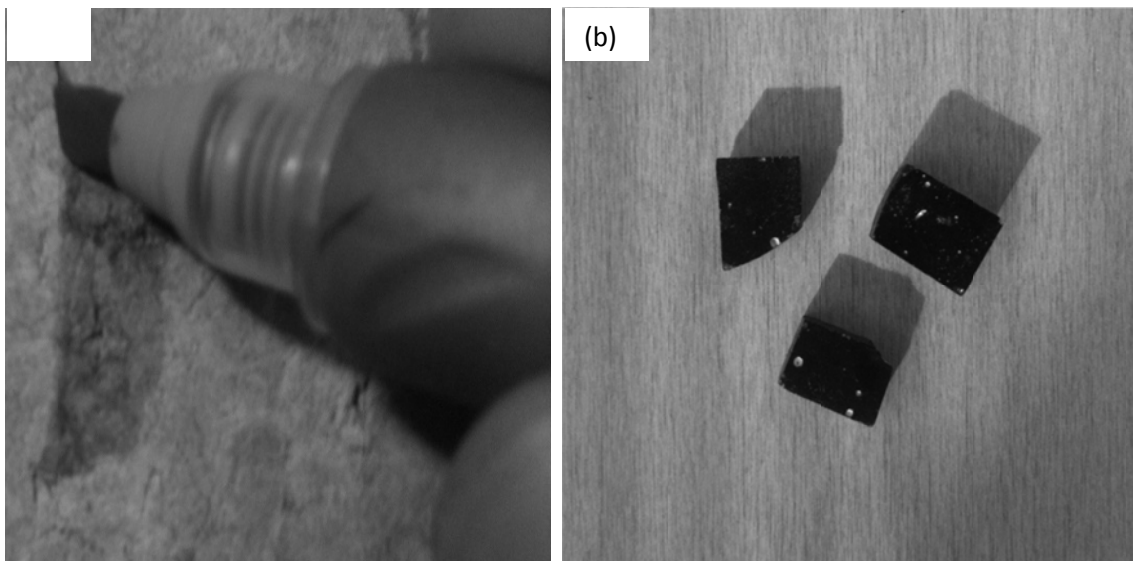
Fig. 4-10 a) Painting the surface of concrete; b) Samples prepared by inked method

In the following sentences, the precision of the both preparation samples are discussed. This author believes that the inked samples provide more reliable and accurate results compared to the epoxy ones based on the following discussions. First, in the epoxy-impregnated technique,

the penetration of epoxy through the whole samples has always been subject to question. It is impossible to be sure whether the epoxy penetrates through all voids inside a sample. Epoxy may not be able to completely penetrate to the impermeable and dense concrete. Secondly, the light colour of epoxy which is supposed to fill the voids makes it difficult to be distinguished by an image analysis software from the remaining parts of concrete which are mostly light gray. Meanwhile, one should be aware of errors which the ink-preparation technique may also bring. Covering the surface of a sample in this method may introduce errors. If a permanent marker is used, the edges of the marker put traces on the sample which disrupts the uniformity of the marked surface. If a spray colour is used, it may generate bubbles on the surface that may be mistakably considered as the air voids of concrete.

The advantages and disadvantages of these two sample preparation techniques have been subject to debates. Jana (2006) performed a comprehensive literature review on different sample preparation techniques. He investigated 20 sample preparation techniques including the epoxy-impregnated method. He concluded that in concrete containing fly ash, air bubbles cannot get impregnated with epoxy. Jana (2006) also concluded that the inked samples can be used for measuring the air-void characteristics of concrete using image analysis. He described a method to increase the contrast between the air void and the surrounding matrix where using this method leads to more accurate results. Several researchers (Robert and Scali 1987, Chatterjii and Gudmundsson 1977, Laurencot et al. 1992, Pade et al. 2002) also implemented the inked samples (white filling materials were used to highlight the air voids against the dark background of surrounding matrix) to evaluate the air-void characteristics where they were confident from the obtained results. Soroushian et al. (2003) showed that the epoxy-impregnated sample does not generally yield crisp boundaries and sharp contrast between air voids versus the body of

concrete. Attempts to improve upon this drawback were defeated. For instance, a technique was also suggested to improve the conventional epoxy impregnation technique using fluorescent and ethanol solution (Soroushian et al. 2003). Although this technique shows promising results, it involves time-consuming immersion of concrete specimens in fluorescent and ethanol solution for several days, and its application is limited to the research reported (Soroushian et al. 2003).

The size of sample whether it is obtained by the epoxy-impregnated method or inked method also plays an important role in the accuracy of the results. Smaller samples may be appropriate when the mortar or paste samples are subjected to test. However, when a concrete sample is tested, a larger cross section area is required since a significant portion of the cross section is occupied by aggregate. Jana (2006) showed that for examining the air-void characteristics of a concrete containing 19-25 mm nominal maximum size aggregate, a cross section area of at least 7700 mm^2 is needed. He also believed that a 27X47 mm section may be adequate for characterization of a cement sample. Chen et al. (2002) used a cylindrical sample with the diameter of 24 mm and height of 15 mm for measuring the microstructure of paste (not concrete) using an optical microscope. They also used a mortar (not concrete) sample of 20X20X15 mm to measure its microstructure. Thus, removing the coarse aggregate from the concrete sample is another task that can be considered to generate more accurate results. In the image analysis process higher number of phases makes it difficult for a person to distinguish them. By removing the coarse aggregates, the existing phases are narrowed down to two phases (cement paste and void) which makes the analysis easier and reliable (although voids at the interfacial transition zone may be eliminated by removing the aggregates which may affect the reliability).

For both epoxy-impregnated and inked samples, a Nikon DXM1200 digital microscopy camera was used to capture coloured digital images with the magnifications of X60 and X100. A magnification in the range of 50 to 100 is the most accepted magnification in the field of concrete air void investigation through the optical microscope (Schutter 2002). A higher magnification causes a loss of the larger voids while a lower one leads to missing smaller pores. The digital microscopy camera used is designed for photography through the microscope. This system provides high quality photo-realistic RGB digital imaging at a resolution of up to 12 million pixels with low noise, and high sensitivity compared to other types of digital microscopy camera as per the manufacturer. Images were captured by the microscope at 3840 x 3072 pixels. Figure 4-11 shows the microscope used in this study.

Fig. 4-11 The optical microscope used in this study

(Nikon Microscopy as of September 15th 2011)

Images of the inked and epoxy prepared samples for mix A20F0P captured by the microscope are shown in Figures 4-12a and 4-12b, respectively. It should be noted that the

captured images did not include any scale. Scales were manually defined for each image using the calibrated ruler provided by the manufacturer. Scale bars were added to the bottom right hand corner of all images. Figure 4-13 shows the calibrated ruler used for setting the scale of the images.
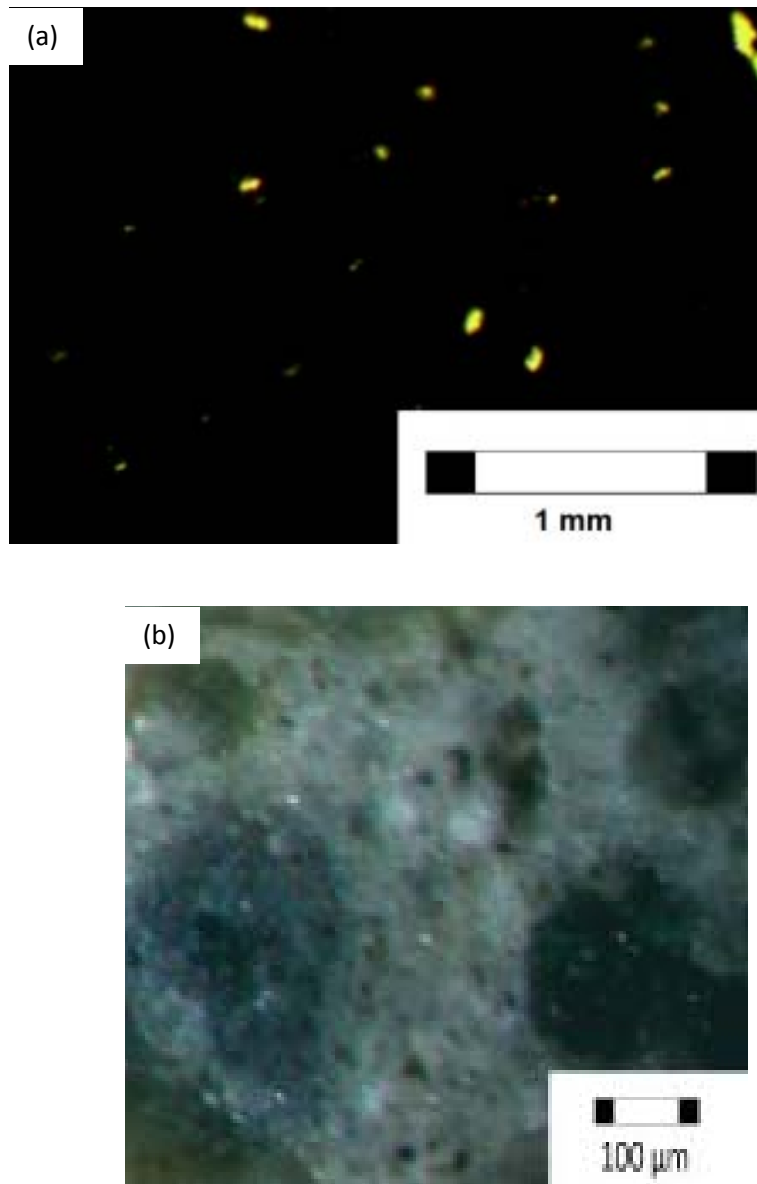
Fig. 4-12 Optical images of A20F0P samples prepared by the

a) inked; b) epoxy- impregnated method
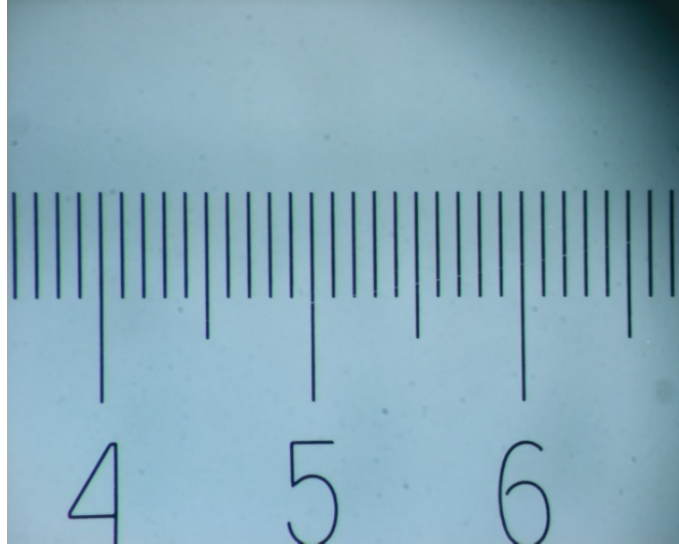
Fig. 4-13 Calibrated ruler used for setting image scale

Recommended (Nemati 2009) ImageJ open source software (Image Processing and Analysis in Java as of September 15th 2011) was employed due to its ease of access, ease of use and accurate analysis. The ImageJ software works in the Java environment. Figure 4-14 shows the interface of the software.

The first step in the image analysis process includes changing the digital image from the RGB format to the 8 bit, 256 gray scale format as the software can only analyze the gray scale photos. Figure 4-15 shows the typical gray scale format of photos taken at two different magnifications. A sample histogram obtained for specimen 20F0P is shown in Figure 4-16. The minimum, maximum, and mean gray scale values of 11.7 million pixels are 0, 255 and 133, respectively.
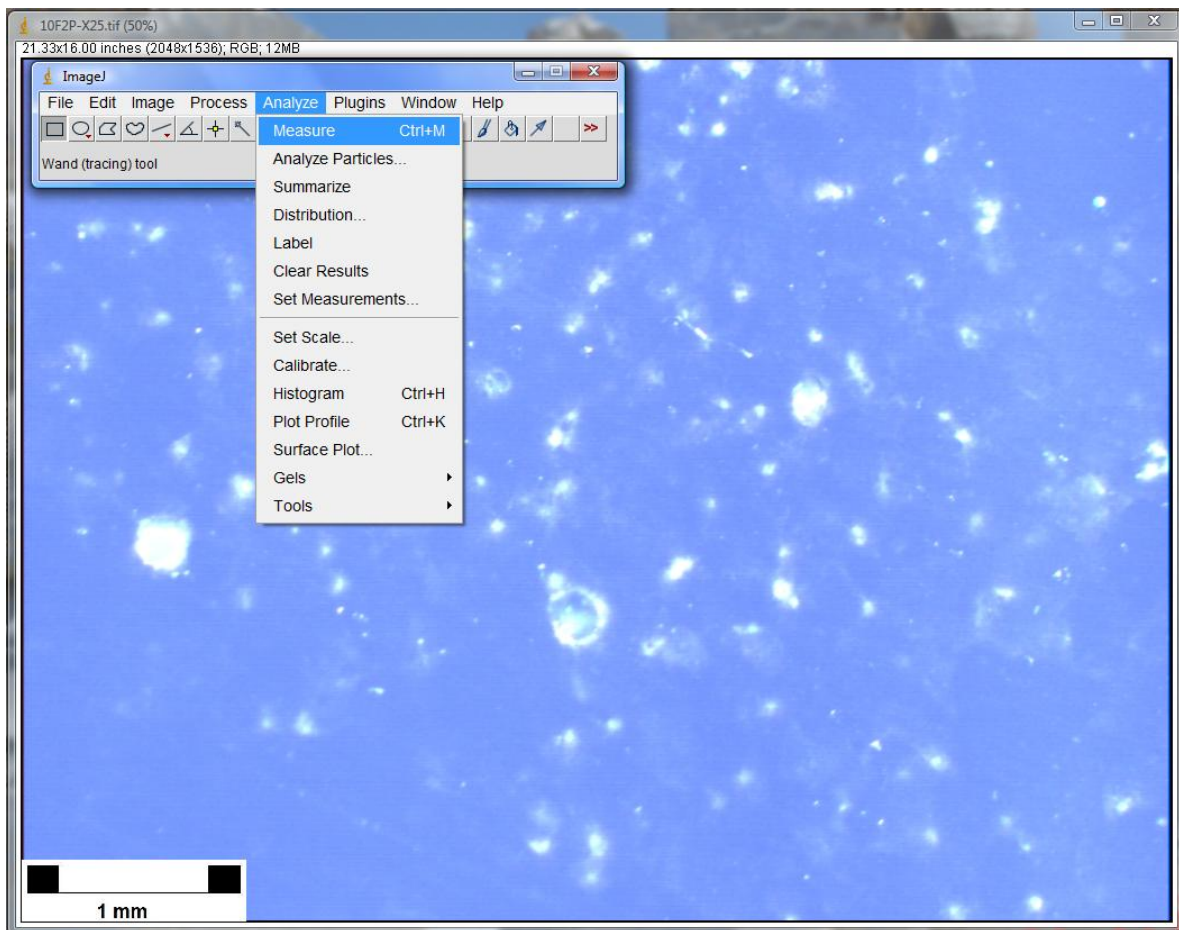
Fig. 4-14 Interface of ImageJ software
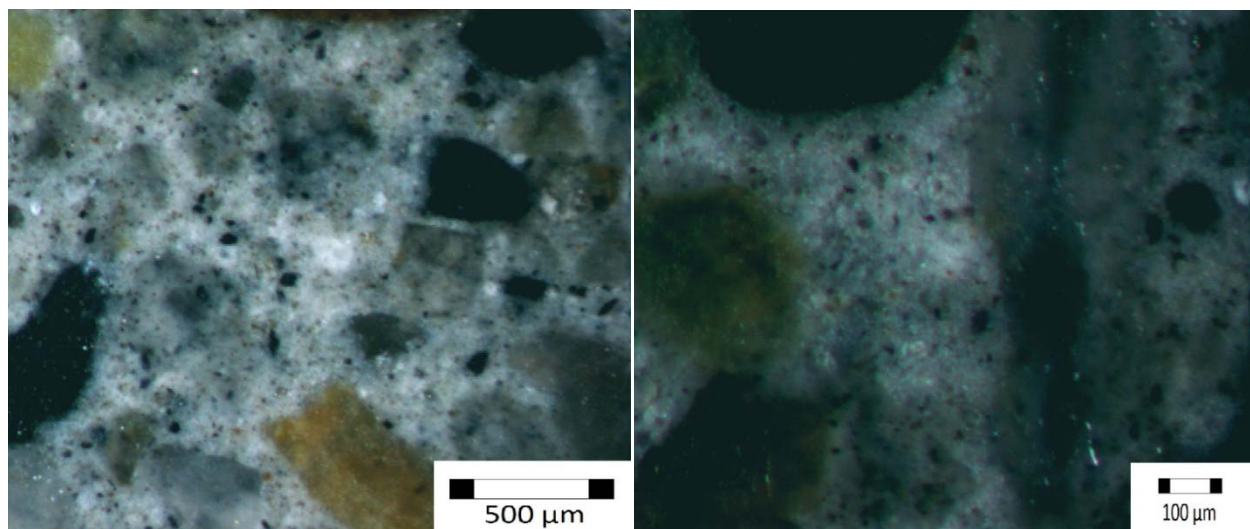
Fig. 4-15 Optical images at two different magnifications
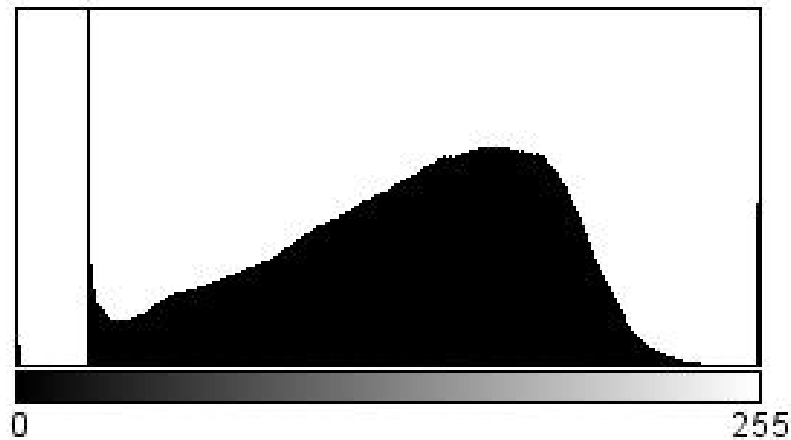
Fig. 4-16 Gray scale value distribution

After the scale of the photo was set, a threshold value of the gray scale was assigned to distinguish voids from aggregate and paste. Defining the threshold value is the most complicated and important part of the image analysis technique. There are several methods to calculate the threshold value automatically including Otsu, Yen, Moments, and Triangle (Kwon 2004). However, none of these methods accurately estimates the threshold value for the samples since three phases (matrix, aggregate, void) exist in each image. A trial and error method was applied to find the best threshold value by comparing the size of some voids in the original and the adjusted image. Using a drawing tool provided by the software, an area approximately 3000x2500 pixels was electronically drawn on the image as the zone of interest. This area was selected in the most homogeneous part of the surface. Using the ImageJ software, the histogram and particle properties (including area and diameter) of the zone of interest were obtained. These measurements were automatically done using tools provided by the software. ImageJ can calculate and displays a grey level histogram of an image defined by the region of interest. To calculate/display the histogram, the Analyze/Histogram tab was selected. In the histogram window the x-axis represents the gray values and the y-axis shows the number of pixels found

for each gray value. The total pixel count, the mean, standard deviation were also calculated using the same tool. The properties of particles were also determined using the Analyze/Analyze particle tab.

By putting size distribution data into the following equations (Powers 1949), the most important characteristics of the air void in concrete were calculated. The spacing factor equations were provided by Powers (1949).

$$A = \frac{V_h}{V} \times 100$$
Eq. 4-9

$$\alpha = \frac{16}{\pi} \times \frac{\sum n_i \times d_i}{\sum n_i \times d_i^2}$$
Eq. 4-10

where, n_i denotes the number of voids with a particular void diameter, d_i and A, V, V_h α are the air void content, volume of selected zone, volume of air voids and specific surface area, respectively.

$$L = \frac{3}{\alpha} \times [1.4 \times (\frac{P}{A} + 1)^{0.33} - 1] \quad \text{if } \frac{P}{A} \geq 4.33$$
Eq. 4-11

$$L = \frac{P}{\alpha A} \qquad \qquad \text{if } \frac{P}{A} < 4.33$$
Eq. 4-12

$$SHF = \frac{4\pi\psi}{(\chi)^2}$$
Eq. 4-13

where, P represents the volume of paste in the composite and A, ψ, χ, L and SHF are the air void content, area and perimeter of voids, spacing factor and shape factor, respectively. Based on the binder and water content, the volume of paste for all mixes was considered as 0.3. It should

be noted that the shape factor for a circle equals one, becoming larger or smaller for other shapes. The closer the shape factor to unity the more accurate are the results of image analysis (Kunhanandan Nambiar and Ramamurthy 2007).

4-3 SUMMARY

In the current chapter, the experimental program including material properties, mix proportions, specimen preparation and test procedures (for the foam index test, air content and density of fresh concrete, compressive strength, ASTM C642 and image analysis method) were explained. In the next chapter, the results of the experiments are presented, analyzed and elaborately discussed.

CHAPTER 5- RESULTS AND DISCUSSION

In this chapter the results of the tests which have been described in Chapter 4 are shown. The results of Series 1, 2 and 3 are explained separately in Sections 5-1, 5-2 and 5-3, respectively. The comparison between the results of these series is discussed in Section 5-4.

Before presenting the results of each series, the results of the foam index test are first discussed. The results show that the foam index of 20-grams fly ash (Class F) with 0, 2.5 and 5% PAC are 49, 41 and 30 ml, respectively. However, previous research by Kulaots et al. (2003) shows that the foam index values for 20-gram fly ash samples could vary from 3 ml to 36 ml, which is lower compared to the results of this study. The lower numbers from Kulaots et al. (2003) can be attributed to the lack of additional carbon (PAC or other types) added to fly ash. As a result, stable foams were more easily created compared to fly ash containing PAC. A decrease in the foam index with an increase in the PAC content is against other results described in this chapter later. As mentioned earlier, this test method is highly dependent on the operator (Zhang and Nelson 2007). The results are inconclusive since one expects the foam index to increase with the addition of PAC. One may blame the low accuracy of the foam index test (due to the visual concept of the test which makes it an operator based test) for the unexpected results. It is worth emphasizing that the results of the foam index is highly dependent to the operator, therefore, one operator may report different foam indexes when performing the foam index test for the same materials and conditions at different times. Also, the foam index results of Genesee fly ash showed the range of 4-6 drops which varied depending on the samples of fly ash taken over 7 months (AMEC 2010). Each month, the power plant tested its fly ash and reported the foam index results. As explained in Chapter 4, in Section 4-1-2, PAC was introduced to the flue gas at the Genesee power plant at a dosage assumed as 2% by weight of fly ash to reduce

mercury emissions. In this investigation because the actual concrete was cast and its air-void structure was measured both directly (using image analysis) and indirectly (via the ASTM C642 standard test method), the results of the foam index tests were not estimated any further.

5-1 RESULTS OF SERIES #1

In this section the fresh and hardened properties of Series #1 which include the compressive strength, density, absorption, air void content, spacing factor, specific surface area and shape factor are described. All individual results are listed in Appendix #1 while the average data is reported in the main text.

5-1-1 Properties of Fresh Concrete

The air void content of fresh concrete is shown in Figure 5-1 with each data point representing the average of three samples. The air void content and the coefficient of variation (C.O.V.) were in the range of 1.3% to 3.3% and 0.0% to 20.4%, respectively. This range is typical of normal concrete not containing any air entraining admixture (Mohammed and Fang 2011). From looking at Figure 5-1, a decrease in the air void content of the fresh mix was generally observed with an increase in the fly ash content. However, in the absence of any AEA, different percentages of PAC contained in the fly ash did not reveal any perceptible influence on the fresh air void content. Such low air void content of concrete containing no AEA was also reported by Lomboy and Wang (2009) where the total air void content of concrete varied in the range of 0.2-2.4%.
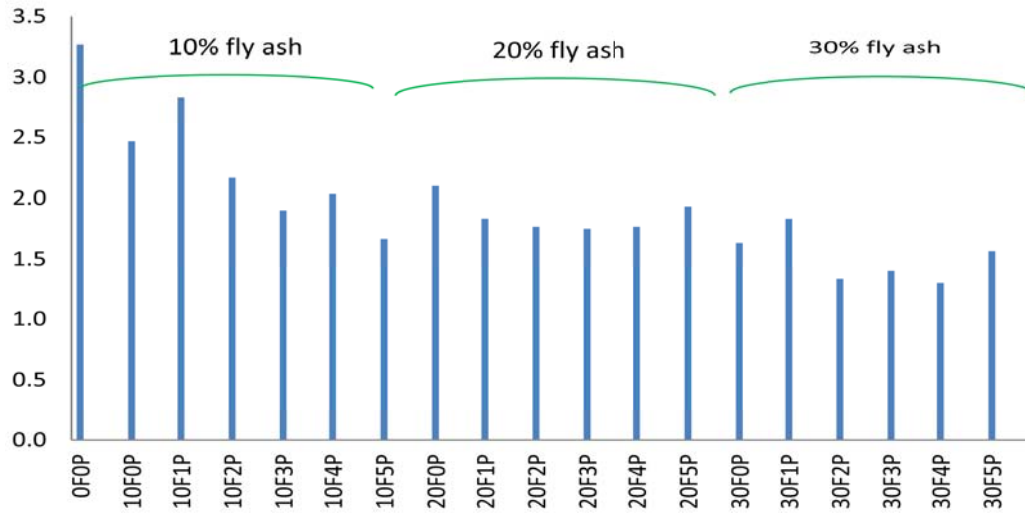
Fig. 5-1 Fresh air void content of Series #1

The fresh concrete density was obtained for all 19 mixes by taking the average of three observations. The variation in the density of the mixes is shown in Figure 5-2. The mixes were designed to reach a target density of 2350 kg/m^3, and it is clear that there was no significant difference between the densities as the volume percentages of fly ash and PAC changed. Zain et al. (1999) showed that the density of concrete (W/C=0.35 and 0.5) containing 10% fly ash varies in the range of 2362-2365 kg/m^3 which is very close to the fresh density of concrete obtained in this study. The C.O.V. of the fresh density also varied from 0.0 % to 0.9 %.
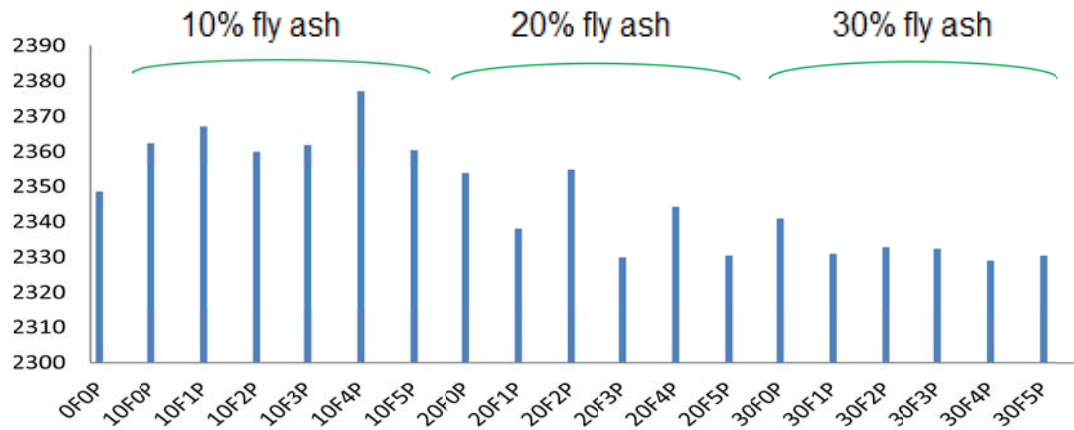
Fig. 5-2 Density of fresh concrete

5-1-2 Compressive Strength

The compressive strength developments for the mixes containing 10%, 20% and 30% fly ash are shown in Figures 5-3a, 5-3b and 5-3c, respectively. The C.O.V. of the compressive strength at 7, 28 and 60 days varies from 1.3% to 8.5%, 0.5% to 8.2% and 2.8% to 14.6%, respectively. As expected, the strength increases with age. A higher volume of fly ash resulted in a lower compressive strength at the earlier ages. Similar reduction of the compressive strength at early ages with an increase in the fly ash percentages was concluded by Pala et al. (2007). A higher content of PAC led to a perceptible decrease in the compressive strength of higher fly ash volume percentages (30%). An increase in the age of the concrete (containing fly ash and PAC) led to an increase in the compressive strength at rates that are typical for conventional concrete. For example, the compressive strength of mix 30F4P (30% fly ash and 4% PAC) at 60 days was more than two times its strength at seven days. Also, the amount of PAC had no significant effect on the compressive strength of concrete for lower quantities of fly ash (10% and 20%). Although other researchers noticed deterioration in the compressive strength due to the presence

69

of unburnt carbon (Lomboy and Wang 2009), the present study shows that adding up to 5% powdered activated carbon may influence the compressive strength only for the series containing the highest fly ash substitution, in this case, 30% by weight of cement. This discrepancy came from the fact that the properties of PAC and unburnt carbon are different (they can be classified as two distinct materials regarding their physical distinctions). According to Hsieh and Tsai (2003), unburnt carbon consists of 73-91% carbon, 2.5-11.5% volatile content, 0.7-1.9% water content and 5-19% ash content. They also showed that the size, specific surface area and pore size of unburnt carbon particles are 1-100 microns, 16-33 m^2/g and 0.02-10 microns, respectively. Its apparent density was also reported as 0.15 g/cm^3 (Hsieh and Tsai, 2003). The properties (specific surface and pore size distribution) of PAC used in this study are shown in Section 4-1-1, showing different physical characteristics compared to unburnt carbon explained earlier in this paragraph. In addition, a higher percentage of PAC does not proportionally lead to a higher unburnt carbon content. Therefore, one may accept that the effect of unburnt carbon and PAC on the compressive strength of concrete can be different. This is seen clearly in Figure 5-4, where at 28 days a higher dosage of PAC led to a lower strength, but only in the mixes with a higher content of fly ash. The same conclusion was reported by Lockert et al. (2005). Their results showed that the addition of a brominated powdered activated carbon at either 1 % or 3 % had no significant effect on the 7 day, 14 day, or 28 day compressive strength of concrete containing up to 20% fly ash. This type of PAC offers exceptional performance as a mercury sorbent while at the same time having a minimal effect on AEA (Lockert et al. 2005). Typical properties of this brominated powered activated carbon were reported as the following values: moisture= 8%, Iodine number> 500 mg/g, tapped bulk density= 35 lbs/ft^3 and bromine=7% (Albermarle as of 25th April 2011).
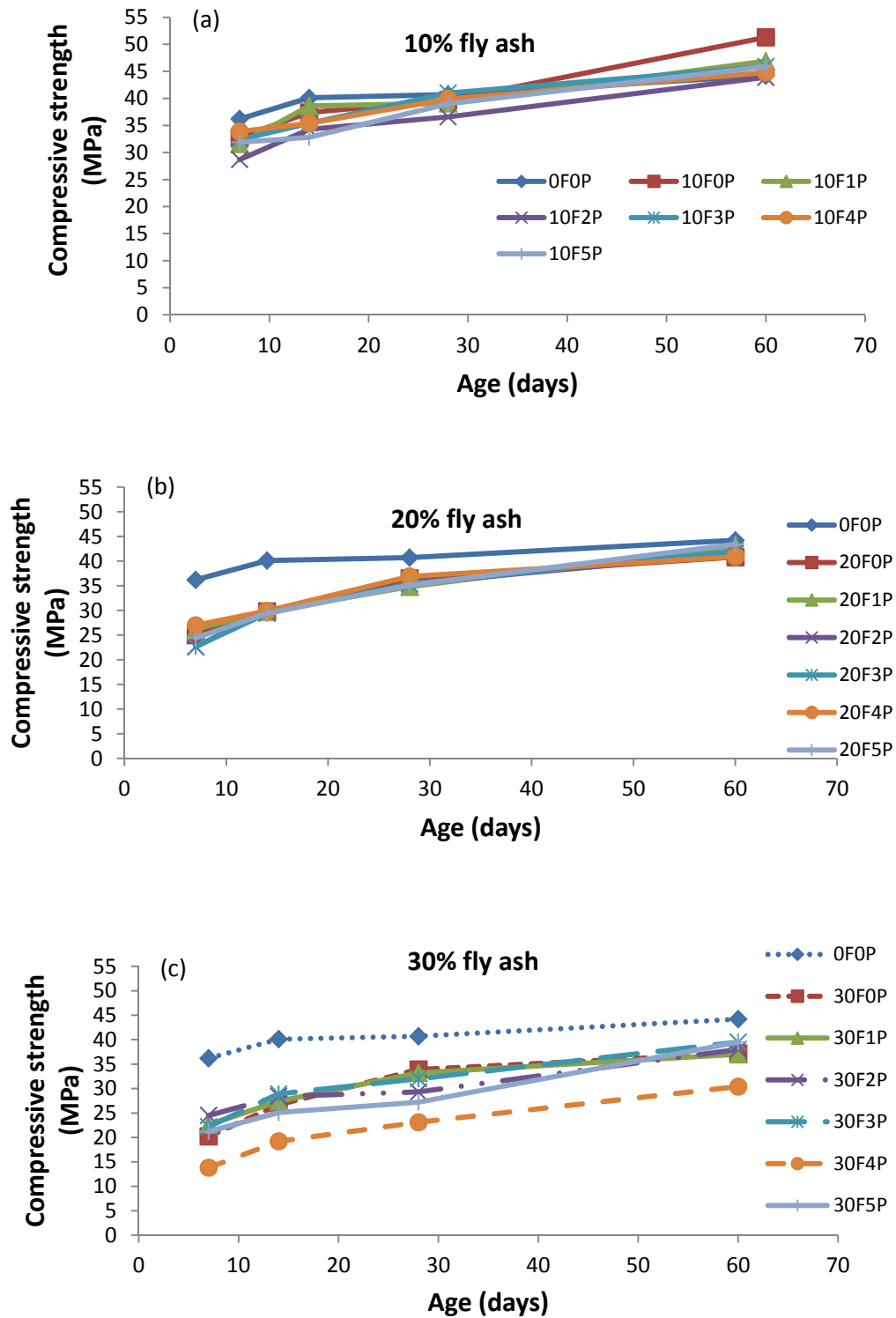
Fig. 5-3 Evolution of compressive strength in concrete for varying fly ash contents:

a) 10%; b) 20%; c) 30%
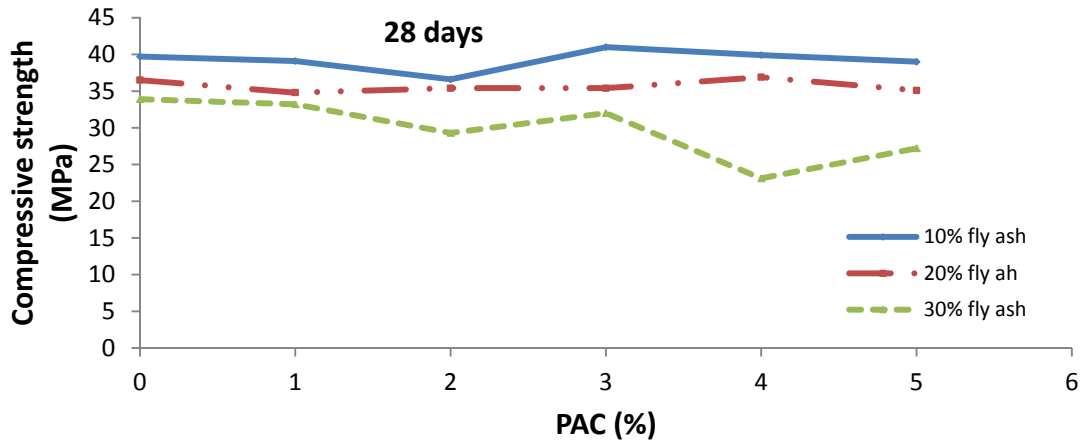
Fig. 5-4 Effect of PAC content on the compressive strength of concrete at 28 days, for increasing fly ash substitution of Portland cement

The similarity between the compressive strength results of the current study and one performed by Lockert et al. (2005) are understandable, with the only main difference of the powdered activated carbons used in both studies being the bromine content. Recall that Lockert et al. (2005) used a higher bromine content powdered activated carbon. In other words, comparing the results of these two studies, one may conclude that the bromine did not affect the compressive strength of concrete. The results of another study performed by Larrimore et al. (2008) confirmed that addition of bromine to fly ash has no effect on the compressive strength of concrete made with the contained fly ash at 3, 7, 14, 28 and 56 days.

5-1-3 Density, Absorption and Volume of Permeable Voids in Hardened Concrete

As mentioned earlier, the 75 mm x 150 mm cylinders were immersed in a boiling water bath as per the ASTM C642 (2006), and the results of the volume of permeable voids for

concrete containing 10%, 20% and 30% fly ash are shown in Figures 5-5a, 5-5b and 5-5c, respectively. The volume of permeable voids for each of the mixes was averaged over three specimens. The C.O.V. of the volume of permeable voids at 7, 14, 28 and 60 days varies from 0.05% to 1.56%, 0.07% to 0.55%, 0.05% to 9.79% and 0.01% to 3.02%, respectively. As expected, the results show that the void volume decreases with age for all levels of fly ash substitution (i.e., 10, 20 and 30% by weight of Portland cement). For example, the total volume of permeable voids for mix 30F2P decreased by 55% from the 7th to the 60th day. However, the rate of this decrease was not constant for different levels of PAC in fly ash and varied with the amount of fly ash. Crouch et al. (2007) showed that an increase in the age of concrete decreased the permeable void volume for 20-50% fly ash replacement. In the present study, the effect of PAC on the permeable void volume of concrete was not obvious. In the case of mixes incorporating 10% fly ash, the results show considerable scatter making it difficult to find a specific trend for permeable void volume as influenced by the PAC percentage. Surprisingly, a higher level of PAC led to a 30% increase in the volume of permeable voids in the presence of the high fly ash replacement of cement. The author faced difficulty in justifying this result. However, the author believes that a higher PAC content indicated a higher content of porous materials inside the mixes wherein these porous materials finally led to a higher volume of permeable voids. Osbaeck and Smith (1985) reported that fly ash can affect the air void content of concrete by increasing the pore volume of a mortar due to its inherent porosity. With lower fly ash content, the effect of hydrated cement, which decreases the porosity of concrete, dominated the effect of PAC. Meanwhile, with high fly ash content, regarding the shortage of cement as well as cement hydration products, the high porosity of PAC material controlled the porosity of

the whole system which led to an increase in the volume of permeable voids. This increase affects the durability of concrete and should therefore be considered.

As seen in Figure 5-6 for specimens tested at 28 days, the mixes containing 30% fly ash reveal that an increase in the percentage of PAC contained in fly ash leads to an increase in the volume of permeable voids. In the mix containing 20% fly ash, the permeable void volume increased up to a PAC dosage of 2%. Beyond 2%, a decrease in the permeable void volume was observed. However, since the volume of permeable voids in 30F1P (30% fly ash and 1% PAC) was smaller than that in 30F2P after 28 days, the compressive strength of the former was higher, which is in agreement with the behaviour of conventional concrete. Ramezanianpour and Malhotra (1995) showed that concrete containing 25% fly ash had lower permeability and lower porosity compared to the plain concrete. That conclusion is in agreement with the results presented in this study where, at all ages, concrete containing 20% fly ash showed lower volume of permeable voids compared to the control mix without fly ash (0F0P).

The bulk density, bulk density after immersion, bulk density after immersion and boiling, absorption after immersion, absorption after immersion and boiling and apparent density for mixes containing 10% fly ash are shown in Figures 5-7a, 5-7b, 5-7c, 5-7d, 5-7e and 5-7f, respectively. The results of the ASTM C642 (2006) test for mixes containing 10% fly ash replacement show no trend with different percentages of PAC and the age of the concrete. Since the results of mixes containing 10% fly ash were almost identical, for example the results of the bulk density after immersion and boiling, it is difficult to find a relationship between them. However, it is generally noted that the apparent density of concrete decreases with age. This generalization was also reported for the ordinary Portland cement concrete (Apaydin 2010). A decrease in the results of absorption after immersion and boiling with an increase in the curing

time can also be observed. Apaydin (2010) also showed that the absorption after immersion and boiling of ordinary concrete decreases with age. The same conclusion (apart from 10F0P and 10F2P) can be also found for the results of the absorption after immersion.
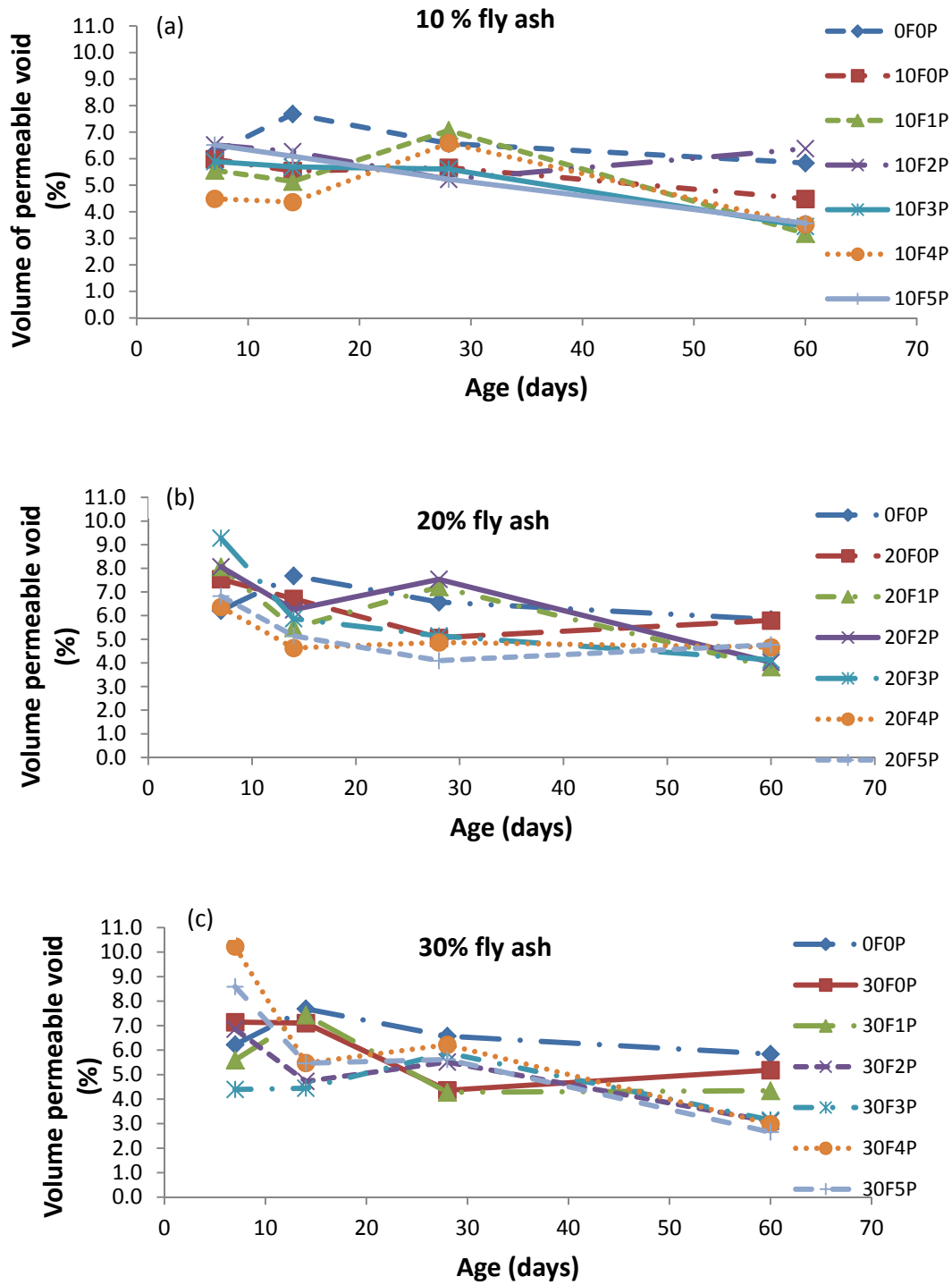
Fig. 5-5 Evolution of permeable voids in concrete due to various contents of fly ash:

a) 10%; b) 20%; c) 30%
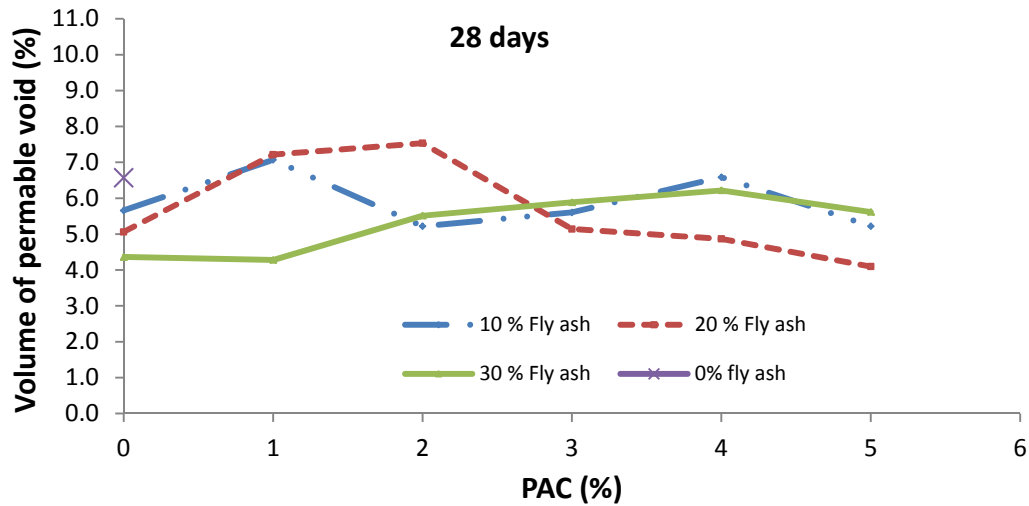
Fig. 5-6 Effect of PAC on the volume of permeable voids in concrete after 28 days

The bulk density, bulk density after immersion, bulk density after immersion and boiling, absorption after immersion, absorption after immersion and boiling and apparent density for mixes containing 20% fly ash are also shown in Figures 5-8a, 5-8b, 5-8c, 5-8d, 5-8e and 5-8f, respectively. The results of the mixes containing 20% fly ash replacement show that the bulk densities of concrete (bulk density-dry, bulk density after immersion and bulk density after immersion and boiling) increased with the age of the concrete. Generally speaking, the apparent density decreased with the age of the concrete, similar to the 10% fly ash replacement mixes. However, it should be noted that the change in the bulk and apparent densities (as indicators of durability) as noted in this study cannot influence the durability of concrete due to their low values. Amer et al. (2008) showed that the mass loss of roller compacted concrete samples in the freeze and thaw test remains the same with the change of unit weight. There are few published data available which address the results of bulk density-dry, bulk density after immersion and

bulk density after immersion and boiling. Crouch et al. (2007) used the ASTM C642 standard test method to determine the air-void characteristics of concrete. They found that the absorption of concrete containing 20% Class F fly ash is almost constant after 180 days. The results of the present study, shown in Figure 5-8, also show that the absorption of most mixes containing 20% fly ash remains constant after 60 days.

Fig. 5-7 ASTM C642 test results: 10 % fly ash replacement. Effect of curing time on a) bulk density dry; b) bulk density after immersion; c) bulk density after immersion and boiling; d) absorption after immersion; e) absorption after immersion and boiling; f) apparent density

79
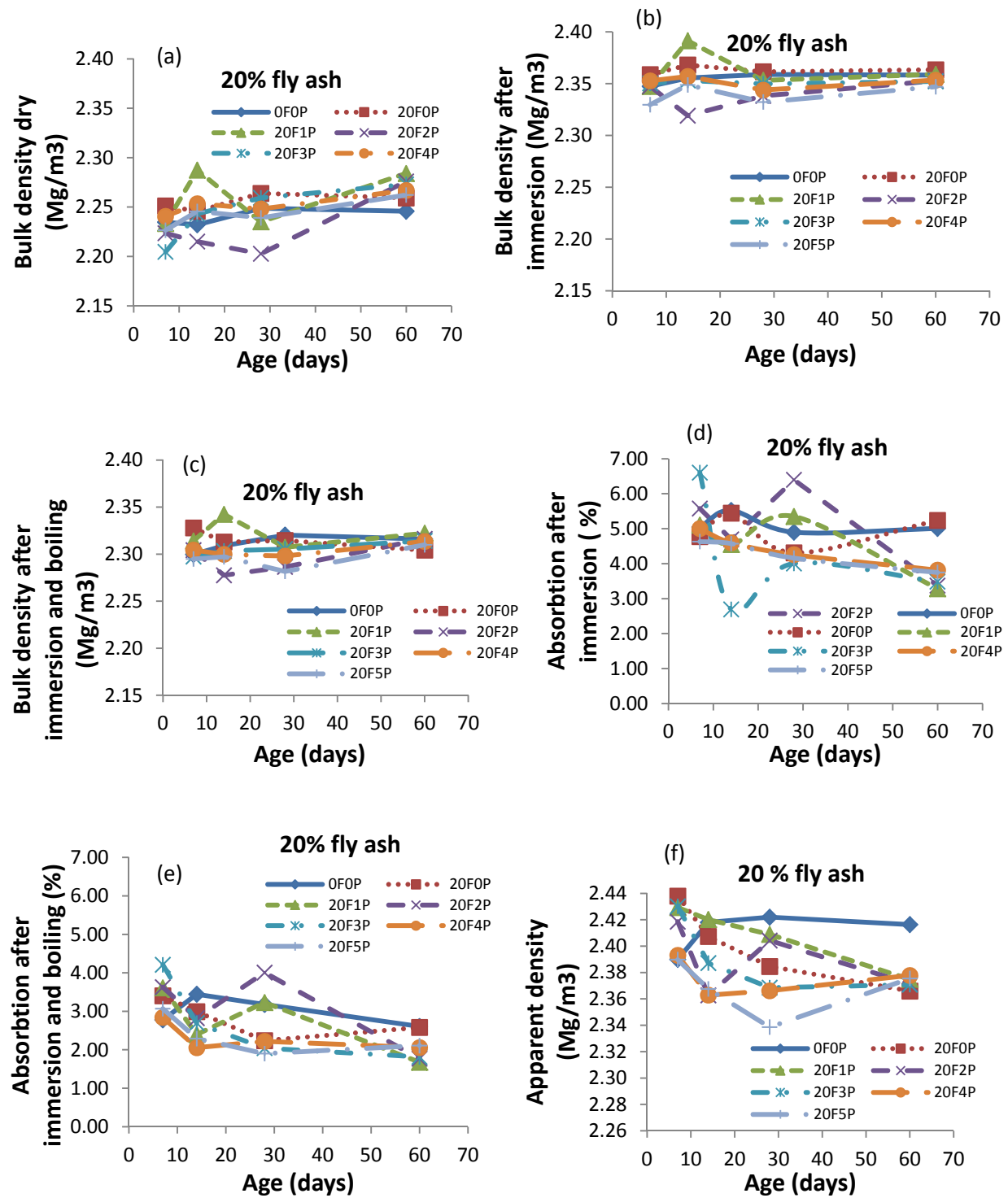
Fig. 5-8 ASTM C642 test results: 20 % fly ash replacement. Effect of curing time on a) bulk density dry; b) bulk density after immersion; c) bulk density after immersion and boiling; d) absorption after immersion; e) absorption after immersion and boiling; f) apparent density

The bulk density, bulk density after immersion, bulk density after immersion and boiling, absorption after immersion, absorption after immersion and boiling, and apparent density for mixes containing 30% fly ash are also shown in Figures 5-9a, 5-9b, 5-9c, 5-9d, 5-9e and 5-9f, respectively. The results of mixes containing 30% fly ash replacement show that the absorption of concrete decreased with age. Crouch et al. (2007) found that the absorption of concrete containing 25% Class C fly ash decreases by 14% at 180 days. The results show that the bulk density after immersion for all mixes with different PAC contents at different ages was in the narrow range of 2.29-2.36 Mg/m^3. The results of the bulk density, dry, also show a narrow range of values. The same conclusion can be drawn for the bulk density after immersion and boiling. However, no specific trend could be found for the apparent density with 30% fly ash replacement of cement. The author believes that since the values of apparent density were quite close, the trend between the PAC content and apparent density at different ages was therefore unclear. Put differently, the errors generated during the test were higher compared to the effect of the PAC content; this led to the scattering. Again, it should be noted that the values of the apparent density lay in a tight range where the difference of its top and bottom is less than 7%. Parande et al. (2011) investigated the micro structural properties of concrete containing fly ash at 0, 5, 10, 15, 20, 25, 30 and 35% replacement. They showed that different amounts of fly ash (or in other words different amounts of unburnt carbon) contained does not affect the bulk density-dry, bulk density after immersion and bulk density after immersion and boiling. In their study, the bulk density-dry, bulk density after immersion and bulk density after immersion and boiling varied at 2.23-2.38, 2.29-2.49 and 2.236-2.60 Mg/m^3, respectively. Nevertheless, it is worth restating that the unburnt carbon and PAC are physically different, see Section 5-1-2.
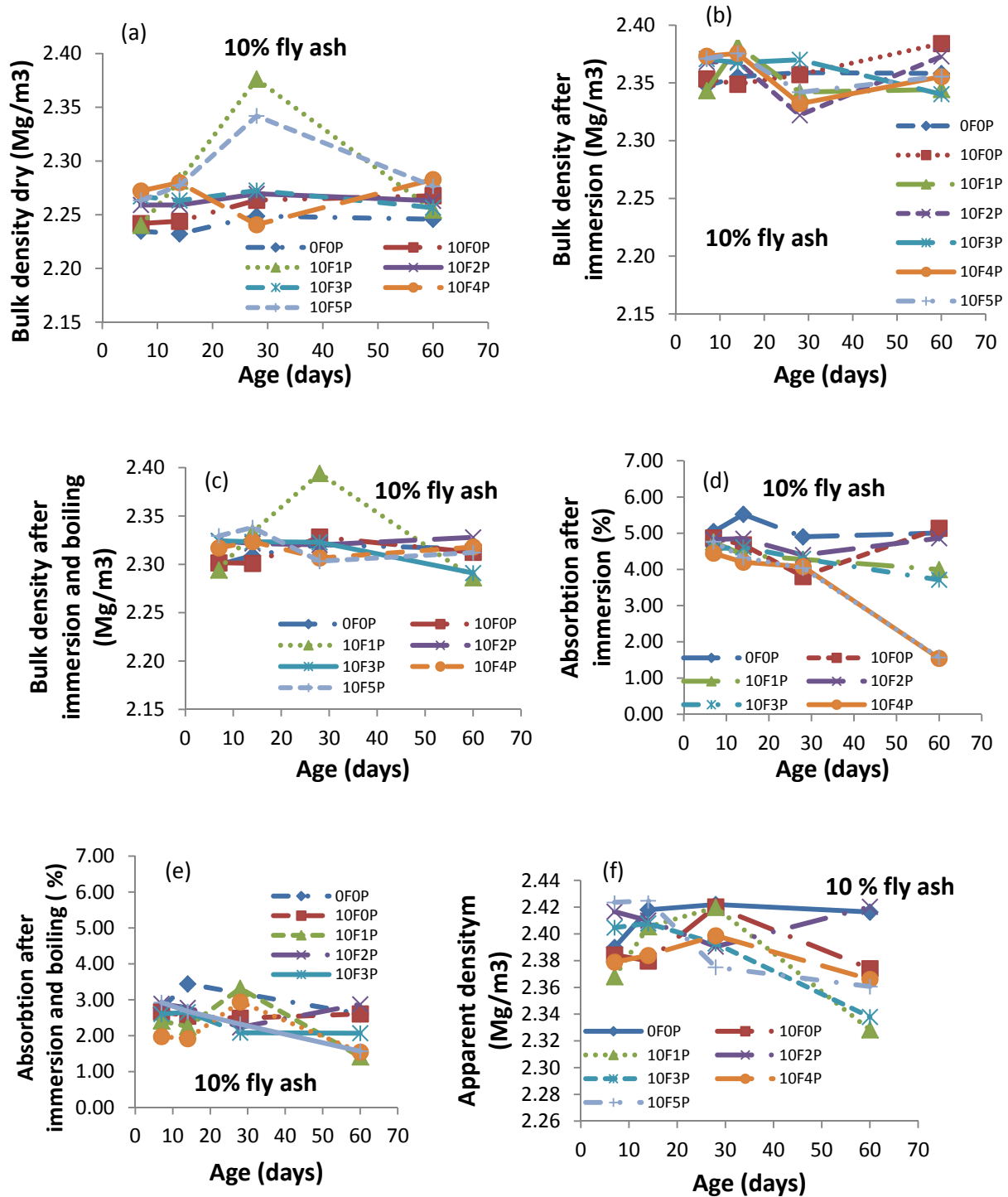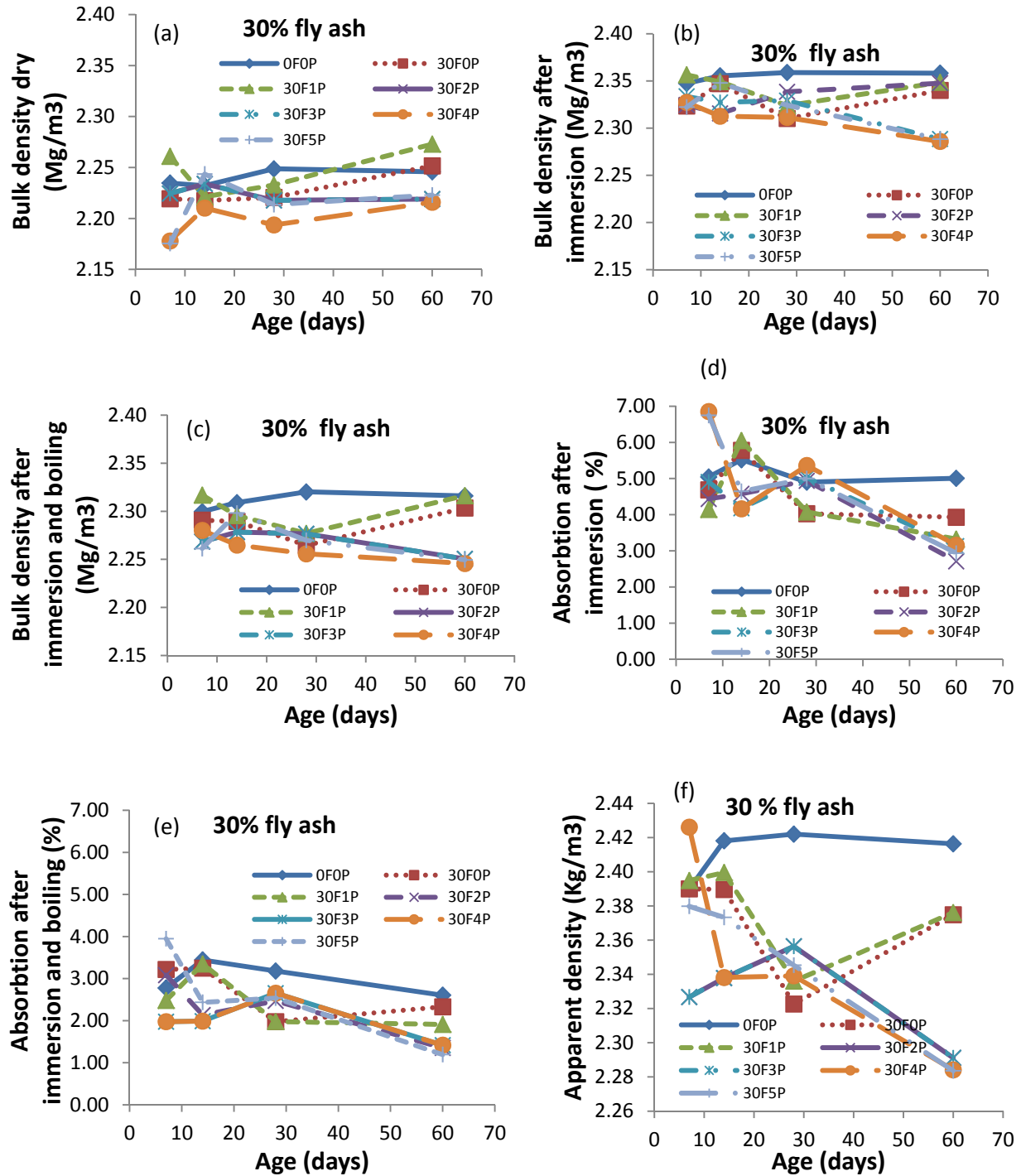
Fig. 5-9 ASTM C642 test results: 30 % fly ash replacement. Effect of curing time on a) bulk density dry; b) bulk density after immersion; c) bulk density after immersion and boiling; d) absorption after immersion; e) absorption after immersion and boiling; f) apparent density

By comparing the fresh and hardened air void content data, it can be concluded that the volume of permeable voids in hardened concrete for any mix was about three times the air void content of the corresponding fresh concrete. While researchers rely on fresh air void content to estimate the freeze-thaw resistance of concrete (Setzer and Auberg 1995), the present investigation indicates that the air-void network of mature concrete should also be assessed by other methods in order to better predict the freeze-thaw resistance. This is especially so when adsorbents such as PAC are present in the mix since the adsorbent affects the porosity over time. Figure 5-5 shows how the porosity of concrete containing different percentages of PAC changed with age.

Note that the air void content of fresh concrete was generally low for the mixes in Series #1 as was shown in Section 5-1-1. Air entrained admixture was not deliberately used in order to allow for the identification of the influence of PAC alone on the air-void system, since only limited data was available in the literature (Golightly et al. 2008). However, in practice the porosity of fresh and hardened concrete may be affected by the interaction between the powdered activated carbon and the air entraining admixture. The increase in the volume of permeable voids that was observed with an increase in the PAC content and associated with higher levels of fly ash is curious as this behaviour is contrary to what is seen in the presence of air entrainers (Nkinamubanzi et al. 2003). In what follows (Sections 5-2 and 5-3), air entrainers were added to yield Series #2 and #3 to investigate their potential interaction and consequent effects on the rheology, strength and air-void network of concrete.

5-1-4 Image Analysis

Figure 5-10 and 5-11 show the air-void distribution and shape factor distribution for the 20F0P sample, respectively.
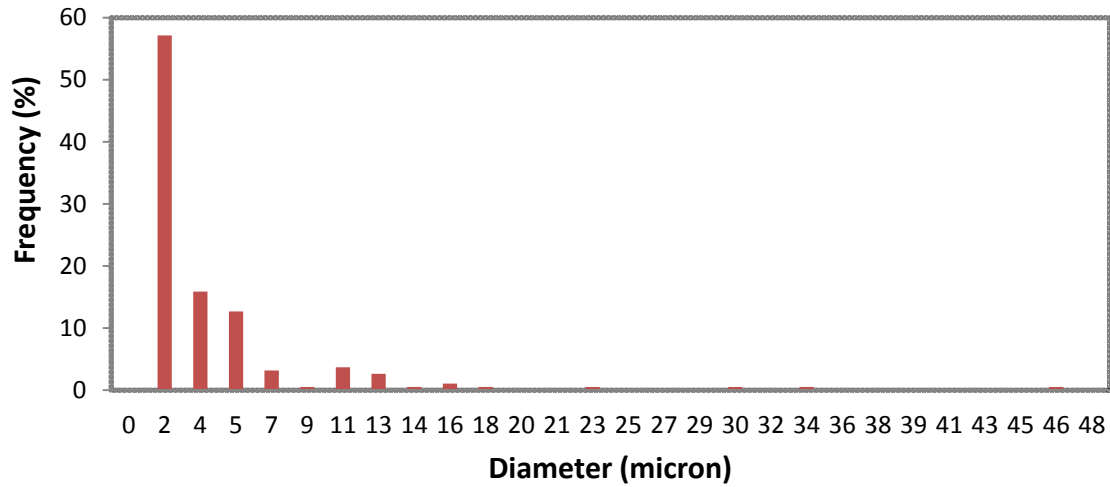
Fig. 5-10 Air-void distribution for 20F0P sample
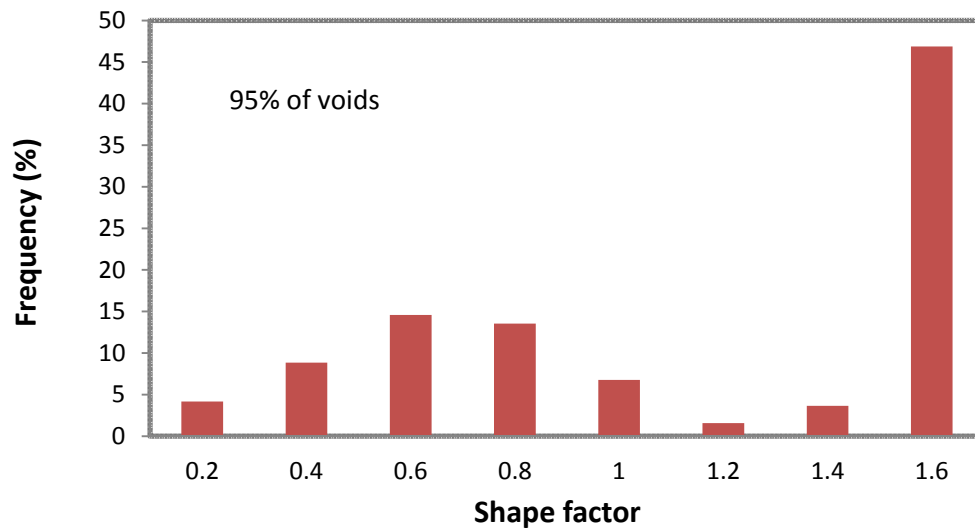
Fig. 5-11 Shape factor for 20F0P

5-1-4-1 The observation on epoxy-impregnated samples

Table 5-1 shows the air void content, specific surface area, spacing factor and shape factor of the epoxy-preparation samples obtained from image analysis process at both 60X and 100X magnifications. The image analysis was performed only on the selected samples containing 0, 2 and 5% PAC.

Table 5-1 Image analysis results of the epoxy-impregnated samples

| | magnification | Sample ID |
		0F0P	10F0P	10F2P	10F5P	20F0P	20F2P	20F5P	30F0P	30F2P	30F5P
Air void content (%)	60	0.52	1.20	1.18	1.18	1.18	1.12	1.80	1.06	1.87	1.00
	100	0.96	1.66	1.20	1.30	1.89	1.33	1.81	1.52	1.93	1.26
Specific surface (1/micron)	60	0.56	0.53	0.54	0.44	0.45	0.36	0.33	0.63	0.50	0.42
	100	0.53	0.47	0.34	0.66	0.28	0.37	0.69	0.26	0.33	0.31
Spacing factor (mm)	60	0.02	0.02	0.02	0.02	0.02	0.03	0.02	0.02	0.02	0.02
	100	0.02	0.02	0.03	0.01	0.03	0.02	0.01	0.03	0.02	0.03
Mean shape factor	60	1.12	1.16	1.08	1.09	1.12	1.11	1.12	1.14	1.14	1.11
	100	1.13	1.04	1.18	1.00	1.03	0.99	1.14	1.03	1.10	1.15

The results of the image analysis compared at different magnifications show different specific surface area and air void content while similar results are obtained for spacing factors, regardless of magnification. The mean ratios of X100 and X60 magnification for the air void

content, specific surface and spacing factor were 1.29, 0.95 and 1.15, respectively. It was also found that both magnifications provide the same shape factor. Put otherwise, one may conclude that use of different magnifications (say X60 and X100) in the image analysis method cannot change the results of shape factor. In the following, only the results of X60 magnification are discussed here as a higher magnification cannot reveal all voids. This is especially true in the case of images taken from the epoxy-impregnated samples.

The results show that the air void content of all samples (except for the reference) was approximately equal and low compared to the typical air void content of concrete containing AEA. This is a reasonable finding since no air-entraining admixtures have been used in Series #1. A low air void content usually raises concerns regarding the low freeze-thaw resistance of concrete. Meanwhile, the results also indicate that all spacing factors are smaller than the maximum 230 micron spacing factor defined by the Canadian code, CAN/CSA A 23.1 (2000) needed for satisfying the freeze and thaw resistance. Figure 5-12 shows a comparison of the air void content obtained by both experimental measurement and image analysis.

It can be concluded that the fresh air void and permeable void content of all the mixes (except 30F2P obtained from ASTM C231-2009) are higher than the air void content obtained from the image analysis. This result could be attributed to the longer curing period for samples evaluated by image analysis. Although Giergiczny et al. (2009) by implementing the image analysis technique showed that an increase in the supplementary cementing material decreases the total volume of permeable voids, a similar trend did not appear in this investigation. The author believes that the lower volume of permeable voids was not obtained at higher fly ash contents in this study as this parameter was measured at early ages. Therefore, fly ash could not completely react with the calcium hydroxide of cement paste to form a denser structure.

86

Saricimen et al. (2000) also reported that the curing time affects the volume of permeable voids of concrete containing fly ash. They showed that the volume of permeable voids decreases with the curing time.
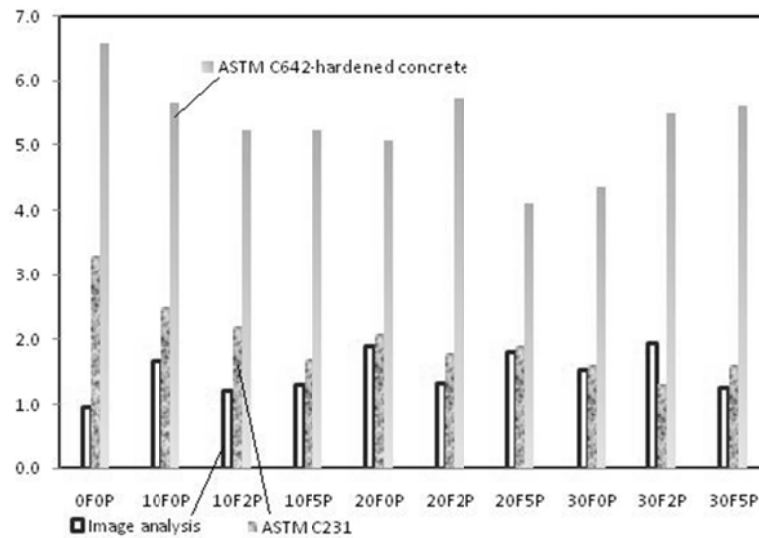
Fig. 5-12 Comparison of the air void content of concrete through test ASTM C231, ASTM C642 and image analysis

Figure 5-13 shows the changes of specific surface area against PAC percentages. A decrease in the specific surface area of concrete due to an increase in PAC indicates that carbon in fly ash has a detrimental effect on the small bubbles.
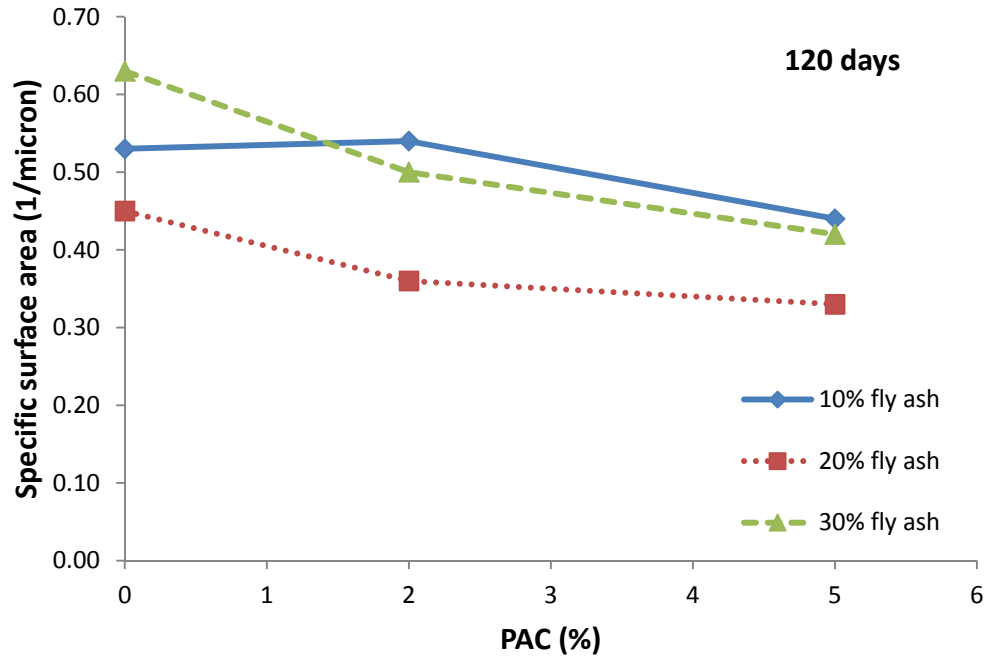
Fig. 5-13 Effect of PAC on the specific surface area

Figure 5-14 shows the effect of PAC on the spacing factor of concrete. The trend remains the same in concrete containing 10% and 30 % fly ash. For 20% replacement, the spacing factor trend does not follow other replacements. Generally speaking, it is difficult to measure the low spacing factors of mixes. The relatively small size sample (cross section area= 500 mm^2) used for the image analysis could be the source of inaccuracy in the results when large coarse aggregate was used in the mixes. As mentioned in Section 4-2-5, Jana (2006) showed that for examining the air-void characteristics of a concrete containing 19-25 mm nominal maximum size aggregate, a cross section area of at least 7700 mm^2 is needed. He also believed that a 27mm X 47mm section would be adequate for the characterization of a cement sample. Chen et al. (2002) used a cylindrical sample with a diameter of 24 mm and height of 15 mm for measuring the microstructure of paste (not concrete) using an optical microscope. They also used a mortar (not

concrete) sample of 20mm X 20mm X 15 mm to measure its microstructure. Toumi and Resheidat (2010) used a cube sample with a 50 mm side to assess (using a flatbed scanner) the air-void characteristics of concrete containing coarse aggregate (maximum aggregate size=12.5 mm). Again, it should be noted that in the current study, concrete containing coarse aggregate (maximum size of 12 mm) was cast and tested. One may expect that a larger sample would be required for concrete samples when their microstructures needed to be measured. Nonetheless, the size of the samples in this study was limited regarding to instrument and equipment restraints. The author believes that if each side of a cube sample is up to 3 times larger than the maximum aggregate size, the sample can be considered for examining the air-void characteristics (Jana 2006). This conclusion was drawn based on Jana's study (2006) showing that for a maximum aggregate size of 19-25 mm, a minimum cross section area of 7700 mm^2 which is equivalent to a 85 mm-side cube is needed. Therefore, for a concrete containing 12 mm coarse aggregate, a cross section area of at least 1300 mm^2 is recommended. It is worth restating that the smaller size was chosen in this study regarding to instrument and equipment restraints.
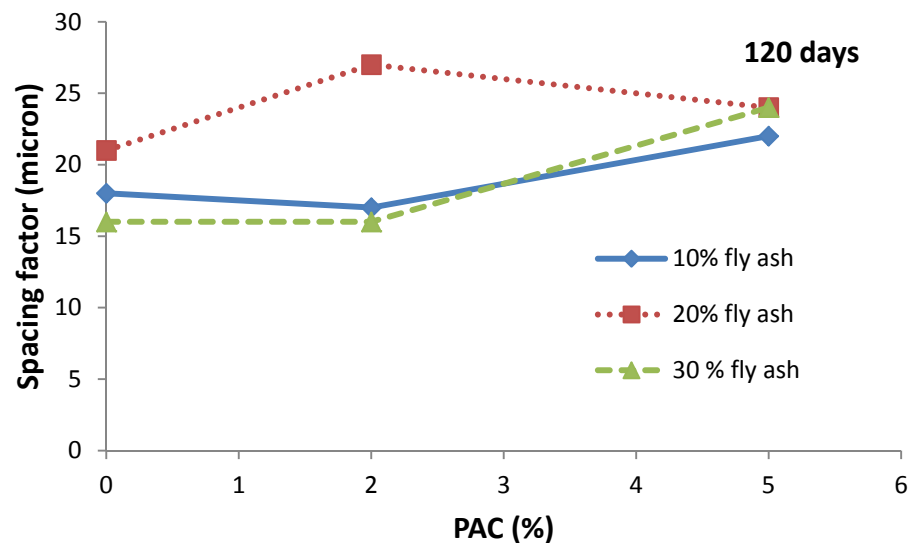
Fig. 5-14 Effect of PAC on the spacing factor

The mean shape factor of the mixes is summarized in Figure 5-15. As mentioned before, the shape factor indicates how close the holes of the voids are to a sphere. The shape factor value is equal to one for a perfect circle and is larger for irregular voids (Kunhanandan Nambiar and Ramamurthy 2007). The mean shape factor (the average of shape factor for voids in the zone of interest) of all mixes is below 1.16, meaning that most voids inside the zone of interest were close to a circular shape. The author believes that closer the shape factor to unity, the more efficient the action of AEA as well as the more accurate the results of the image analysis (Kunhanandan Nambiar and Ramamurthy 2007). Put differently, in this case there is no interruption from other sources that leads to the generation of a near-perfect spherical bubble. Furthermore, a higher shape factor indicates the possibility of merging air voids, showing that the air voids are not uniformly distributed. It is well known that air void distribution plays an important role in the durability properties of concrete (Stutzman 1999). Toumi and Resheidat (2010) showed that the air void distribution is one of the indicators needed to be considered. Kunhanandan Nambiar and Ramamurthy (2007) showed that for foam concrete containing fly ash, the median shape factor remains constant in the range of 1.10-1.23 which confirms the results of the current study.
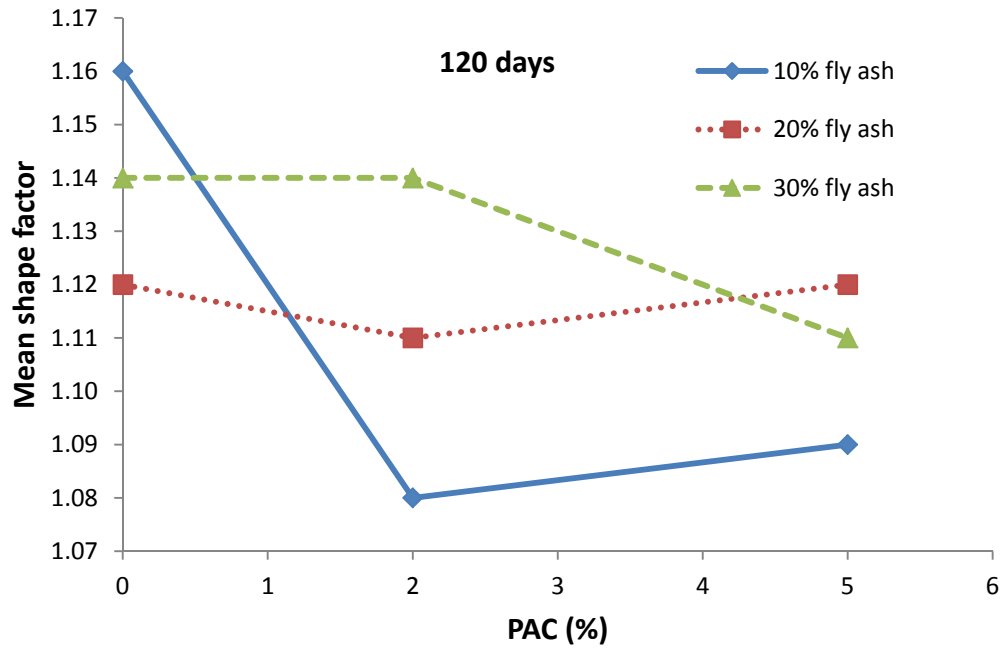
Fig. 5-15 Effect of PAC on the mean shape factor

5-1-4-2 The observation on ink-prepared samples

Table 5-2 shows the air void content, specific surface area, spacing factor, and shape factor of the ink-prepared samples obtained by the image analysis process in both 60X and 100X magnifications.

Table 5-2 Image analysis results of the ink-prepared samples

	magnification	Sample ID									
		0F0P	10F0P	10F2P	10F5P	20F0P	20F2P	20F5P	30F0P	30F2P	30F5P
Air void content (%)	60	0.40	2.86	2.97	2.62	1.64	2.41	0.51	0.58	0.44	0.41
	100	0.34	2.82	2.42	1.76	0.62	1.59	0.19	0.32	0.20	0.24
Specific surface (mm^{-1})	60	131	14	45	21	87	31	70	100	31	146
	100	262	11	58	55	162	42	133	166	230	190
Spacing factor (mm)	60	0.11	0.45	0.14	0.33	0.10	0.22	0.19	0.13	0.45	0.10
	100	0.06	0.59	0.12	0.15	0.08	0.20	0.15	0.10	0.08	0.10
Mean shape factor	60	0.70	0.96	0.69	0.77	0.68	0.72	0.62	0.63	0.67	0.72
	100	0.79	0.67	0.72	0.73	0.74	0.78	0.55	0.62	0.69	0.73

Again, the image analysis was only performed only on the selected samples containing 0, 2 and 5 percent PAC. The results of the ink-prepared samples show that the air void content of samples measured with X60 magnification was higher compared to the samples measured with X100. Also, it is seen that the specific surface area of X100 samples was higher compared to the X60 ones. The results of the spacing factor were erratic as in some cases the X100 images showed a higher spacing factor, while in most cases the spacing factor of the X60 images had the higher spacing factor. However, the results of the mean shape factor demonstrated that there is no difference between the results of different magnifications. The effect of PAC on the spacing

factor of concrete containing different percentages of fly ash at X60 and X100 magnification is shown in Figures 5-16a and 5-16b, respectively. The results of both magnifications, X60 and X100, are presented in this figure.
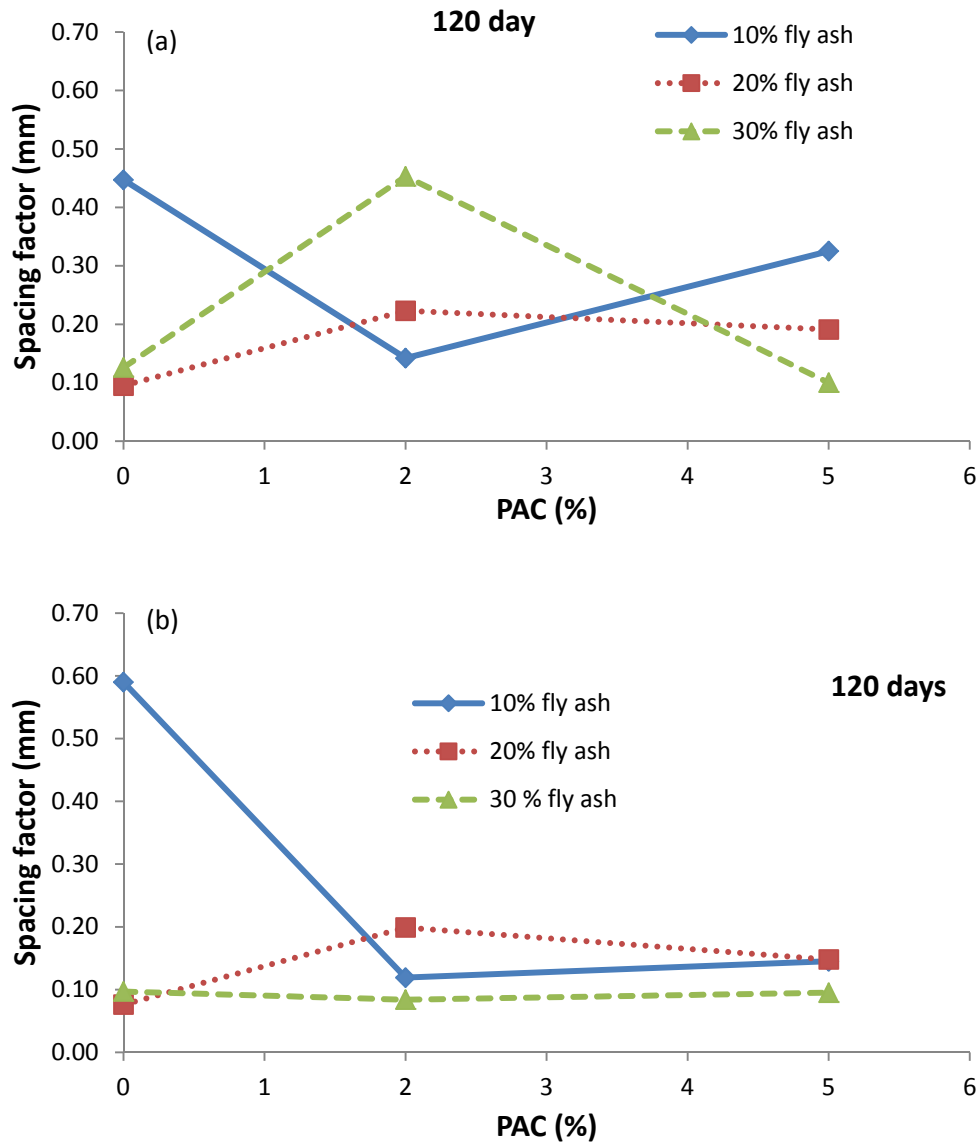
Fig. 5-16 Effect of PAC on the spacing factor: a) X60; b) X100

By looking at Figure 5-16, it is seen that for higher percentages of PAC the spacing factor does not change. The results of the spacing factor for X60 magnification were too scattered

making them difficult to interpret. Cox and De Belie (2007) investigated the effect of fly ash on the durability, microstructure and strength of concrete. They showed that concrete containing 35% fly ash had a 16% lower spacing factor compared to the plain concrete after 1 and 3 months. There are few published reports to address the effect of low volume fly ash on the spacing factor and specific surface area of concrete. Sabir and Kouyiliali (1991) showed that concrete with a lower pozzolanic percentage has a lower spacing factor although the air void content remains constant. Also, Giergiczny et al. (2009) demonstrated that the use of blended cement containing 30% slag resulted in a corruption of the air void distribution in hardened air-entrained concrete, exhibited by an increase in the spacing factor of the air voids by about 100 microns. It is worth restating that although the chemical properties of fly ash and slag are different, the former is likely to mimic the latter in corrupting the spacing factor. In other words, both fly ash and slag show the same action on the spacing factor of voids. This could be the reason why the scattered results obtained in this study is in agreement with results found by Giergiczny et al. (2009). A comparison of the results of the spacing factor shows that X60 magnification led to higher values compared to X100.

The effect of PAC on the specific surface area of concrete containing different percentages of fly ash at X60 and X100 magnification is shown in Figures 5-17a and 5-17b, respectively. The results of both magnifications, X60 and X100, are presented in this figure. At both magnifications, the specific surface area of concrete containing a higher fly ash percentage, 30%, was higher compared to other mixes. In a study performed by Giergiczny et al. (2009) for concrete mixes containing steel slag, the above conclusion was not achieved. They reported that the replacement of cement by 30% slag decreased the specific surface area of voids by 10–11 mm^{-1}. This difference may likely be attributed to the absence of PAC in their study. Also, it

seems that the nature and the chemical properties of fly ash and slag are different which led to different results for the specific surface area though they have a similar impact on the spacing factor. The author could not find a published study reporting the effect of both fly ash and PAC on the specific surface area of concrete. Therefore, the above comparison was performed in order to compare the effect of cementitious materials on the specific surface area of concrete containing AEA. In mixes with 20% fly ash replacement, the specific surface area did not change upon the addition of a high percentage of PAC (5%). The effect of PAC on the shape factor at the X60 and X100 magnification is shown in Figures 5-18a and 5-18b, respectively.
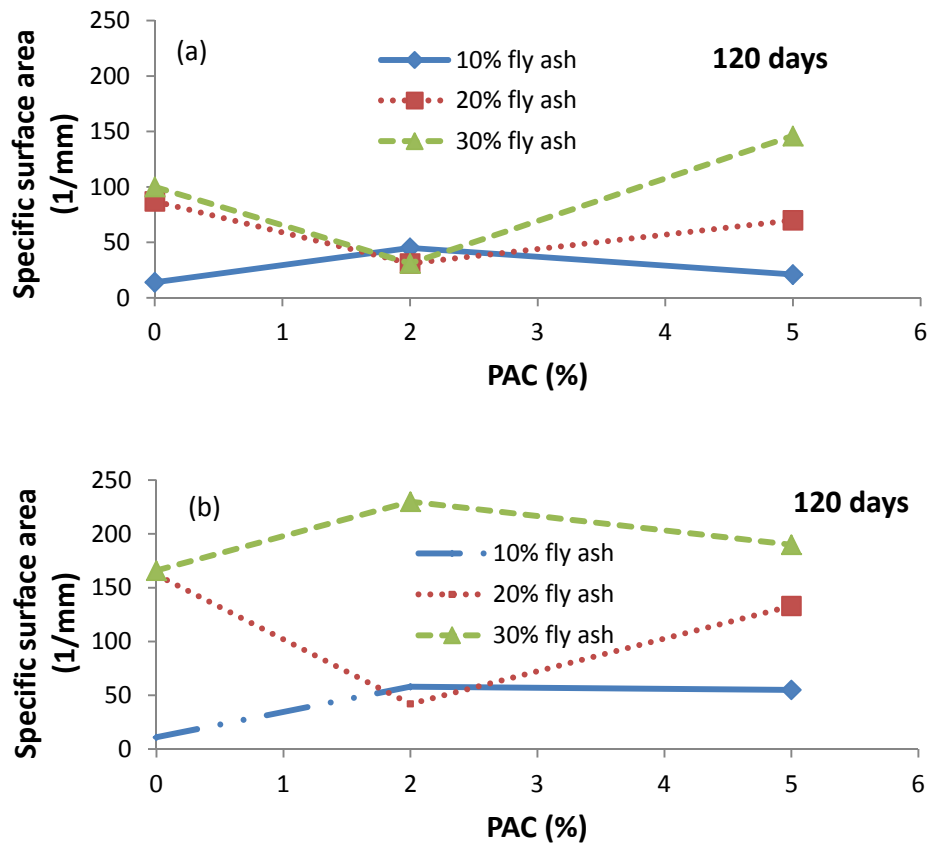
Fig. 5-17 Effect of PAC on the specific surface area: a) X60, b) X100
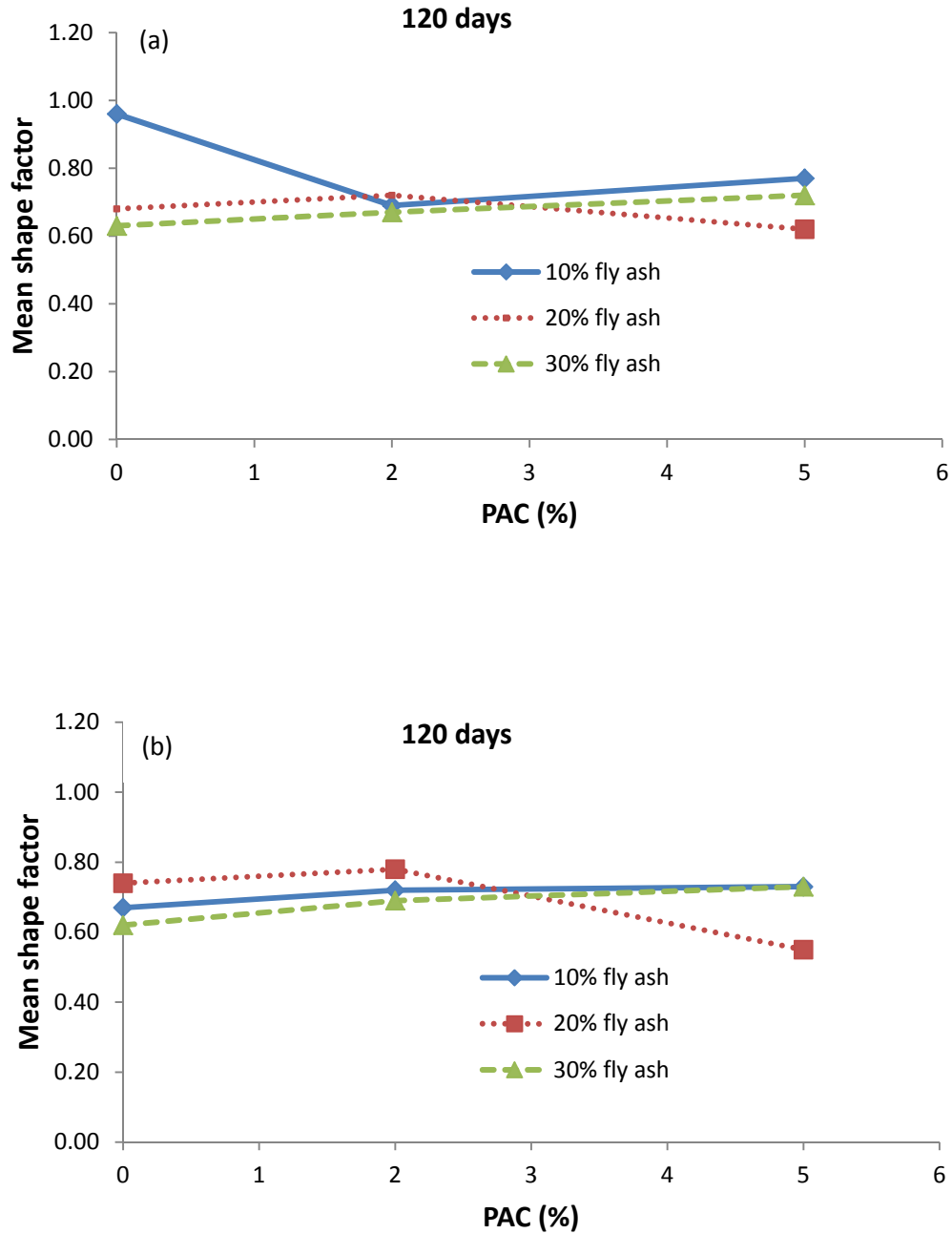
Fig. 5-18 Effect of PAC on the mean shape factor: a) X60; b) X100

The results show that at both magnifications, PAC had no significant effect on the mean

shape factor of concrete containing a different percentage of fly ash. However, only in the case

of 20% fly ash at the X100 magnification, it is seen that with a higher PAC content (20F5P) the mean shape factor dropped by 20% compared to 20F0P. It should be noted that the shape of the bubbles does not play an important role in the durability performance of concrete (Poonguzhali et al. 2008). It should be reminded that closer the value of the shape factor to unity, the higher the accuracy of the results of an image analysis.

5-1-4-3 Comparison of the air-void characteristics obtained from both sample preparation techniques

Since the spacing factor and specific surface area of concrete were not determined by other techniques (for instance ASTM C457 standard test method) it is impossible to judge the accuracy of the results obtained from the epoxy-impregnated and inked samples. A comparison of the results shows that the specific surface area and spacing factor of the mixes were significantly higher in the inked samples than the epoxy-impregnated samples. The results also reveal that the values of the mean shape factor for inked samples were lower than unity, whereas in the epoxy-impregnated samples those values were higher than one. The reader should be informed that a perfect circle has a shape factor of unity where an increase in the irregularity of a void increases the shape factor. Nevertheless, the author believes that the inked samples provide more reliable results. This is because in the inked sample voids can be more easily distinguished from solids. As mentioned in Section 4-2-5, this step plays an important role in the accuracy of the results.

5-2 RESULTS OF SERIES #2

In this section the fresh and hardened properties of Series #2 which included AEA at 0.5% of the total binder weight are described. The results of fresh concrete, compressive strength, ASTM C642 Standard Test Method and image analysis for Series #2 are provided in this section. All individual results and statistical information are listed in the Appendix #2.

5-2-1 Properties of Fresh Concrete

Figure 5-19 shows the air void content of fresh concrete. It is seen that by increasing the PAC content the air void content decreased. This means that PAC adsorbed part of the AEA.
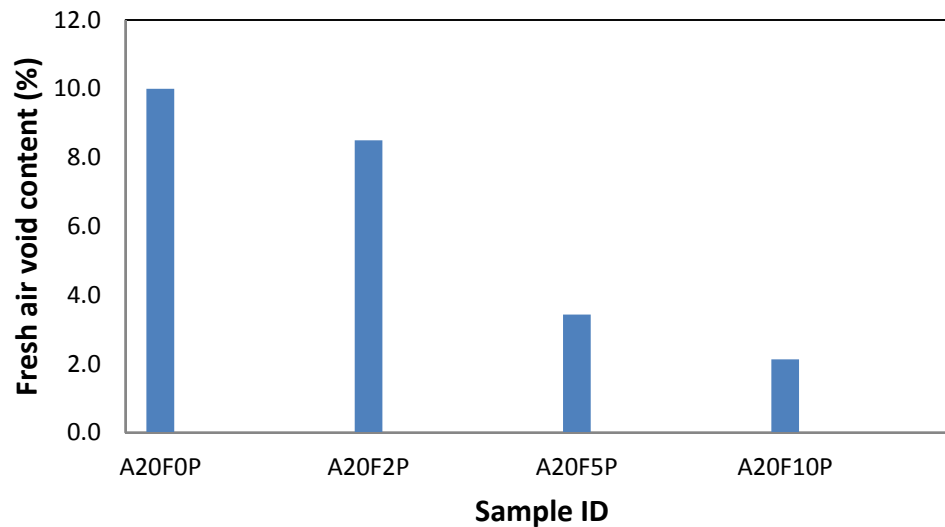
Fig. 5-19 Air void content of fresh concrete

In this series, since AEA was used, the differences in air void content were significant and it was easier to track the changes in air void content as the mix composition varied. The results show that by adding 10% PAC by weight of fly ash, A20F10P, the air void content of fresh concrete

decreased by 79% compared to A20F0P containing 0% PAC. This may cause some concerns regarding the large decrease in the air void content, because as mentioned earlier, the air void content is one of the chief factors affecting the freeze-thaw resistance. In a study by Baltrus and Lacount (2001) the effect of unburnt carbon on AEA demand was investigated. They showed that the adsorption of AEA by unburnt carbon leads to a longer equilibrium time as per the foam index test. They also concluded that the higher rate of adsorption of AEA by unburnt carbon explains the decrease in entrained air observed over time for concrete made using high levels of unburnt carbon fly ash. Hill et al. (2009) revealed that fly ash containing 1% PAC increases the AEA demand for gaining a 6% air void content by about 4 times compared to the plain concrete. Pederson et al. (2008) also showed that the particle size and the surface chemistry of carbon in fly ash impact on AEA adsorption and its demand. They found that the AEA adsorption capacity of carbon decreases with an increase in particle size. They also showed that an increase of the carbon surface area increases the specific foam index.

The results of density are shown in Figure 5-20. The results show that there is no significant difference between the densities of fresh concrete. The densities of the mixes were in the range of 2124 - 2184 kg/m^3, which is in accordance with the density of normal weight concrete. The constant unit weight (2260-2325 kg/m^3) of mixes with different fly ash percentages was also reported by Lomboy and Wang (2009). In a study performed by Hale et al. (2008), the fresh density of concrete containing 20% fly ash was reported as 2250 kg/m^3, showing good agreement with the results of Figure 5-20.
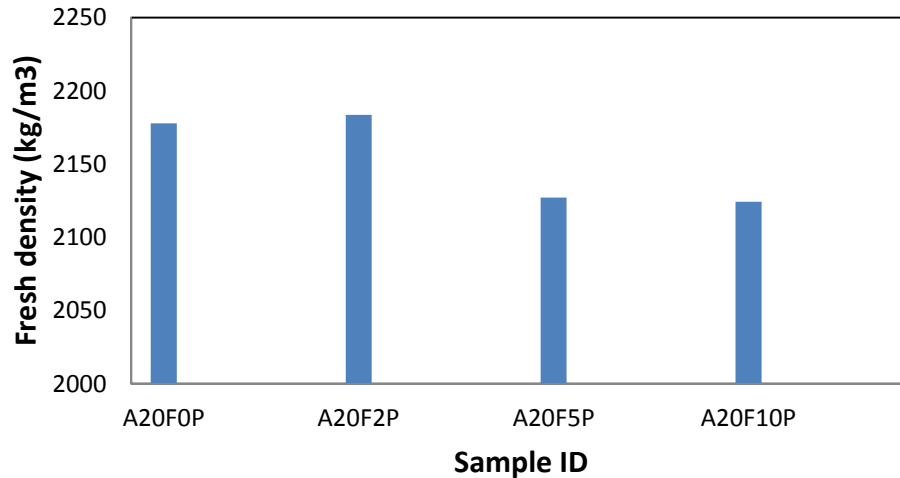
Fig. 5-20 Density of fresh concrete

5-2-2 Compressive Strength

The effect of PAC on the compressive strength of hardened concrete after 7, 28 and 60 days is shown in Figures 5-21a, 5-21b and 5-21c, respectively. The C.O.V. of the compressive strength at 7, 28 and 60 days varied from 2.5% to 11.9%, 3.4% to 16.3% and 0.8% to 10.6%, respectively. The results show that at all ages examined, an increase in the PAC content increased the compressive strength of the mixes. This result was expected, as with higher dosages of PAC, the air void content decreased, and it is known that a lower air void content leads to a higher compressive strength (Lamond 2006). It should be noted that some believe that the effects of carbonaceous solids on concrete (including discolouration, poor air entrainment behaviour and mixture segregation) do not cause any impact on the compressive strength (Freeman et al. 1997). In other words, the compressive strength of concrete may not be affected by increasing the carbon content. It is likely that the type and content of carbon play an important role, but this was not investigated in the present study.
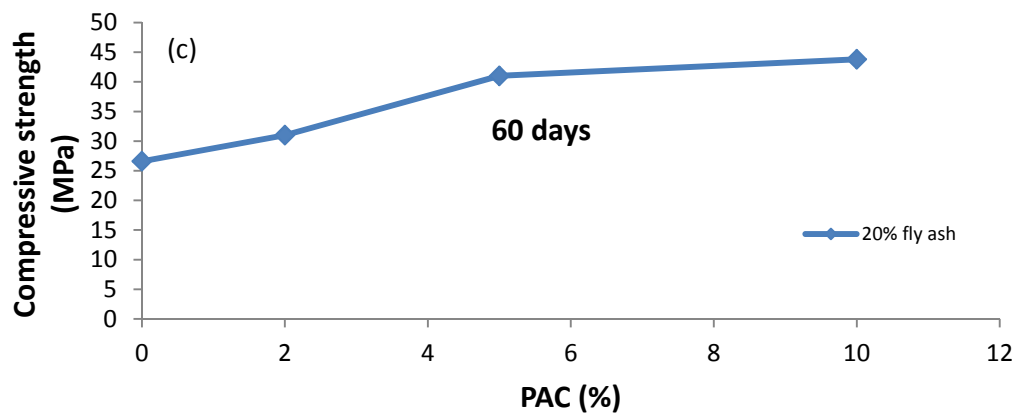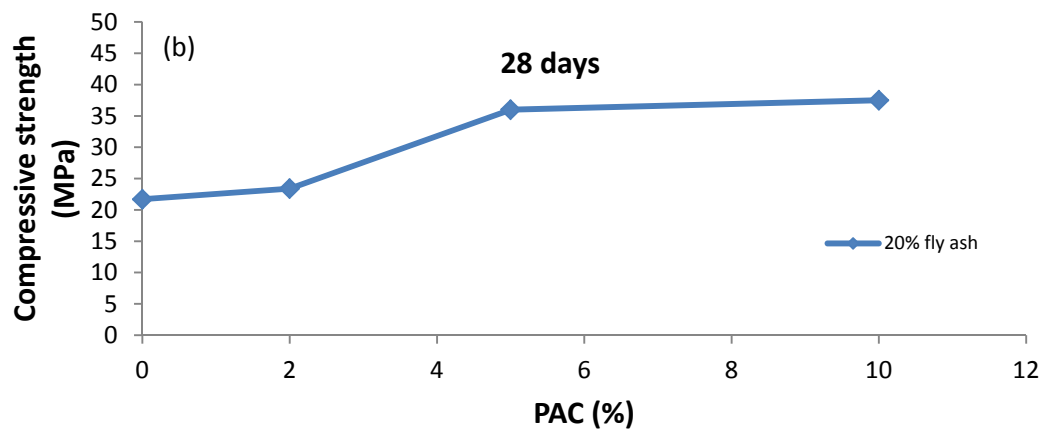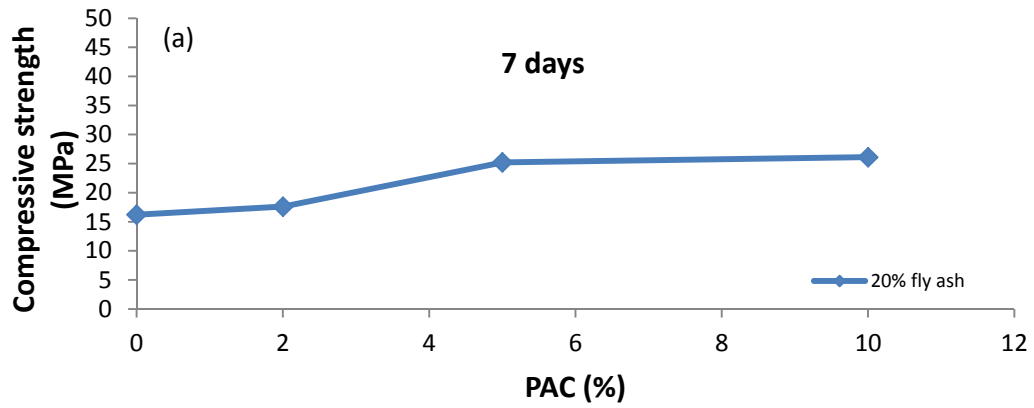
Fig. 5-21 Compressive strength of concrete with 20% fly ash for specimens cured for a) 7 days;

b) 28 days; c) 60 days

The effect of the age of concrete on its compressive strength is shown in Figure 5-22. The results show that with an increase in the age of the concrete the compressive strength increased as expected. For all four mixes, it is seen that the compressive strength of concrete cured for 60 days increased by 65% compared to the 7-day old concrete. The results also show that the compressive strength increased with a PAC content of 5% (A20F5P) or 10% (A20F10P) compared to that with only 2% PAC (A20F2P). This can be attributed to the reduction of the air void content in A20F5P compared to that in A20F2P.
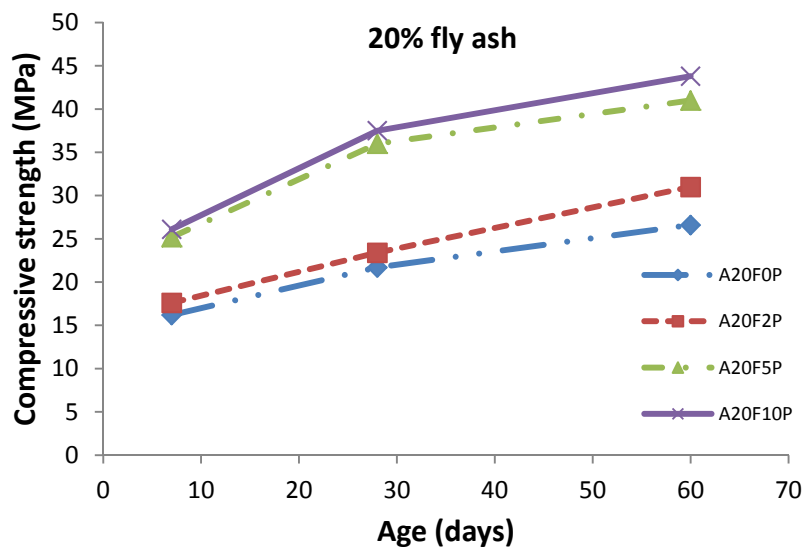
Fig. 5-22 Effect of age of concrete on compressive strength

5-2-3 Density, Absorption and Volume of Permeable Voids in Hardened Concrete

The volume of the permeable voids is shown as a function of the age of test and PAC content in Figures 5-23a and 5-23b, respectively. The C.O.V. of the volume of permeable voids at 7, 28 and 60 days varies from 2.3% to 12.1%, 1.9% to 7.1% and 1.4% to 9.0%, respectively.

The results show that the longer-cured concrete had a lower volume of permeable voids. Increasing the hydration of the cement led to a filling of the air voids with the hydration product. As a result, the concrete with higher curing periods had lower permeable voids. Also, the results show that at the given age, the PAC percentage did not influence the volume of permeable voids.
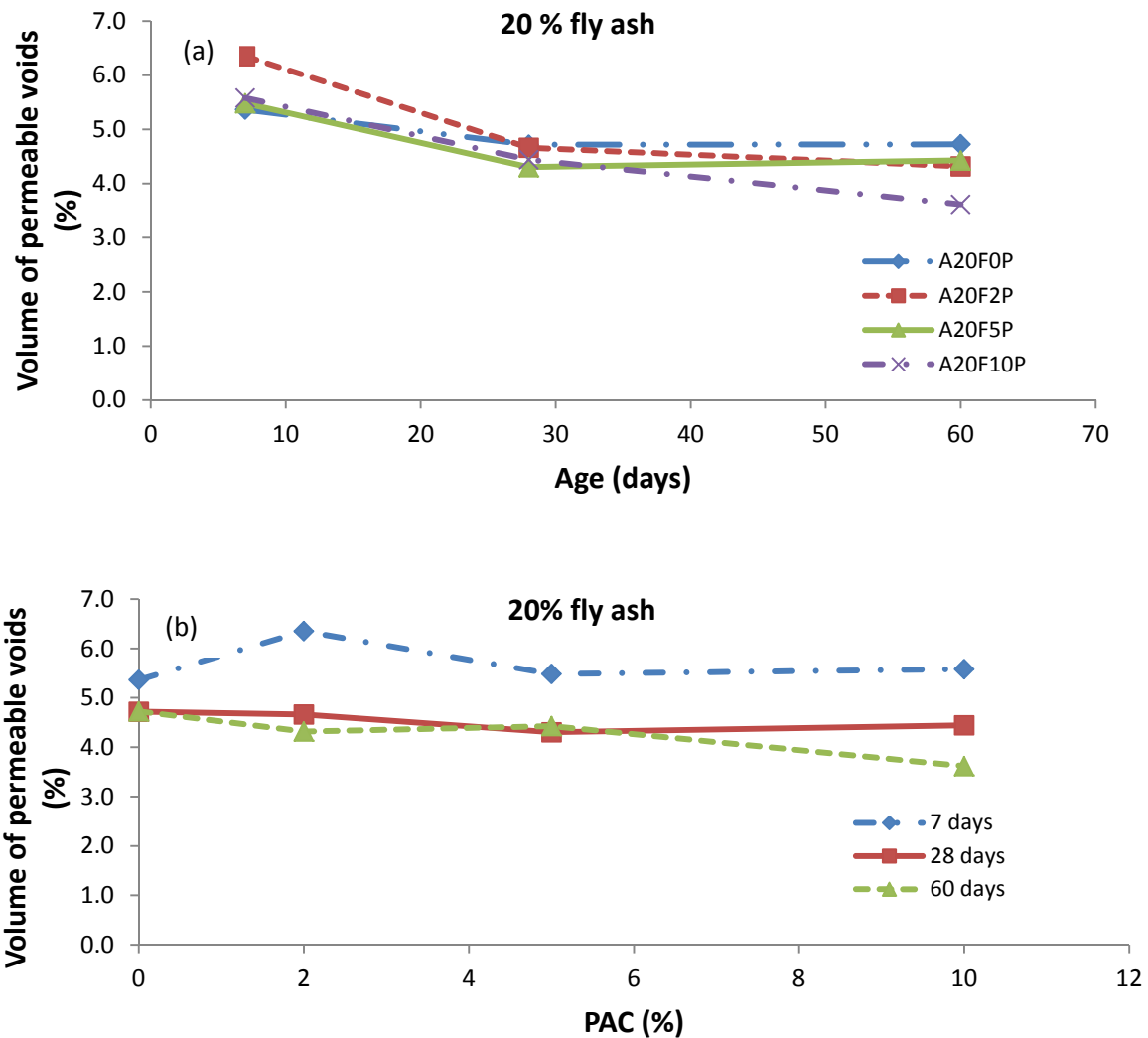
Fig. 5-23 Volume of permeable voids affected by a) curing time; b) PAC content

By looking at Figure 5-23, it can be concluded that there were no changes in the results of the volume of permeable voids when 2, 5 and 10 % of PAC were added. This trend was valid for

7 and 28-day concrete. However, adding 10% PAC (A20F10P) to concrete cured for 60 days decreased the volume of permeable voids by 23%. Lomboy and Wang (2009) compared the results of concrete with and without AEA which is similar to Series #1 and 2 of this study. They concluded that concrete with AEA had slightly lower compressive strength but higher porosity compared to concrete without AEA. The current study confirms their findings. Also, Saricimen et al. (1992) carried out a series of tests on concrete containing 20% fly ash replacement. Their results showed that the volume of permeable voids in concrete containing 20% fly ash and cured for 7 days, was lower compared to the plain concrete due to pozzolanic reactions. Similar results and trends for 20% fly ash replacement were also reported by Haque and Kayyali (1989).

The absorption after immersion and boiling is shown as a function of the PAC content and age at testing in Figures 5-24a and 5-24b, respectively. The results show that with an increase in the age of concrete, the absorption after immersion and boiling decreased in all mixes. Also, it is seen that for 7 and 28-day old concrete, an increase in the PAC content did not affect the boiling absorption, which is similar to the results for the volume of permeable voids. In a study by Zhou et al. (2007) the effect of fly ash containing concrete friendly PAC on the air-void characteristic of concrete was investigated. This concrete friendly PAC was a brominated carbon-base mercury sorbent which adsorbs very little of the concrete AEA. They concluded that the air void content and slump of concrete containing concrete friendly PAC contained fly ash were the same as the reference concrete. They also demonstrated that concrete friendly PAC does not influence the stability of air voids. The typical properties of a concrete friendly PAC were reported in Section 5-1-2. Meanwhile, it is worth restating that the concrete friendly PAC adsorbs the mercury but it has no detrimental effect on the air-void characteristics of concrete. It

should be noted that in this study, however, a conventional powdered activated carbon was used, as per the intent of the local thermal power plant.
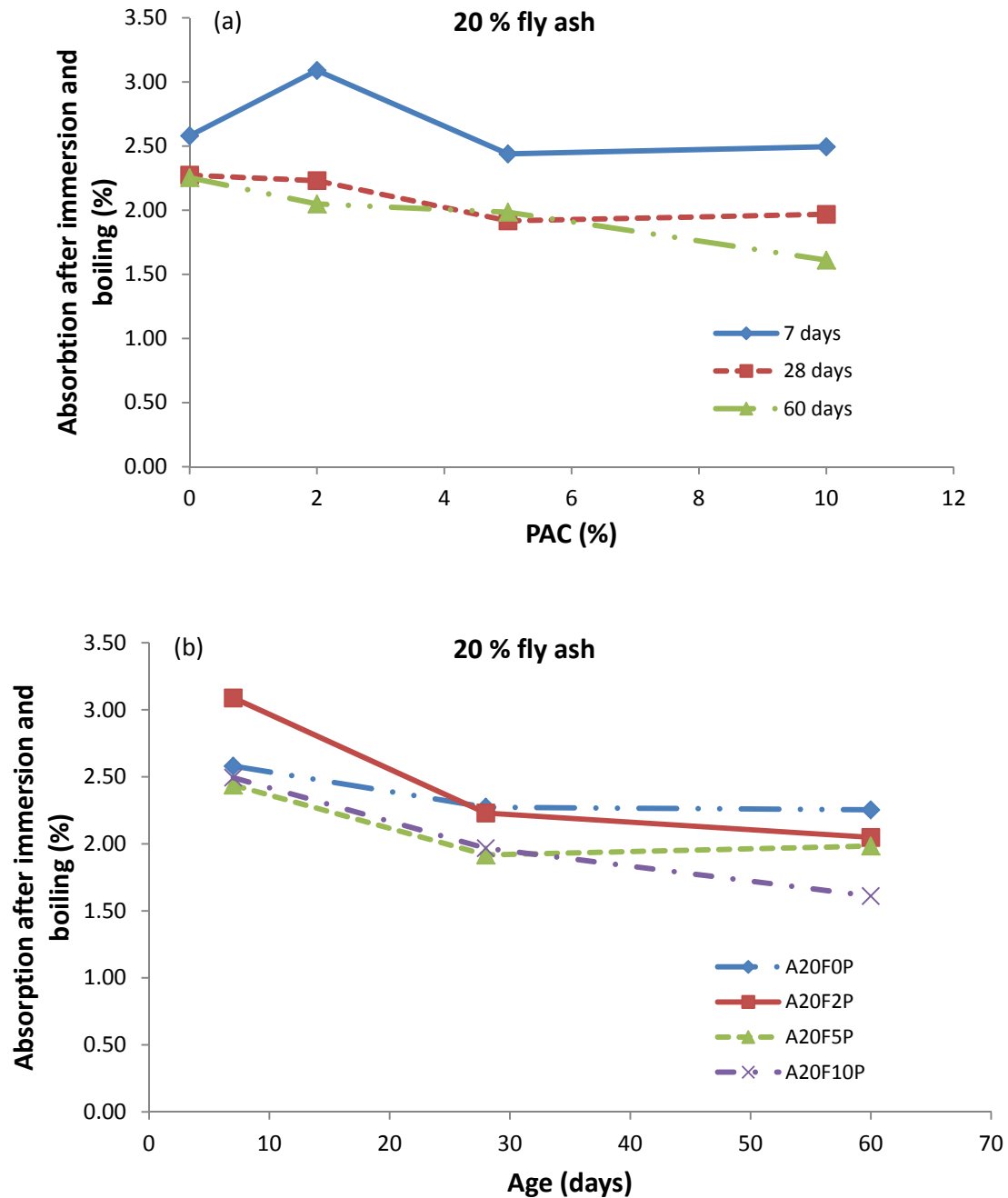
Fig. 5-24 a) Effect of PAC on the boiling absorption; b) effect of aging time on the boiling absorption of concrete containing fly ash and PAC

5-2-4 Image Analysis

5-2-4-1 The observation on epoxy-impregnated samples

Figure 5-25 shows the air void content of hardened concrete obtained by the image analysis method. In the first part, the results of the epoxy-prepared samples are presented. Later, the results of the ink-prepared samples are discussed.
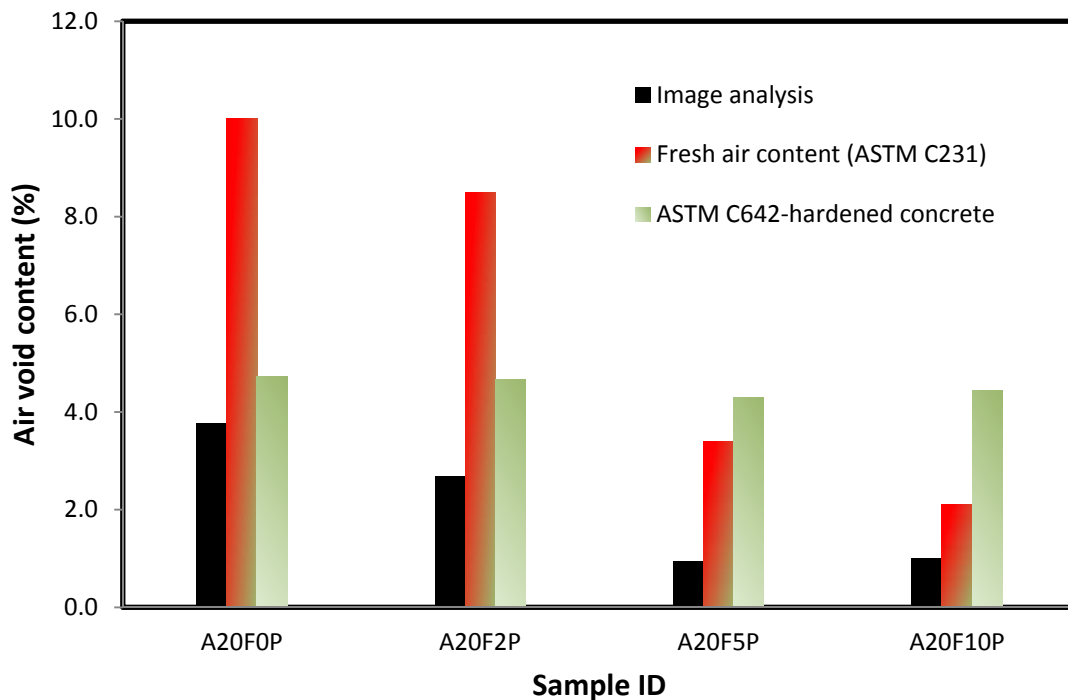
Fig. 5-25 Comparison of the air void content obtained by different test methods

The results of the image analysis indicate that the air void content of the mixes decreased when the PAC percentage increased. This trend is in agreement with the air void content of fresh concrete. However, the order of the results of the image analysis and fresh air void content values was completely different. It is observed that the fresh air void content was about two times higher than the air void content obtained by image analysis.

Figure 5-26 shows the effect of PAC on the spacing factor. It is clear that an increase of the PAC content led to an increase of the spacing factor. This is expected due to the lower air void content of the mixes with a higher PAC content. The results show that adding 10% PAC (A20F10P) increased the spacing factor by 43%. A higher spacing factor reveals that the distance between voids is higher; in other words, fewer voids exist in the paste due to the effect of the PAC on the absorption of AEA. This increase in the spacing factor might have a negative effect on the concrete which is exposed to freeze-thaw cycles. As stated in Section 3-4-3, according to Powers (1949), the lower the spacing factor the more durable the concrete will be.
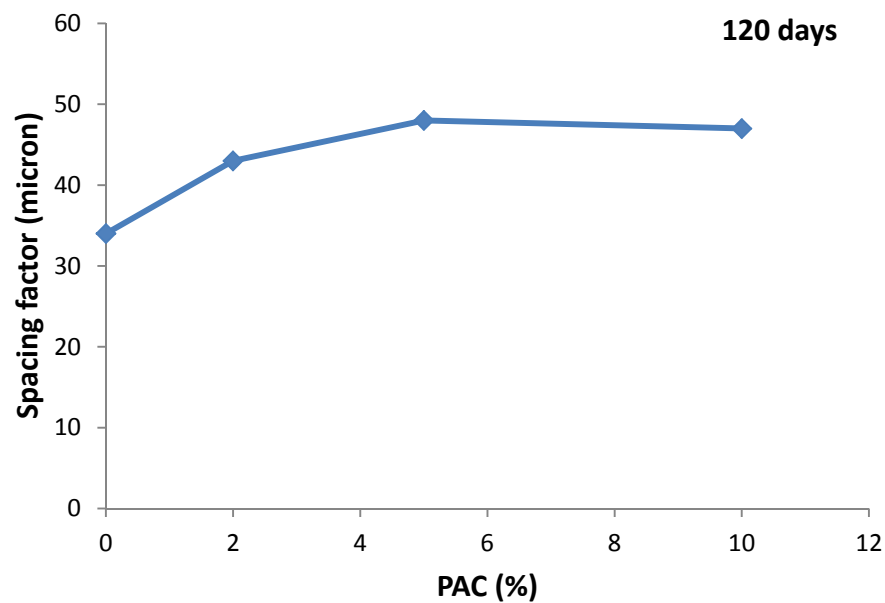
Fig. 5-26 Effect of PAC on the spacing factor of concrete with FA at 20% of binder

The effect of PAC on the specific surface area is illustrated in Figure 5-27. In general, it is evident that an increase in PAC leads to an increase in the specific surface area. A 44% increase in the specific surface area was observed when 10% of PAC was added to the mix compared to the mix without PAC. One may expect that PAC affected the larger air voids by eliminating them which led to a higher specific surface area.
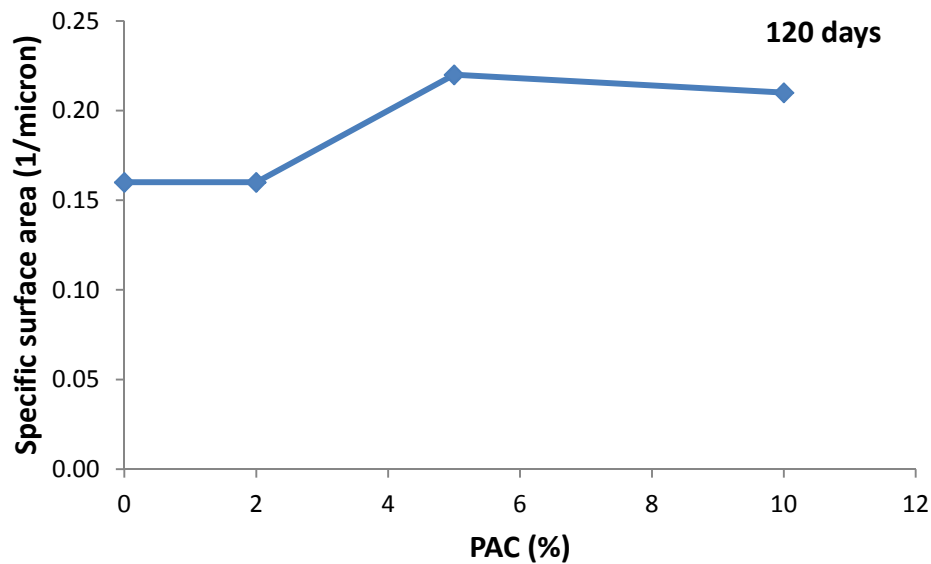
Fig. 5-27 Effect of PAC on the specific surface area

Figure 5-28 illustrates the results of the mean shape factor for mix with different PAC content. Similar to Series #1, the shape factors were in limited ranges and no specific changes can be seen in the values as the PAC quantity changed. It should be noted that the above results are related to the image analysis of specimens which were prepared using the epoxy-impregnated technique. In Section 5-2-4-2 the results of the image analysis technique performed on the ink-

prepared samples are presented. Two magnifications were used in presenting the air-void characteristics of the mixes.
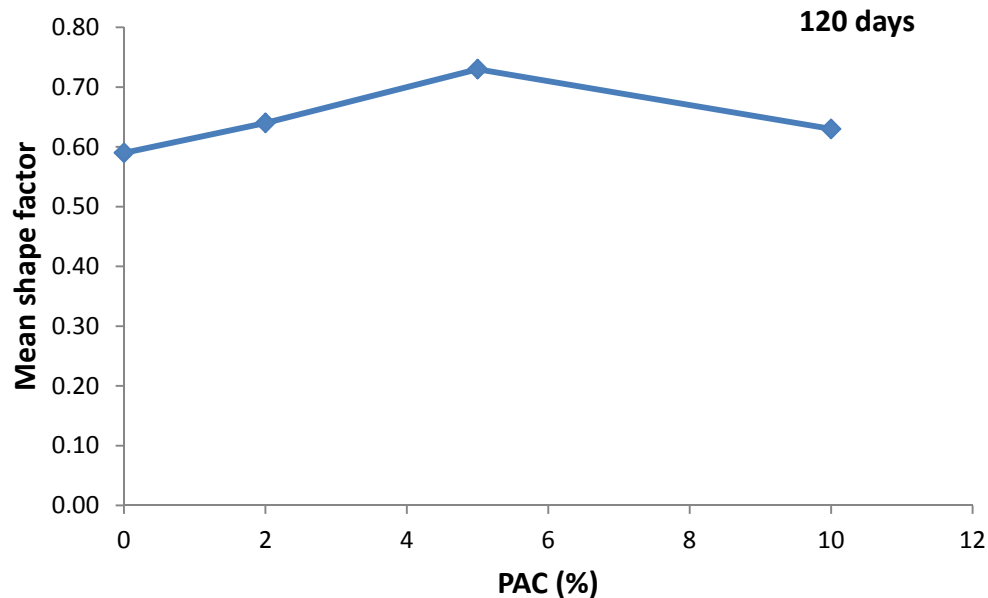
Fig. 5-28 Effect of PAC on the mean shape factor

5-2-4-2 The observation on ink-prepared samples

The results of the ink-prepared samples are summarized in Table 5-3. The results indicate that the air void content of mixes measured by the X60 magnification was higher compared to the X100 magnification. However, it was found that the air void content decreased by increasing the PAC percentage for both magnifications. This result (obtained from the image analysis method) is in agreement with the results of the air void content of fresh concrete obtained by the ASTM C231 (2009) standard test method. It can be seen that both magnifications, X60 and X100, resulted in the same values for the spacing factor and mean shape factor, but the results of the specific surface area show different values for these two magnifications.

Table 5-3 Results of the image analysis method for ink-prepared samples

	Magnification	Mix ID			
		A20F0P	A20F2P	A20F5P	A20F10P
Air void content (%)	60	9.13	4.28	4.48	1.00
	100	5.92	2.38	2.86	1.13
Specific surface (mm^{-1})	60	21.00	49.00	20.00	43.00
	100	35.00	85.00	28.00	38.00
Spacing factor (mm)	60	0.08	0.07	0.24	0.38
	100	0.07	0.07	0.21	0.37
Mean shape factor	60	0.71	0.70	0.66	0.65
	100	0.71	0.78	0.80	0.68

The effect of PAC on the specific surface area obtained at the lower magnification, X60, is presented in Figure 5-29. In this case, the results were very scattered, and no conclusion could be drawn. However, it can be seen that the specific surface area was within the range of 20-49 mm^{-1}. Zhang and Wang (2006) used the Rapid Air Test to evaluate the specific surface area of concrete containing 15% fly ash. The results of the current study confirm the results of the study conducted by Zhang and Wang (2006), as they showed that the specific surface area of mixes changed in the range of 21.8-60.0 mm^{-1} depending on the mixing time (it should be noted that

the mixing time was not a factor investigated in the current study). However, the same mixes were tested by Zhang and Wang with another technique, Air Void Analyzer, and the results show that the specific surface area changes in the range of 20.7 mm^{-1} 28.0 mm^{-1} (Zhang and Wang 2006).
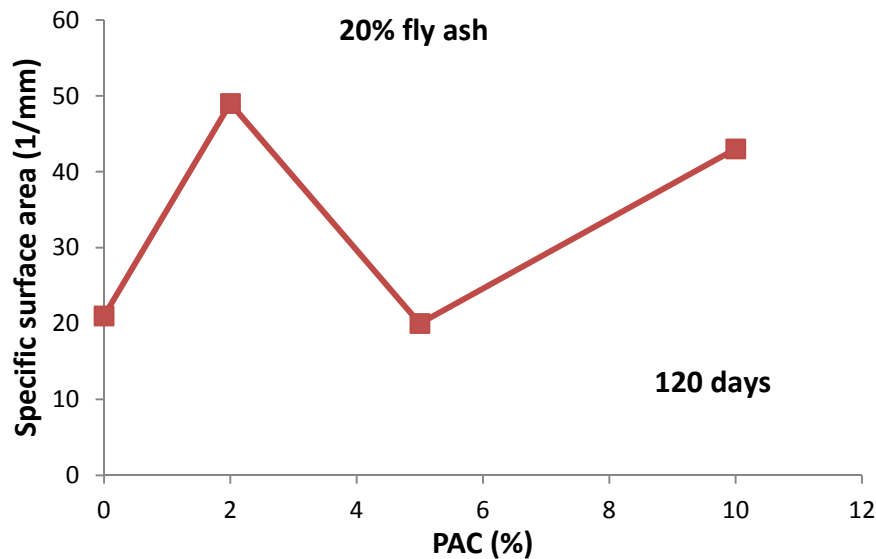
Fig. 5-29 Effect of PAC on the specific surface area

Figure 5-30 shows the results of the spacing factor obtained at the lower magnification (X60). It is seen that an increase in the PAC content led to an increase in the spacing factor. By adding 10% PAC to the plain concrete mixture (A20F0P), the spacing factor increased by about four times. This happened in mixes with a higher PAC content as the air void content was lower in those mixes. This led to an increase in the distance between air voids. It is worth restating that the difference between Figures 5-26 and 5-30 is due to the application of different preparation techniques. Whereas the specimens described by Figure 5-26 were obtained from epoxy-

impregnated method, the specimens described by Figure 5-30 were obtained from the inked preparation method.
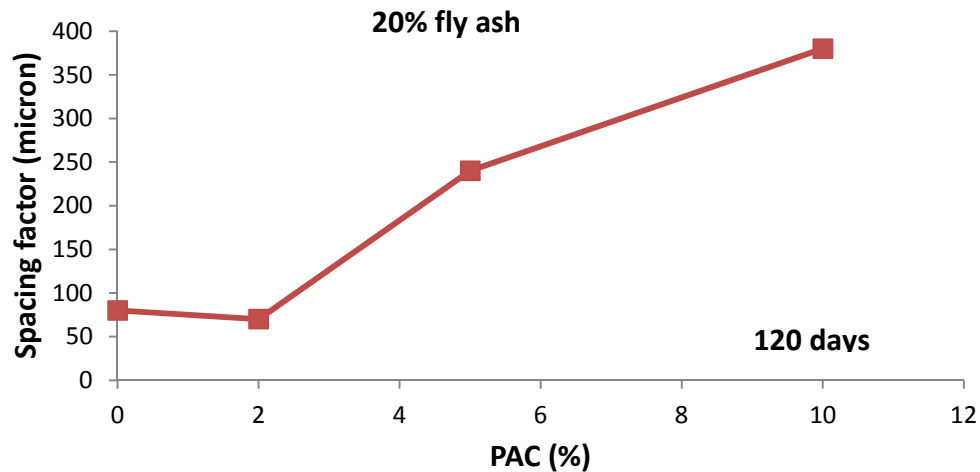
Fig. 5-30 Effect of PAC on the spacing factor of concrete with FA at 20% of binder

Figure 5-31 shows the results for the mean shape factor obtained at the lower magnification (X60). The results show that the mean shape factor was within a narrow range of 0.65 to 0.71. However, a drop in the shape factor is seen in the mixes with a higher PAC content. The results show that the shape factor decreased by 8% with an increase of PAC content from 0% to 10%. This drop indicates that with the higher PAC content, the shape of the voids became more irregular compared to a perfect spherical void. One may assume that merging the perfect spherical voids resulted in making the voids with the irregular shape. It is also possible that in the mixes with a higher PAC content the entrained air replaced with the entrapped air which led to a lower shape factor compared to the mixes with a lower PAC content.
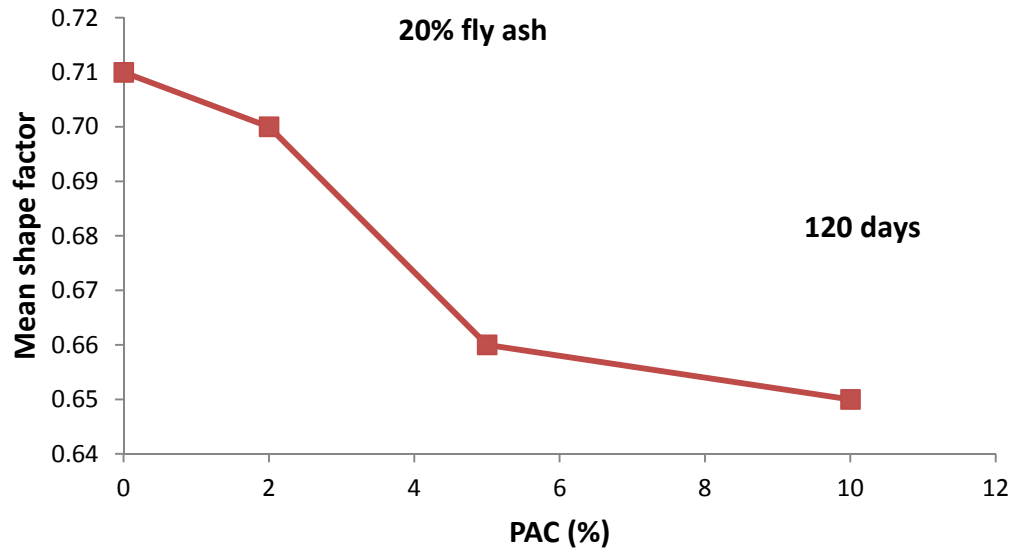
Fig. 5-31 Effect of PAC on the mean shape factor

5-2-4-3 Comparison of the air-void characteristics obtained from both sample preparation techniques

In this section, the results of the air-void characteristics obtained from both sample preparation techniques are compared. The results of the air void content shows that the inked samples led to values closer to the values of the fresh air void content, compared to the epoxy-impregnated samples. Specifically, the air void content of the epoxy-impregnated samples was almost 2 times lower than that of fresh concrete, whereas good agreement can be seen between the results of inked samples and the fresh concrete. The results of the spacing factor for the inked samples (at X60 magnification) vary from 80 to 380 microns whereas the values for the epoxy-impregnated range between 34 to 47 microns. Recall that the air void content of fresh concrete for A20F10P was measured at about 2%. CAN/CSA A 23.1 (2000) suggests that a maximum spacing factor of 230 microns can be obtained in concrete containing AEA; (high air void

113

content can be achieved in concrete containing AEA). However, the results from the epoxy-impregnated samples show a low spacing factor despite the low air void content of concrete. Meanwhile, a higher spacing factor (380 microns) reported for the inked sample of A20F10P is reasonable when compared to the suggested CAN/CSA A23.1 value. Therefore, it can be concluded that the result of the spacing factor obtained from the inked-samples provides a more accurate value compared to the epoxy-impregnated ones. Also, with regard to the specific surface area values found in this study, the inked samples led to a closer value to other studies compared to the epoxy-impregnated ones. While the specific surface area of inked samples containing 20 percent fly ash varies between 20 mm^{-1} to 49 mm^{-1}, this parameter was measured as about 200 mm^{-1} for the epoxy-impregnated samples. Recall that Zhang and Wang (2006) reported the specific surface area of concrete containing 15% fly ash as about 40 mm^{-1}. Therefore, it can be concluded that similar to the air void content and spacing factor, the inked samples provided more reliable results for the specific surface area compared to the epoxy-impregnated ones. Nonetheless, it should be emphasized that since no third technique was implemented, it is difficult to judge the accuracy of the results of the spacing factor and specific surface area. However, based on the above discussion, and that in Section 4-2-5, the visual inspection of the prepared samples and the images obtained from both techniques convinced the author that the inked samples can provide more reliable results compared to the epoxy-impregnated one.

5-3 RESULTS OF SERIES #3

In this section, the fresh and hardened properties of Series #3 are described. One can find the results of the performance of fresh concrete, compressive strength at different ages, the ASTM C642 (2006) Standard Test Method and image analysis in this section. All individual results with the coefficient of variations are listed in Appendix #3. Recall that in this series, an air-entraining admixture at 0.5% of the total binder weight and fly ash from the Genesee power plant were used to investigate the effect of AEA on concrete made with fly ash. The AEA was used at the same content as those used in Series #2 and Genesee fly ash replaced up to 80% of the cement weight. As mentioned before, this fly ash came from a power plant where PAC was directly injected into the flue gas ahead of the precipitator. It is worth restating that the PAC content of the Genesee fly ash was evaluated earlier in Section 4-1-2 and taken here as and assumed value of 2% by weight of fly ash.

5-3-1 Properties of fresh concrete

The results for the air void content of fresh concrete are presented in Figure 5-32. The C.O.V. of the air void content varied from 0.0 to 2.8 %. As can be seen, the air void content of all mixes was in a narrow range between 8.7% and 13.0% and an increase in fly ash did not change the air void content of the concrete.
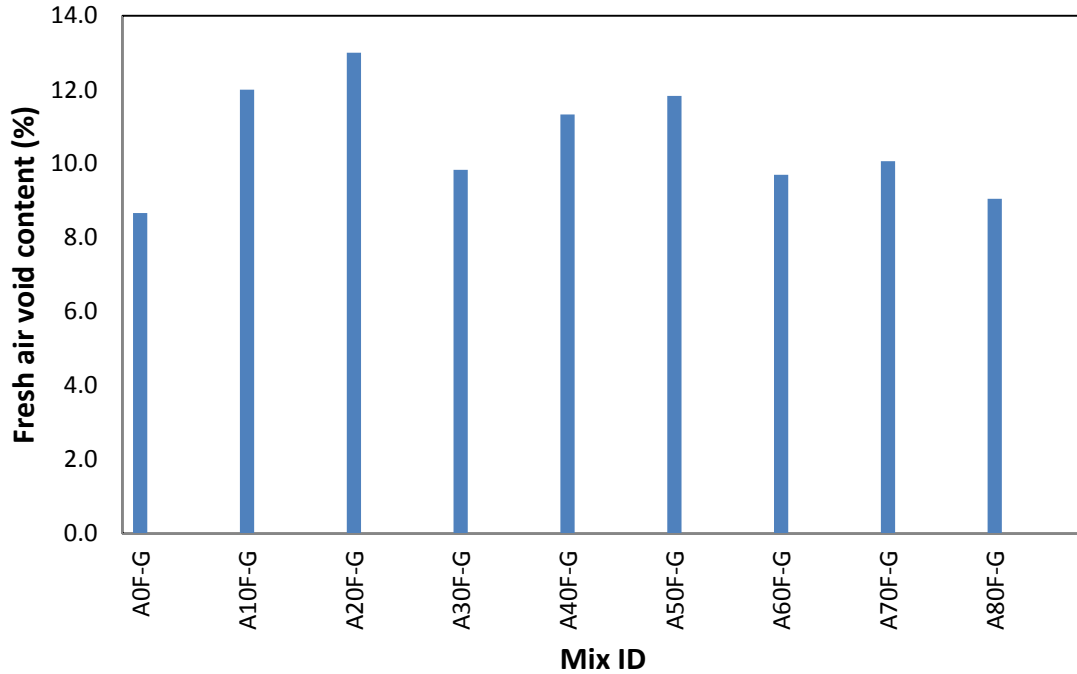
Fig. 5-32 Air void content of fresh concrete for Series #3

It is worth restating that limestone and silica fume were used in the mixes containing 70% and 80% fly ash. However, these powers cannot affect the air void content and absorption of concrete. At the fresh stage, it is too early for silica fume to react with the hydration product. On top of that, the order of magnitude of surface area for PAC is considerably higher compared to both silica fume and limestone. Therefore, one may ignore the effect of silica fume and limestone on the air void characteristics of high volume fly ash concrete. Meanwhile, at the later ages, silica fume cannot access to sufficient calcium hydroxide as the cement content was too low in those mixes. Concrete containing up to 80% fly ash did not show a decrease in the air void content compared to concrete without fly ash. As a result, it does not appear to be a challenge to entrain air for concrete in its fresh state. Recall that the PAC content of the Genesee fly ash was assumed as 2% of this pozzolanic admixture. So, one may assume that since A20F2P and A20F-G contain the same amount of PAC, they should display a similar air void content.

116

Nonetheless, the air void content of A20F-G was 50% higher compared to A20F2P which shows that PAC adsorbs more AEA when the PAC was added during the post-production process compared to fly ash being injected with PAC in front of the precipitator. Expanded discussion of this observation is provided in Section 5-4. The results of a study conducted by Hill et al. (1997) show that the adsorption properties of carbon play a role in AEA's performance. In other words, a higher content of fly ash, which leads to a higher content of carbon, does not necessarily affect the air entrainment. Their conclusion corresponds to the results for the air void content of fresh concrete obtained in this study. Meanwhile, it should be noted that the nature of the carbon discussed by Hill et al. (1997) is different from that of PAC, in that they used the loss of ignition (LOI) index to quantify the carbon content. This difference may lead to a varied performance compared to those with the same nature of carbon.

The density of fresh concrete is shown in Figure 5-33. Similar to the other series, the fresh density of the mixes was in the range of normal weight concrete (ACI 211 2009). Chaudry (2005) showed that the average fresh density of HVFA concrete with 50% fly ash replacement by weight was 2372 kg/m^3, a 10% higher density compared to the fresh density obtained in this study. The results of a study by Siddique (2004) show that the density of HVFA concrete (40%, 45 and 50% fly ash replacement) varies in the range of 2398-2401 kg/m^3 which shows a difference of 12% compared to the results in Figure 5-33. In a study performed by Malhotra (1990), the density of concrete containing 60% fly ash in binder, without AEA, was reported as 2365 kg/m^3; a value which confirms the density of concrete containing high volume of fly ash reported by other researchers including Siddique and Khatib (2010).
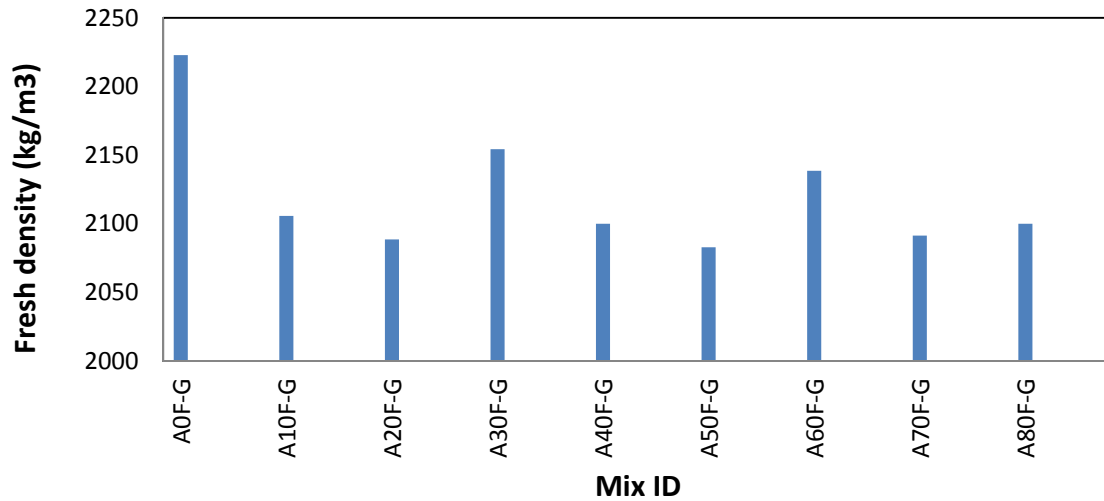
Fig. 5-33 Density of fresh concrete for Series #3

5-3-2 Compressive Strength

The results for the compressive strength are shown in Figure 5-34. The C.O.V. of the compressive strength at 3, 14, 28 and 60 days varies from 1.0% to 14.6%, 0.7% to 7.5%, 1.9% to 6.8% and 1.7% to 7.5%, respectively.
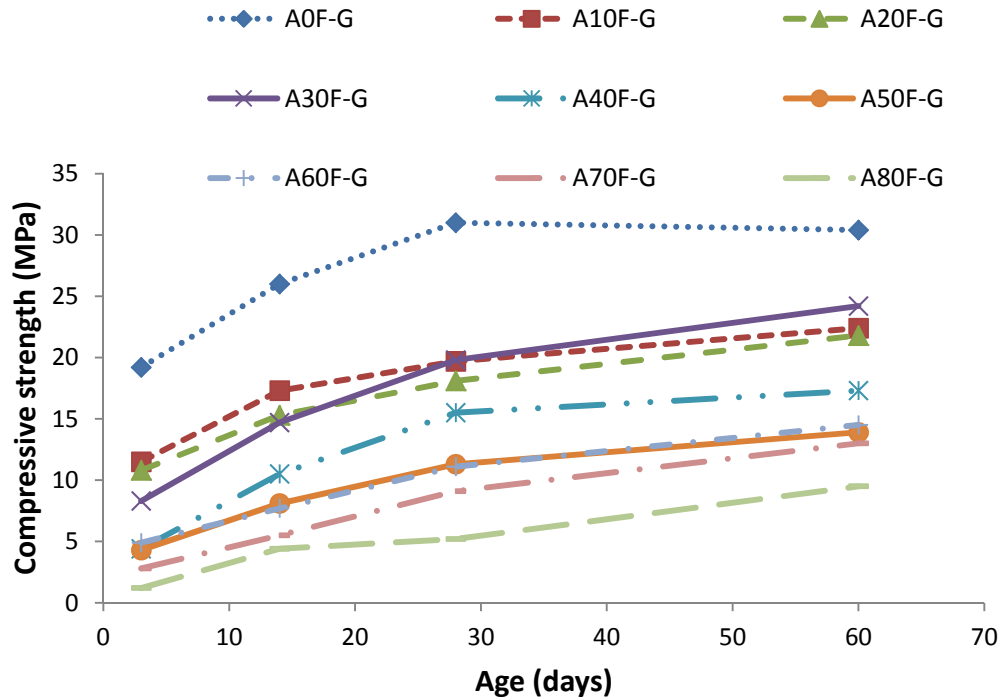
Fig. 5-34 Compressive strength of Series #3 mixes at different ages

For all mixes, it is seen that an increase in the age of the concrete led to an increase in the compressive strength. However, the rate of the increase varied depending on the percentage of fly ash replacement. For example, the gain in strength for the plain concrete with no fly ash (A0F-G) stopped after approximately 30 days, while the rate of increase of the compressive strength for the A80F-G sample was the highest from 30 days to 60 days. In hindsight, it should be noted that since a high volume of fly ash was used in Series #3, the compressive strengths should have been measured after longer curing times, say 120 days, due to the slower reaction rate of fly ash (Poon et al. 2000). As concrete kept gaining strength after 60 days for all mixes (except the plain one), it is impossible to make a conclusion about the final compressive strength of the mixes. One may also notice that in some mixes (A70F-G and A80F-G) limestone and silica fume were used where those powders could have an influence on the final compressive

strength. This conclusion can also be found in Figure 5-35 which shows the effect of fly ash percentage on the compressive strength of concrete cured for different durations. A decrease in the compressive strength is observed at all ages with an increase in the fly ash content. The obtained results are in good agreement with the results of a study performed by Nkinamubanzi et al. (2003). They showed that at early ages, the compressive strength of high volume fly ash concrete (W/B=0.32 and 55% fly ash replacement) was lower compared to that of plain concrete. They also showed that at 1 and 7 days the compressive strength of high volume of fly ash concrete was 58% and 26% lower compared to the plain concrete. Recall that the W/B ratio of the current study is higher than that used in Nkinamubanzi et al. (2003)'s. study The effect of the fly ash content and the age of concrete on the compressive strength of HVFA concrete containing up to 80% fly ash were also investigated by Montgomery et al. (1981). They found that HVFA concrete (cement/fly ash ratio= 40/60 by volume, without AEA) had a lower compressive strength compared to plain concrete at different ages. Meanwhile, they cured their samples up to 1 year, increasing the strength of the samples to 200%. In a study performed by Ramezanianpour and Malhotra (1995), concrete samples containing 58% fly ash which were cured under different conditions, were tested under uniaxial compression. Their results showed that HVFA leads to a lower compressive strength compared to plain concrete when the samples were cured up to 180 days.
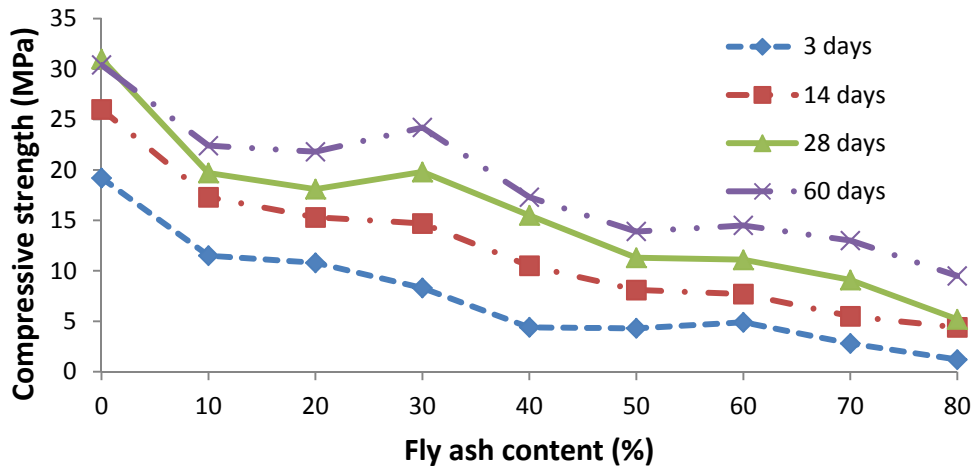
Fig. 5-35 Effect of fly ash content on the compressive strength

5-3-3 Density, Absorption and Volume of Permeable Voids in Hardened Concrete

The volume of permeable voids is presented as a function of fly ash content and the age at testing in Figures 5-36a and 5-36b, respectively. The C.O.V. of the volume of permeable voids at 3, 14, 28 and 60 days varied from 0.6 % to 3.7 %, 0.4 % to 38.8 %, 1.2 % to 35.8 % and 3.6 % to 91.8% %, respectively. The results show that with an increase in age, the volume of permeable voids decreased. This conclusion held true in all mixes but plain concrete, which showed the opposite trend. The volume of permeable voids for the plain concrete at 3, 28 and 60 days was obtained as 6.2%, 7.1% and 8.4%, respectively. The values of the volume of permeable voids at 28 days and 60 days were only 14% and 18% higher compared to the 3 and 60-day cured samples, respectively. Apaydin (2010) showed that the values of the volume of permeable voids of plain concrete (no fly ash) at 60 and 90 days are almost the same (the reported difference is less than 10%) compared to 28-day cured samples. The same conclusion can be drawn in the current study as the results showed no significant change.
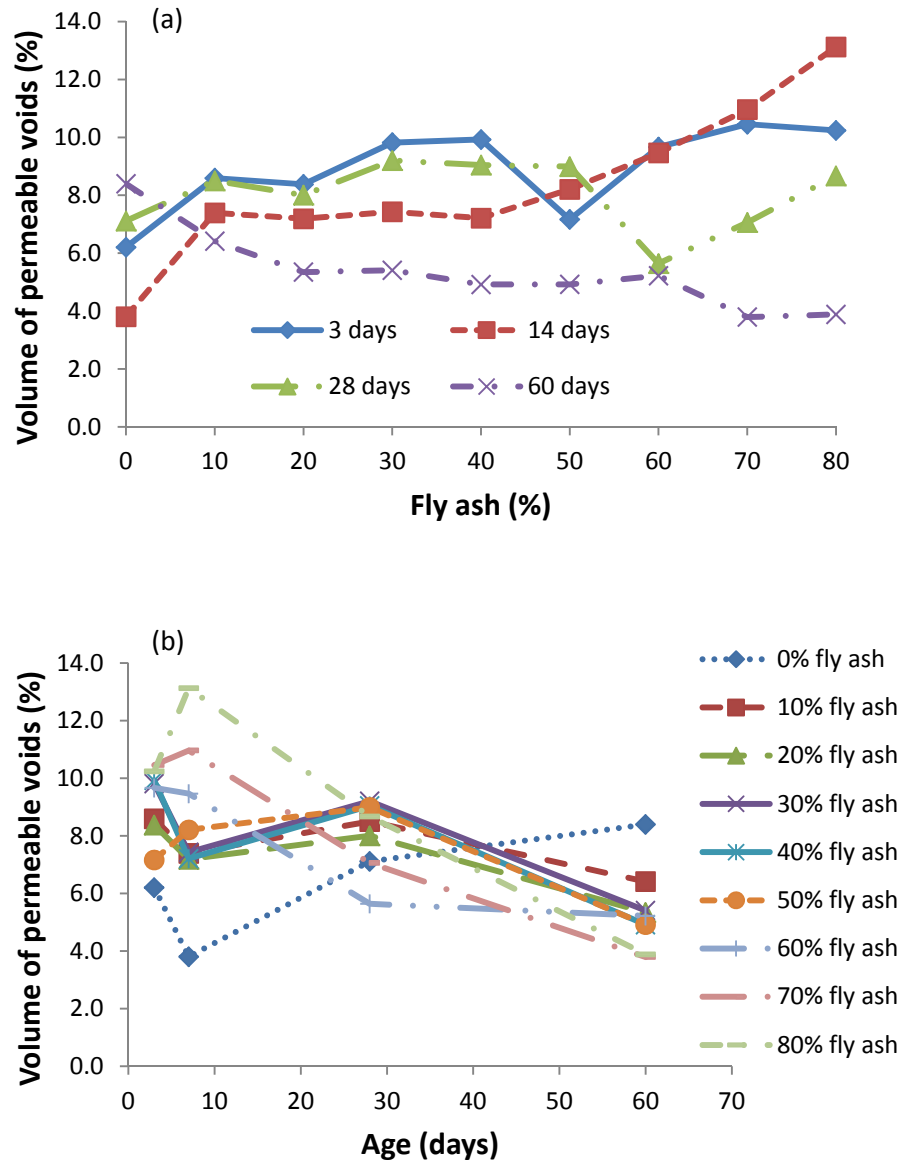
Fig. 5-36 Volume of permeable voids as affected by a) fly ash content; b) age of test

It can also be seen that an increase in the fly ash content resulted in an increased volume of permeable voids after 14 days of curing while a decrease was noticed after 60 days. After 14 days of curing, an 80% increase in the fly ash content increased the volume of permeable voids of the concrete by 200%; at 60 days, the volume of permeable voids decreased by 50%. In other words, there is no clear relationship between the fly ash content and the volume of permeable

voids. Meanwhile, Dinakar et al. (2008) believed that the fly ash content has a significant bearing on the volume of permeable voids in concrete. They showed that in concrete incorporating high volume of fly ash (up to 85 % of cement replacement) the corresponding permeable voids were higher. They concluded that this might be due to the high paste volumes and high water content, which resulted in increased porosity.

The effect of fly ash content on the apparent density, bulk density after immersion, absorption after immersion, and absorption after immersion and boiling is shown in Figures 5-37a, 5-37b, 5-37c and 5-37d, respectively. In general, the results are very scattered to draw any concrete conclusions. However, one may conclude that the absorption of concrete containing higher amounts of fly ash (A70F-G and A80F-G) is higher compared to concrete with a lower fly ash content (A10F-G).

The effect of the age of the concrete on the absorption after immersion and bulk density after immersion is shown in Figures 5-38a and 5-38b, respectively. One may conclude that the absorption of concrete decreased with the age of the concrete, while there was no visible trend for the case of bulk density.
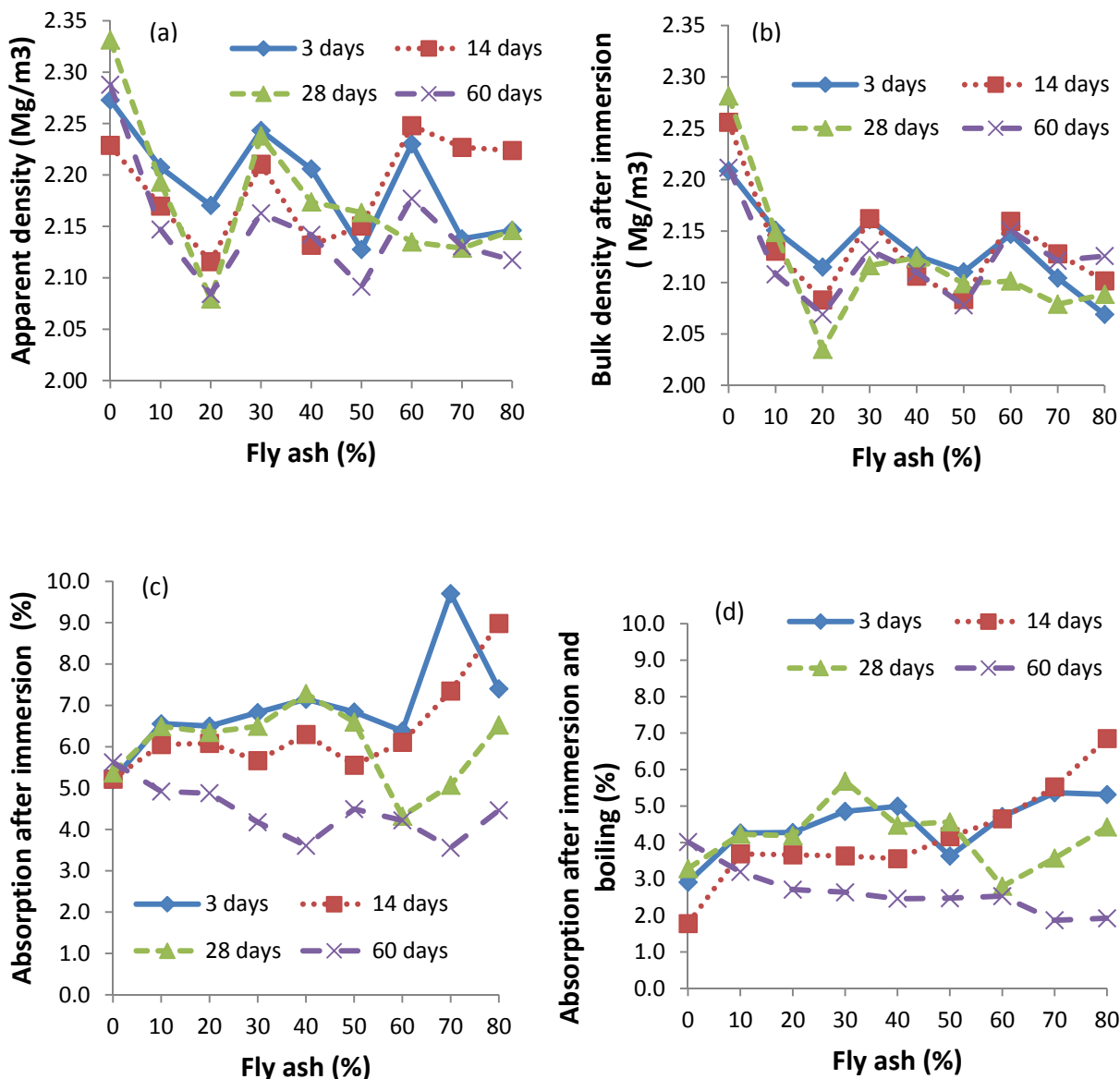
Fig. 5-37 Effect of fly ash content on the a) apparent density; b) bulk density after immersion; c) absorption after immersion; d) absorption after immersion and boiling
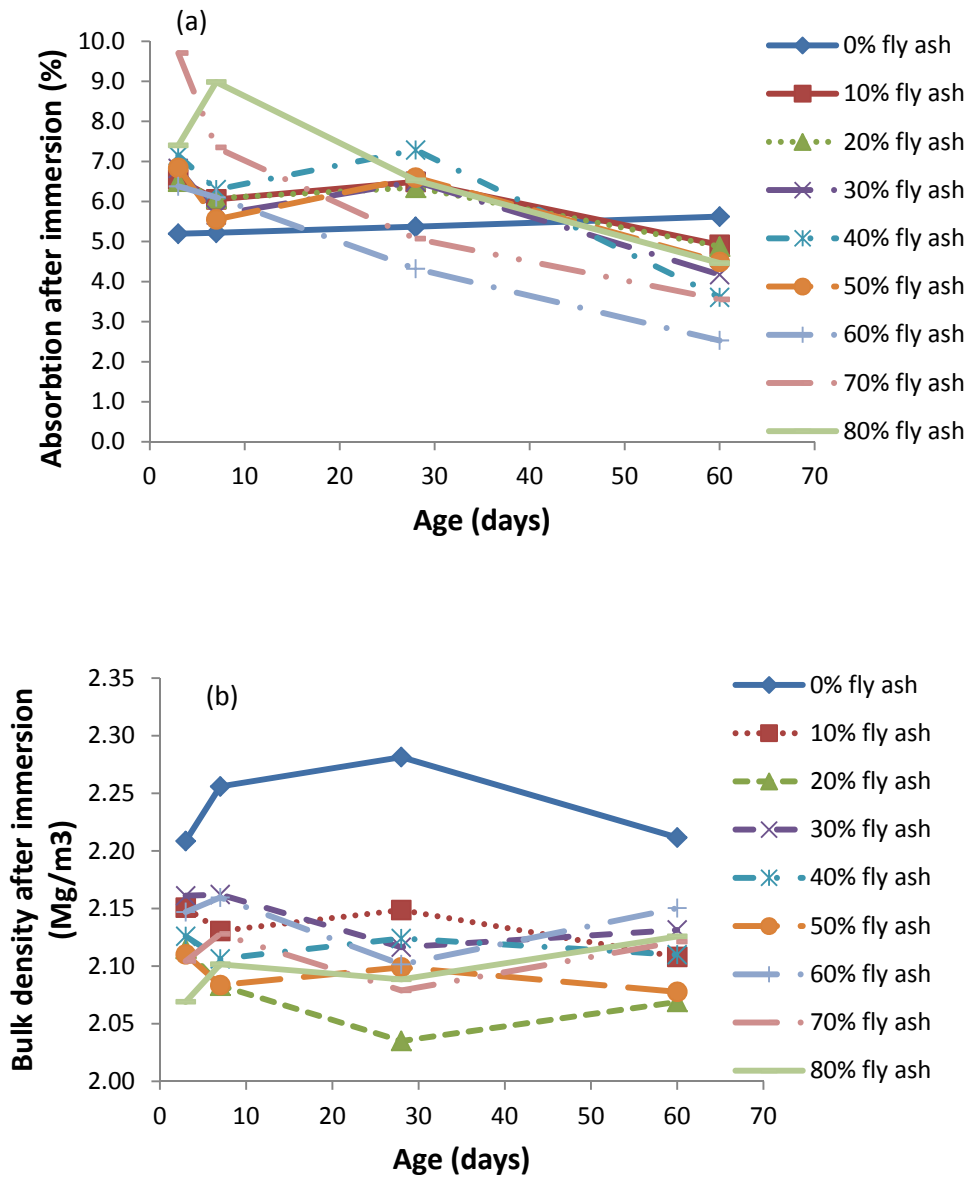
Fig. 5-38 Effect of age of concrete on the a) absorption after immersion; b) bulk

density after immersion

5-3-4 Image Analysis

The air void content of hardened concrete obtained by the image analysis method at the X60 and X100 magnifications is shown in Figures 5-39a and 5-39b, respectively. It should be noted that in Series #3, the samples were prepared solely via the ink method.

The results of the image analysis show that a high fly ash content does not affect the air void content of concrete. Therefore, one should not be concerned with the freeze-thaw resistance of concrete containing this type of fly ash. The results of image analysis with X60 magnification show that the three methods gave the same orders of magnitude for air void content. However, in the case of X100 magnification, the image analysis technique gave a lower air-content compared to the ASTM C231 and ASTM C642 test methods. It can be concluded that a lower magnification, say X60, is more reliable and therefore recommended.

The results for the specific surface area at the X60 and X100 magnifications are shown in Figures 5-40a and 5-40b, respectively. It was found that the order of specific surface area at the X100 magnification was about 10 times higher than at X60. The results of a study carried out by Glinicki and Zielinski (2008) revealed that an increase in the fly ash content by up to 40% leads to an increase in the spacing factor by 0.05– 0.10 mm and decreases the specific surface area by 9–12 mm^{-1}. However, in another study, Naik et al. (1995) demonstrated that an increase in fly ash replacement by up to 70% increases the specific surface area of concrete. These conflicting trends were also found in the current investigation. The author believes that although the results seem scattered, they were actually in the narrow range of 0.006 to 0.038 microns^{-1}.
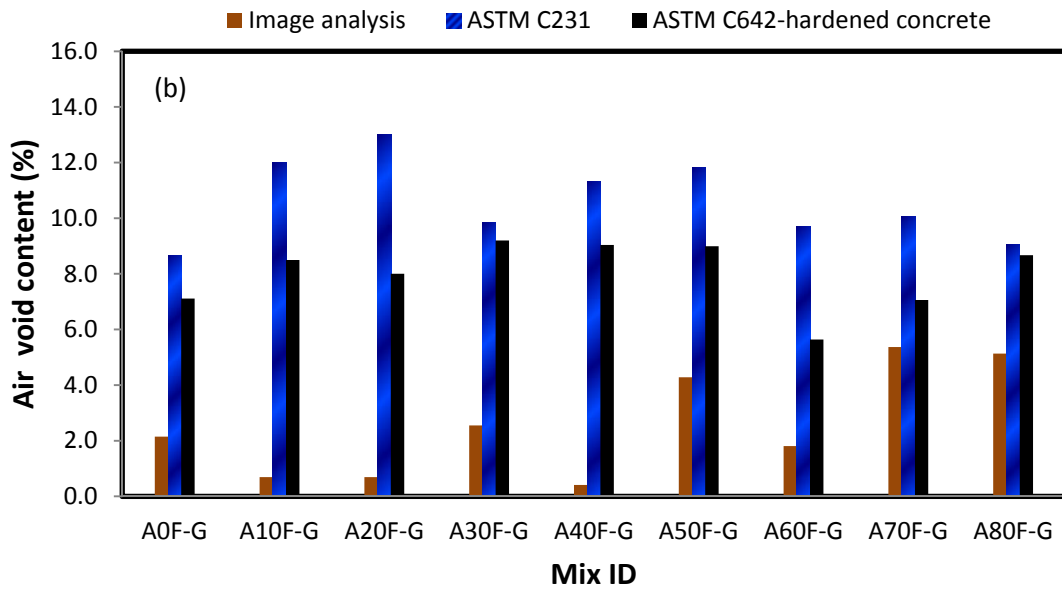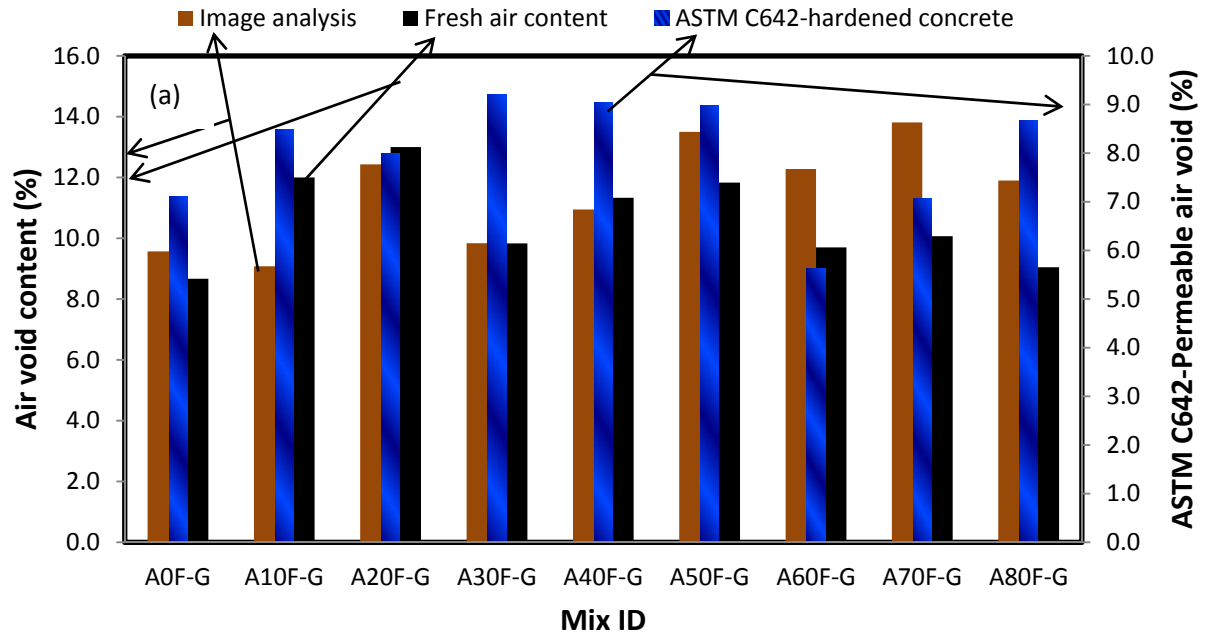
Fig. 5-39 Comparison of the air void content obtained by different methods: a) X60; b) X100
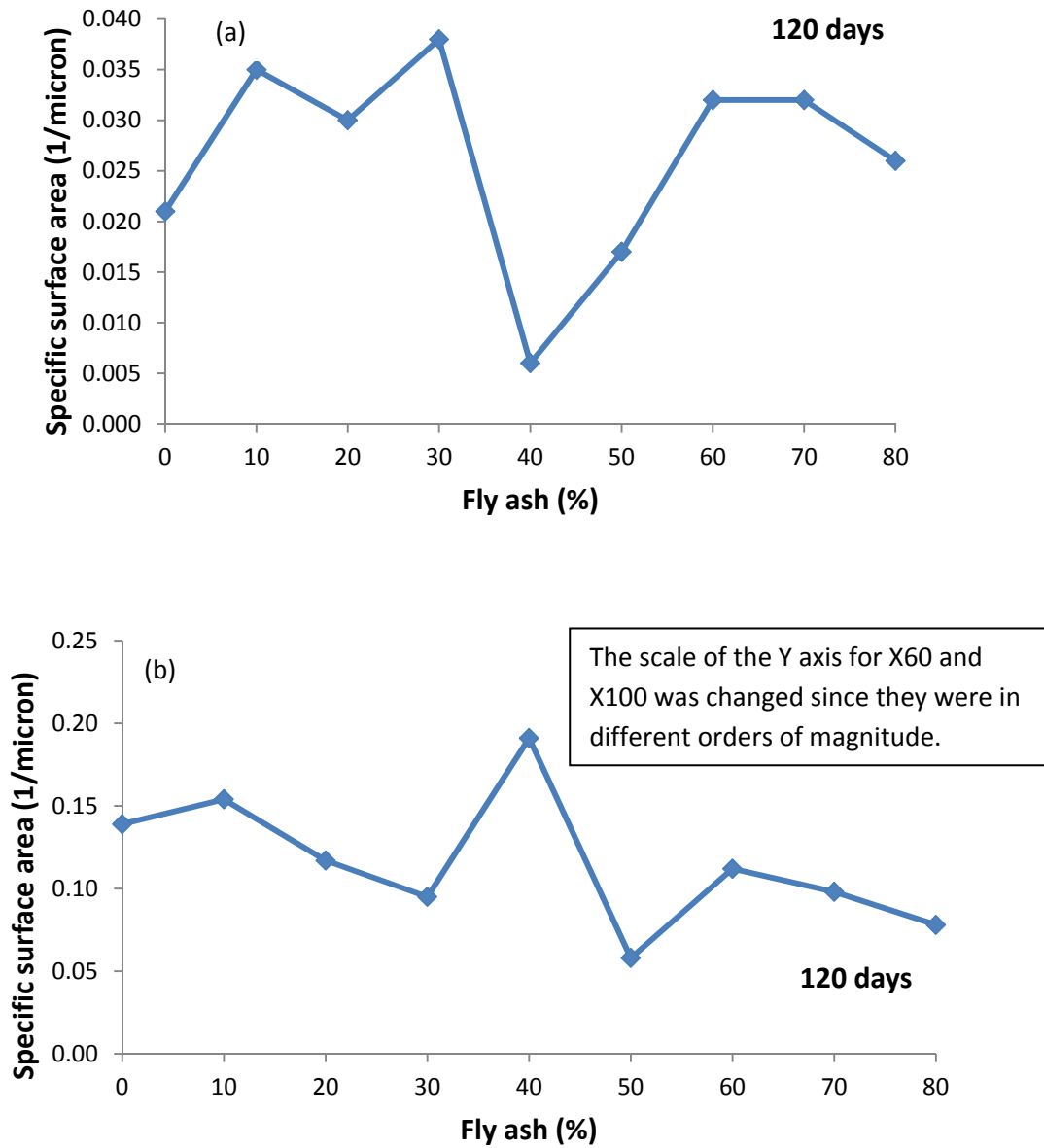
Fig. 5-40 Specific surface area: a) X60; b) X100

The results for the spacing factor at the X60 and X100 magnifications are shown in Figures 5-41a and 5-41b, respectively. The average of the spacing factors for different fly ash volumes obtained from the lower magnification, i.e. X60, is at a higher value compared to the higher magnification, i.e. X100. Pistilli (1983) showed that AEA in a higher soluble alkali Class C fly ash produces higher values for the spacing factor. Also, Naik et al. (1995) revealed that in HVFA concrete, an increase in the fly ash percentage decreases the spacing factor. Their results showed that 70% fly ash replacement in concrete decreased the spacing factor by 65%. Cox and De Belie (2007) measured the spacing factor of concrete containing both 50% and 67% fly ash. Their results showed that the spacing factor of concrete containing 50% fly ash decreased by 25% and 37% compared to plain concrete after 1 and 3 months, respectively. Reductions in the spacing factor for concretes incorporating 67% fly ash were also reported as 17% and 58% (Cox and De Belie 2007). However, the current study cannot confirm their results.

As discussed in Section 4-2-5, it seems that if the image analysis technique was performed on the cement mortar samples instead of on the concrete samples, the results would have been more accurate. It is recommended in the future to have a mortar sample containing cement, fly ash and PAC. Since there is no coarse aggregate in said sample, the air voids and the background can be more easily and more reliably distinguished. Recall that, aggregate is a porous material and its pores can be unintentionally included as the air voids of concrete.
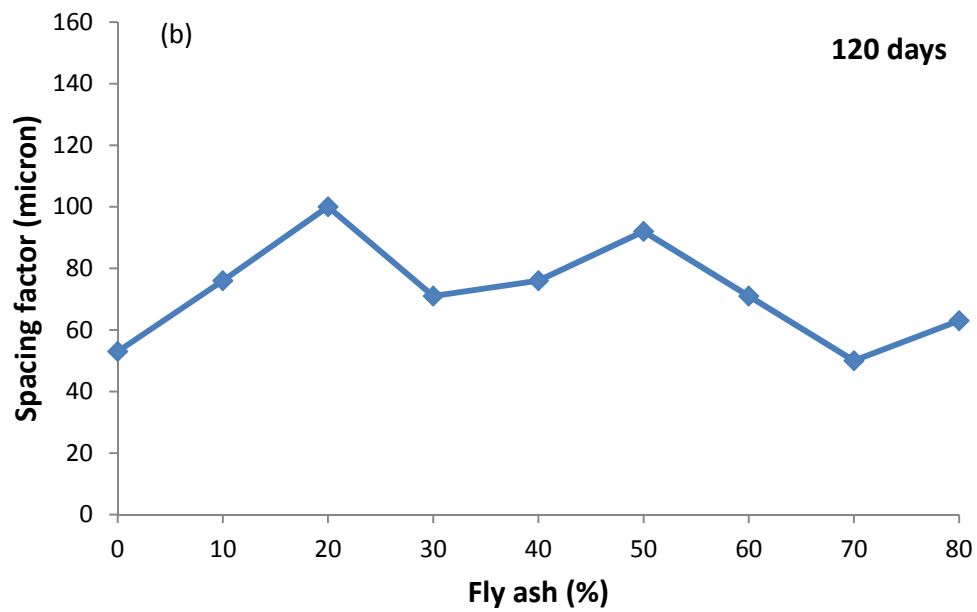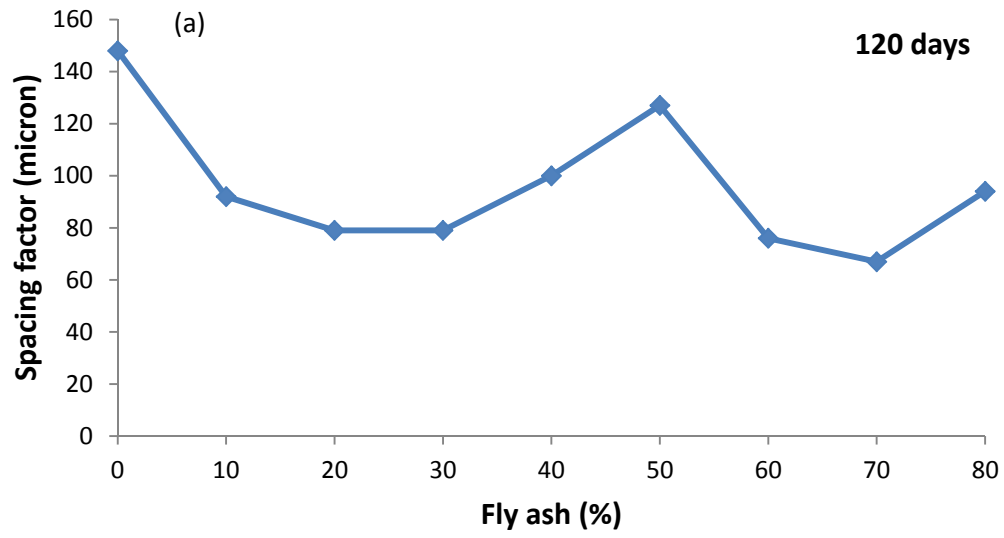
Fig. 5-41 Spacing factor: a) X60; b) X100

5-4 COMPARISON OF THE RESULTS

In Sections 5-1 to 5-3, the results of individual series were presented. In this section, these results are compared in hopes of drawing conclusions across the parametric study. This comparison will lead to a better understanding of the effect of PAC on the properties of concrete. Based on the different parameters examined in this study, the effect of the air entraining admixture and the mode of PAC addition are discussed in this section

.

5-4-1 Effect of Air Entraining Admixture

The effect of the air entraining admixture on the properties of concrete was determined by Series #1 and Series #2. In both series, mixes were prepared with 20% fly ash replacement and 0, 2 and 5% of PAC. In Series #1, no AEA was used whereas in Series #2 AEA was used at 0.5% of the total binder weight. Table 5-4 shows that as expected, the air void content of mixes containing AEA (Series #2) was higher compared to that of Series #1. It was also concluded that the fresh density of mixes with AEA was lower by 7-8 % (7, 7 and 8% for 0, 2 and 5% PAC, respectively) compared to the plain concrete with no AEA. Figure 5-42 and Table 5-4 show the fresh densities of mixes including and excluding AEA. AEA creates more pores in the concrete, which leads to lower density.

Table 5-4 Comparison of Series #1 and Series #2

	Series #1 (no AEA)			Series #2 (with AEA)		
PAC (%)	PAC=0%	PAC=2%	PAC=5%	PAC=0%	PAC=2%	PAC=5%
Air void content (%)	2.1	1.8	1.9	10.0	8.5	3.4
Density (kg/m^3)	2354	2355	2330	2178	2184	2127
Compressive strength (MPa)	36.5	35.4	35.1	21.7	23.4	36.0
Specific surface area (1/micron)	0.45	0.36	0.33	0.16	0.16	0.22
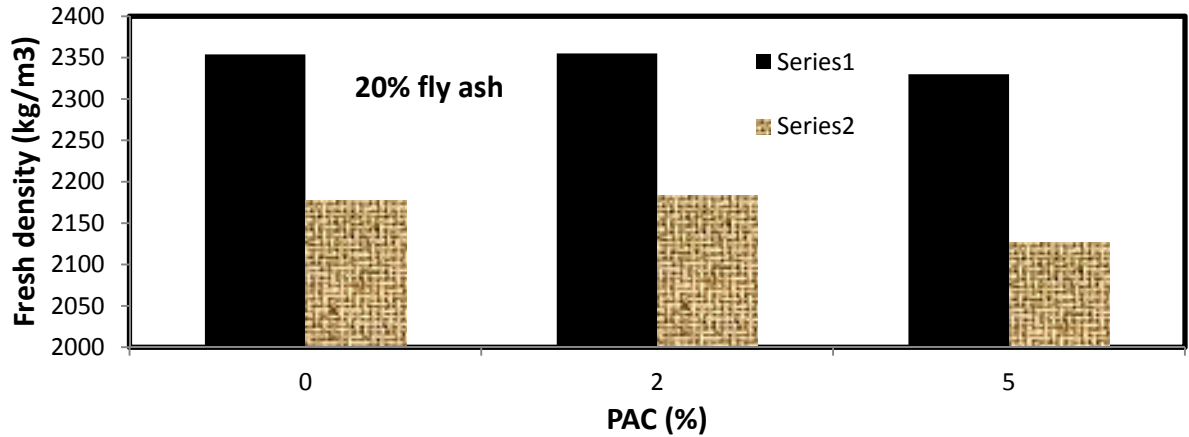
Fig. 5-42 Comparison of fresh density of Series #1 and 2

The comparison of results (A20F0P with 20F0P and A20F2P with 20F2P) from compression testing in Table 5-4 shows that mixes with AEA had a lower strength as expected. It is known that for each percent of air void, 5% of compressive strength is lost (Klieger and Lamond 1994). Figure 5-43 shows the comparison of compressive strength in both Series #1 and #2.
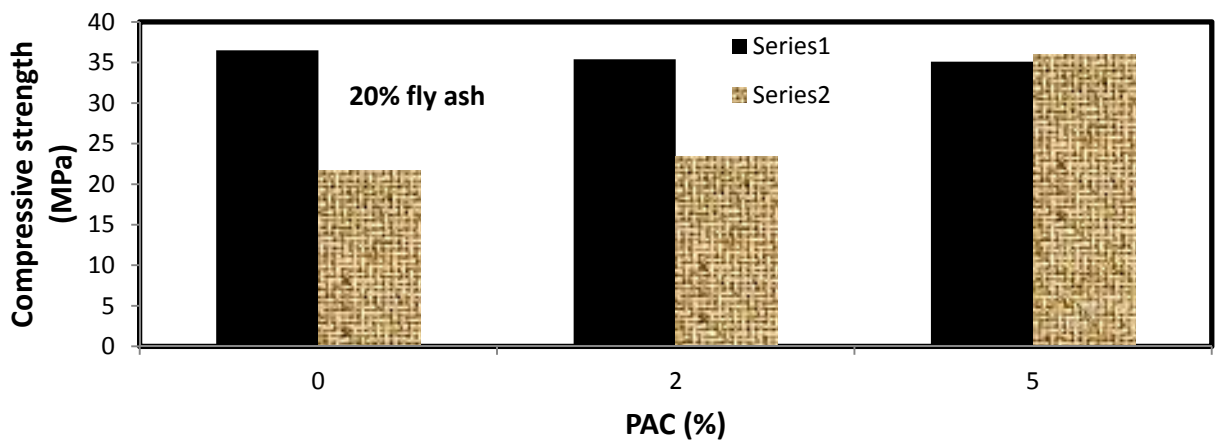
Fig. 5-43 Comparison of compressive strength of Series #1 and 2

The compressive strength of mixes at 28 days varies from 35 MPa to 37 MPa in Series #1 while for different PAC contents the compressive strength changed from 22 MPa to 37 MPa

when AEA was used. In mixes containing 20% fly ash and 5% PAC, the same compressive strength was measured for concrete with and without AEA (A20F5P and 20F5P). It was shown that a higher PAC content (5%) adsorbed more AEA, and resulted in a low air void content which can be attributed to the same compressive strength compared to the mix with no AEA. In general, with little or no PAC, AEA led to a higher air void content, and as a result, a lower compressive strength.

The volume of permeable voids at 28 days was the same for the mixes containing 0 and 5% of PAC in both the air entrained and non-air entrained concrete. However, in the mixes with 2% PAC, the volume of permeable voids of concrete with no AEA showed an increase by 60% compared to the mix with AEA (A20F2P). The absorption of concrete after immersion and boiling at 28 and 60 days is shown in Figures 5-44a and 5-44b, respectively. The results of absorption after immersion and boiling are also compared, see Figure 5-44, which indicates that at 7, 28 and 60 days the boiling absorption of concrete containing AEA (Series #2) is generally lower compared to the mixes of Series #1 (no AEA). In other words, AEA led to a decrease in the absorption of concrete. It is known that concrete with a higher air entrained content attributes to a concrete with higher porosity. Nonetheless, the lower slump in Series #1 compared to Series #2 (it can be seen from Appendices #1 and #2 that the slump of the mixes in Series #1 was about 3 times lower compared to the mixes in Series #2) may have led to a higher content of entrapped air in concrete in regard to the compaction deficiency, which attributed to the higher water absorption for concrete with no AEA compared to concrete containing AEA. It was also demonstrated that air-entrained concrete is more resistant to absorption compared to plain concrete (Perlite Info as of October 21th 2011), something in agreement with the results of this

study. Meanwhile, Klieger and Hanson (1961) showed that the water absorption of lightweight, air entrained concrete is similar to those for the non-air entrained mixes.
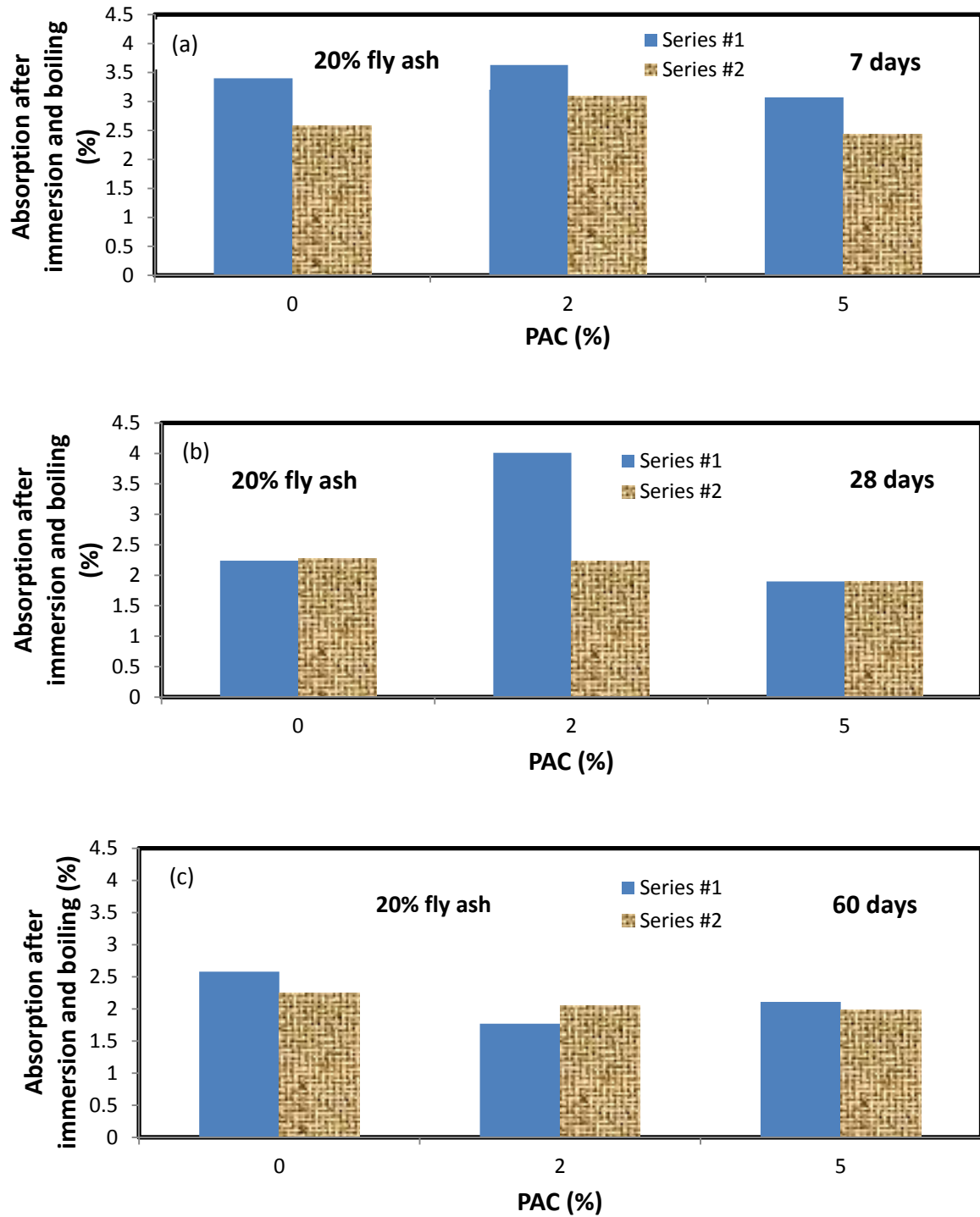
Fig. 5-44 Absorption after immersion and boiling at a) 7 days; b) 28 days; c) 60 days

Finally, comparing the results of specific surface area, Table 5-4, demonstrates that specific surface area of Series #1 was 1.5-3.0 times higher compared to Series #2. This is likely because in Series #2, the small air-entrained bubbles merged together to create bigger bubbles which would lead to a lower specific surface area, though the size of entrapped bubbles is generally bigger than air-entrained bubbles.

5-4-2 Effect of Mode of PAC Addition

In this section, mixes containing 20% fly ash replacement of cement by weight and 2% PAC from Series #2 and #3 were selected and compared. This comparison helps to examine the effect of PAC addition method on the properties of concrete. This comparison of mixtures is valid, as the percentage of cement replacement with fly ash and the PAC percentage were the same for both mixes. Nonetheless, as discussed in Chapter 4, the chemical composition of Genesee fly ash and Class F fly ash was slightly different which could affect AEA effectiveness. On top of that, PAC was sourced from different suppliers which may have some influence though they showed the same physical properties. Figure 5-45 and Table 5-5 show the comparison of Series #2 and Series #3.

Table 5-5 Comparison of Series #2 and Series #3

Series	#2	#3
Mix ID	A20F2P	A20F-G
PAC	2%	2% (see Section 4-1-2)
Air void content (%)	8.5	13.0
Volume of permeable voids (%)	4.7	8.0
Fresh density (kg/m^3)	2183	2089
Compressive strength-28 days (MPa)	23.4	18.1
Spacing factor (microns)	70	79
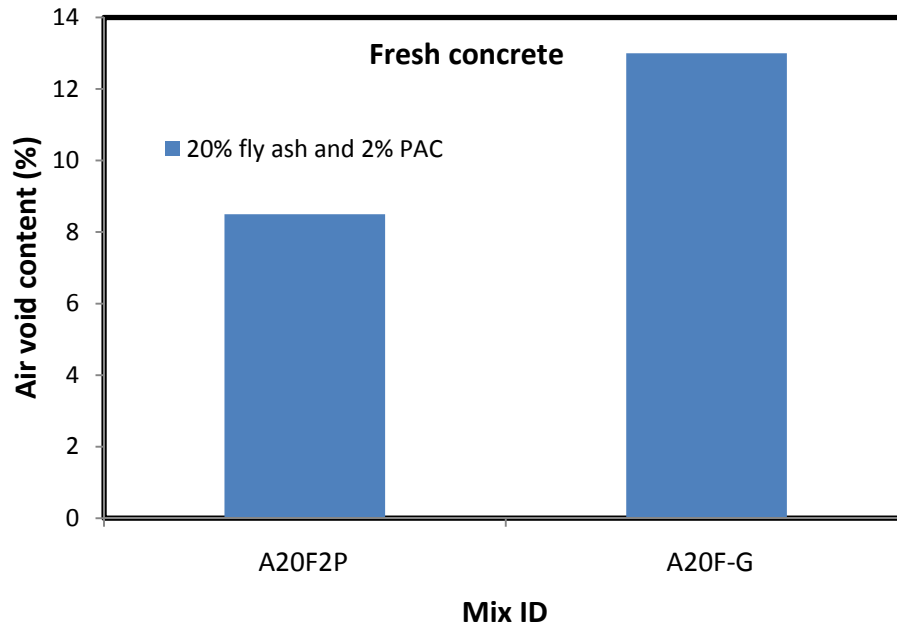
Fig. 5-45 Comparison of fresh air void content in Series # 2 and #3

As shown in Figure 5-45 and Table 5-5, the fresh air void content of A20F-G was 50% higher compared to A20F2P. It shows that PAC adsorbs more AEA when added during the post process production compared to when it is injected with PAC in front of the precipitator. Based on this finding, it can be concluded that fly ash already treated with PAC in the power plant resulted in a higher air void content when the same amount of AEA was used.

It is worth restating that the Genesee Power Plant used a PAC (Power PAC Premium from the ADA company), which was similar to the PAC used in this study though they are not identical, see Section 4-1-1. Recall from Section 4-1-2 that the PAC inclusion of the Genesee fly ash was assumed as 2%, therefore the same amount of PAC was included in both mixes. Thus, it can be concluded that the effectiveness of PAC to adsorb AEA decreases when it is injected in front of the gas precipitator.

Table 5-5 shows that the fresh density of A20F0P was higher compared to A20F-G, as the former contains a lower air void content. This means that when PAC is added during the post process production, it leads to a higher density. As Table 5-5 shows, at 28 days, the compressive strength of mixes containing 20% fly ash was 23.4 and 18.1 MPa for series 2 and 3, respectively. These results show that the compressive strength of concrete made with already-treated fly ash (from the Genesee power plant) was lower compared to the concrete made with Class F fly ash, where PAC was added during the post process production. Powdered activated carbon when injected in front of the gas precipitator, introduces fly ash that results in a lower compressive strength. The lower compressive strength in Series #3 is in agreement with its higher air void content compared to Series #2.

Figure 5-46 shows the volume of permeable voids for A20F2P and A20F-G. It is seen that the volume of permeable voids of Series #3 was higher compared to Series #2, as it showed higher air void content. One may conclude that when PAC is injected in front of the gas precipitator, it results in a higher volume of permeable voids. In other words, when PAC is manually and separately added to a concrete mix during the post process production, a concrete with a lower volume of permeable voids can be achieved.
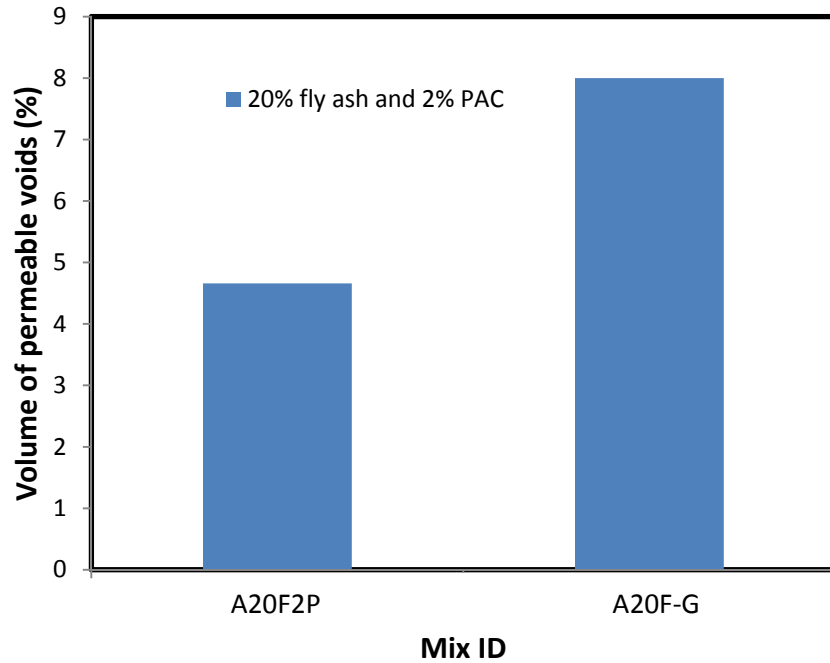
Fig. 5-46 Comparison of permeable void in Series # 2 and #3

The spacing factor of Series #2 and Series #3 is also compared in Table 5-5. It can be seen that A20F-G and A20F2P had almost the same values for the spacing factor. The spacing factor of concrete made with already-treated fly ash was 10% higher (this difference is likely to be insignificant) compared to concrete made with Class F fly ash where PAC was added during the post production process.

CHAPTER 6- SUMMARY

This study has focused on the effects of PAC on the air-void characteristics and consequent properties of concrete containing fly ash. For achieving this goal, laboratory tests were performed to evaluate the effect of powdered activated carbon on the air void network of concrete. Three series of mixes were designed to evaluate the effect of powdered activated carbon, PAC, on the fresh and hardened properties of concrete. Concrete with both normal and high volume fly ash were cast. The fresh properties were examined included the air void content and density of fresh concrete. The permeable void and compressive strength of hardened concrete at four different ages were also measured. Finally, the air void content, specific surface area, spacing factor and shape factor of hardened concrete were determined using the image analysis technique.

The results of concrete containing 20% fly ash and different PAC percentages (Series #1 and #2) show that AEA led to a higher air void content which contributed to lower compressive strength in those concrete. The results show that the compressive strength of concrete from Series #3 containing 20% fly ash made with already treated fly ash from the Genesee power plant was lower compared to concrete made with Class F fly ash where PAC was added during the post process production. It was shown that when PAC was injected in front of the gas precipitator, it results in a higher volume of permeable voids compared to when PAC was added during the post process production.

Based on the discussion in Chapter 5, the author summarized that more accurate and reliable results can be assessed through the inked samples. This is because the voids can be more easily distinguished from the solids in the inked-prepared sample. Therefore, it is recommended

that the ink-prepared sample should be implemented in any future study using image analysis for studying the air-void characteristics of concrete.

Based on the results of Series #2, it was found that higher volume percentage of PAC, for instance beyond 5%, if added after fly ash is precipitated, affects the air void content and other air-void characteristics of concrete. However, the actual amount of PAC included in fly ash may be much lower than the applied percentages in this study. For instance, the fly ash obtained from the Genessee power plant was found to have only 2% PAC by weight. Also, based on the comparison of Series #2 and #3, the effect of PAC on air void content was found to be lower when it was included during the production of fly ash compared to those added in the fly ash before casting concrete. In other words, when PAC was injected in front of the gas precipitator, it adsorbed lower amount of AEA compared to when PAC was added during the post process production. In general, based on the results of this investigation it was found that the fly ash if injected with PAC in front of the precipitator has insignificant effect on the parameters including the air void content and spacing factor which affect durability (specifically freeze and thaw resistance) of concrete.

CHAPTER 7- RECOMMENDATIONS

Based on the experiences obtained in this investigation, the following recommendation are made for future studies.

- In this study only one batch of fly ash from the Genesee power plant was investigated. To generalize the findings, variation of fly ash from other power plants should be tested. Therefore, it is recommended that different fly ash samples injected with PAC from power plants across North America should be investigated in the near future.

- Other types of PAC, for instance brominated PAC, and another class of fly ash (Class C) can be used in future studies to examine their effects on the air-void network of concrete.

- It is expected that further investigation is required to allow derivation of quantitative relationships between the voids at fresh and hardened states.

- It is recommended to employ the permeability and freeze/thaw resistance tests. The mercury intrusion porosimeter test that enables measurement of a wider range of voids should be performed in future investigations.

- In the future studies, measuring of the properties of HVFA concrete should be extended to at least 3 months.

- Regarding the presence of mercury in the fly ash containing PAC, it is recommended in the next step to assess the effect of concrete containing mercury on the health issues.

- It is recommended to use a third image analysis method, for instance ASTM C457, so that one may compare its result with the other two sample-preparation techniques, described here.

- It is recommended that the image analysis technique be performed on the paste samples alone (instead of sample with coarse aggregates) and on bigger samples, to better understand the air-void characteristics.

REFERENCES

- AAD Document Control, "Mercury information clearinghouse", final report, University of North Dakota- US Department of Energy, 2006, 354 p.

- Abell, A. B., Willis, K. L., Lange, A. D., "Mercury intrusion porosimetry and image analysis of cement-based materials", *Journal of Colloid and Interface Science, 1999, Vol.* 211, pp. 39–44.

- ACI 211, Proportioning concrete mixtures, ACI 211 committee, 2009.

- Ahmaruzzaman, M., "A review on the utilization of fly ash", *Progress in Energy and Combustion*, Vol. 36, 2010, pp.327–363.

- Aizpuru, A., Malhautier, L., Roux, J. C., Fanlo, J. L., "Biofiltration of a mixture of volatile organic compounds on granular activated carbon", *Biotechnology and Bioengineering*, Vol. 83, 2003, pp. 479–488.

- "Albermarle", Accessed April 25th 2011, www.albemarle.com/fw/filemanager.

- Allen, T., "Particle size measurement", *Chapman and Hall,* UK, 1975, 454 p.

- AMEC, "Fly ash analysis-final report", Job number: CA17575, Canada, 2010.

- Amer, N., Storey, C., Dellate, N., "Effect of density on the mechanical properties and durability of roller compacted concrete", PCA R&D Serial No. 2940, *Portland Cement Association*, 2008.

- American Coal Ash Association, 2001 and 2004 Coal Combustion Product (CCP) Production & Use Survey Report.

- Apaydin, B., "Comparison of mechanical properties of boron modified active belite cement and ordinary Portland cement concrete", MSc. Thesis, Atilim University, Turkey, 2010, 51 p.

- ASTM C39, "Standard test method for compressive strength of cylindrical concrete specimens", *ASTM International*, West Conshohocken, PA, 2010.

- ASTM C128, "Standard test method for density, relative density (specific gravity), and absorption of fine aggregate", ASTM International, 2007, PA, USA.

- ASTM C231, "Standard test method for air content of freshly mixed concrete by the pressure method", *ASTM International,* 2009, PA, USA.

- ASTM C260, "Standard specification for air-entraining admixtures for concrete", *ASTM International,* 2010, PA, USA.

- ASTM C457, "Standard test method for microscopical determination of parameters of air-void system in hardened concrete", *ASTM International,* 2010, PA, USA.

- ASTM C618, "Standard specification for coal fly ash and raw or calcined natural pozzolan for use in concrete", *ASTM International,* 2008, PA, USA.

- ASTM C642, "Standard test method for density, absorption, and voids in hardened concrete", *ASTM International*, PA, 2006.

- ASTM C1202, "Standard test method for electrical indication of concrete's ability to resist chloride ion penetration", *ASTM International*, PA, 2005.

- Badger, R., Clark, B., Sahu, S., Thaulow, N, Lee, R., "Backscattered electron imaging to determine the water-cement ratio of hardened concrete", *Transportation Research Center*, No. 1775, 2001, pp. 17-20.

- Baltrus, J., LaCount, R., "Measurement of adsorption of air-entraining admixture on fly ash in concrete and cement", *Cement and Concrete Research*, Vol. 31, Issue 5, 2001, pp. 819-824.

- Bansal, R., Goyal, M., "Activated Carbon Adsorption" Panjab University, Chandigarh, India, 2005, 520 p.

- BASF, MB-AE 90, BASF, 2007, "Product data sheet", 2 p.

- CRC Press, An imprint of Taylor and Francis Group, 2005, 498 p.

- Berndt, M.L., "Properties of sustainable concrete containing fly ash, slag and recycled concrete aggregate", *Construction and Building Materials*, Vol. 23, 2009, pp. 2606–2613.

- Bentz, D., Ferraris, C., "Rheology and setting of high volume fly ash mixtures", *Cement & Concrete Composites, Vol.* 32, 2010, pp. 265–270.

- Beusse, R., "Evaluation report: additional analyses of mercury emissions needed before EPA finalizes rules for coal-fired electric utilities", Report No. 2005-P-00003, 2005, 61 pages.

- Boel, V., Audenaert, K., De Schutter, G., Heirman, G., Vandewalle, L., Desmet, B., Vantomme, J., "Transport properties of self compacting concrete with limestone filler or fly ash", *Materials and Structures,* Vol. 40, 2007, pp. 507-516.

- Bourdtte, B., Ringot, E., Ollivier, J. P., "Modelling of the transition zone porosity", *Cement and Concrete Research*, Vol. 25, 1995, pp. 741– 751.

- Cameron Carbon Incorporated, "Activated carbon and adsorption systems", Accessed September 15th 2011, http://www.cameroncarbon.com/.

- Cameron Carbon Incorporated, ``Activated carbon: manufacture, structure and properties``, 2006, US, 11 p.

- CAN/CSA A 23.1, "Concrete Materials and Methods of Concrete Construction/Methods of Test for Concrete", *Canadian Standard Association*, 2000, 362 p.

- Canadian Council of Ministers of the Environment, Canada-wide standards for mercury emissions from coal-fired electric power generation plants, 2006, 15 p.
- Care, S., "Effect of temperature on porosity and on chloride diffusion in cement pastes", *Construction and Building Materials*, Vol. 22, 2008, pp. 1560–1573.

- CCME, "Canada-wide standard for mercury emissions from coal-fired electric power generation plants", progress report, 2008, 54 p.

- Chatterjii, S., Gudmondsson, H., "Characterisation of entrained air bubble systems in concrete by means of an image analyzing microscope", *Cement and Concrete Research*, Vol. 7, 1977, pp. 423-428.

- Chaudhry, R., "Use of high volume fly ash concrete in underground structures", Delhi MRTS Project, 2005. 21 pages.

- Chen, J., Zampini, D., Walliser, A., "High-pressure epoxy impregnated cementitious materials for microstructure characterization", *Cement and Concrete Research*, Vol. 32, 2002, pp. 1-7.

- CIRCA, Canadian Industries Recycling Coal Ash, "Fly ash: its origin, applications and the environment", Fact sheet #1, 2006, 2 p.

- Claisse, P., Elsayad, H., Shaaban, G., "Absorption and sorptivity of cover concrete", *Journal of Material in civil Engineering*, Vol. 9, 1997, pp. 105-110.

- Cnudde, V. Cwirzen, A., Masschaele, B., Jacobs, P. J. S., "Porosity and microstructure characterization of building stones and concretes", *Engineering Geology*, Vol. 103, 2009, pp. 76–83.

- Cook, R. A., Hover, K. C., "Experiments on contact angle between mercury and hardened cement paste", *Cement and Concrete Research*, Vol. 21, 1991, pp. 1165–1175.

- Cox, K., De Belie, N., "Durability behavior of high-volume fly ash concrete", Ghent University, Ghent, Belgium, 2007, 9 p.

- Crouch, L.K., Hewitt, R., Byard, B., "High volume fly ash concrete", *World of Ash (WOCA)*, 2007, Northern Kentucky, USA.

- CTRE, "Improving variability and precision of air-void analyzer (AVA) test results and developing rational specification limits", *Center for Transportation Research and Education*, Iowa State University, phase I report, 98 p.

- Derenne, S., Sartorelli, P., Bustard, J., Stewart, R., Sjostrom, S., Johnson, P., McMillian, M., Sudhoff, F., Chang, R., "TOXECON clean coal demonstration for mercury and multi-pollutant control at the Presque Isle Power Plant", *Fuel Processing Technology*, Vol. 90, 2009, pp. 1400-1405.

- "CXI Corporate", Accessed 15th September 2011, http://www.concrete-experts.com/pages/Newsletter/03/03.htm.

- Diamond, S., "Mercury porosimetry: an inappropriate method for the measurement of pore size distributions in cement-based materials", *Cement and Concrete Research,* Vol. 30, 2000, pp. 1517–1525.

- Dinakar, P., Babu, K. G., Santhanam, M., "Durability properties of high volume fly ash self compacting concretes", *Cement & Concrete Composites*, Vol. 30, 2008, pp. 880–886.

- Dombrowski, K., Padilla, J., Richardson, C. Fisher, K., Campbell, T., Chang, R., Eckberg, C., Hudspeth, J., Pletcher, S., "Evaluation of low-ash impact sorbent injection technologies at a Texas lignite/PRB fired power plant" *Proceeding of the International Conference on Air Quality VI*, Arlington, VA, September 24-27, 2007.

- Elahi, A., Basheer, P. A. M., Nanukuttan, S. V., Khan, Q. U. Z., "Mechanical and durability properties of high performance concretes containing supplementary

146

cementitious materials", *Construction and Building Materials*, Vol. 24, 2010, pp. 292–299.

- Elsen, J., "Automated air void analysis on hardened concrete results of a European intercomparison testing program", *Cement and Concrete Research*, Vol. 31, 2001, pp. 1027-1031.

- Feldman, R.F., Beaudoin, J. J., "Pretreatment of hardened hydrated cement pastes for mercury intrusion measurements", *Cement and Concrete Research*, Vol. 21, 1991, pp. 297– 308.

- Felix, L. C. M.; Munoz, L. A. B., "Representing a relation between porosity and permeability based on inductive rules", Journal of Petroleum Science and Engineering, Vol. 47, 2005, pp. 23-34.

- "Fraunhofer", Accessed September 15th 2011, http://www.hoki.ibp.fhg.de/wufi/grundl_poros_e.html.

- Freeman, E., Gao, Y., Hurt, R., Suuberg, E., "Interactions of carbon-containing fly ash with commercial air-entraining admixtures for concrete", *Fuel*, Vol. 76, No. 8, 1997, pp. 761-765.

- Gao, Y. M.; Shim, H.; Hurt, R.; and Suuberg, E., "Effects of carbon on air entrainment in fly ash concrete: the role of soot and carbon black", *Energy and Fuels*, Vol. 11, 1997, pp. 457-462.

- Gebler, S.; and Klieger, P., "Effect of fly ash on the air void stability of concrete", *American Concrete Institute*, SP 79, 2005, pp. 103-142.

- Giergiczny, Z., Glinicki, M., Sokolowski, M., Zielinski, M., "Air void system and frost salt scaling of concrete containing slag blended cement", *Construction and Building Materials*, Vol. 23, 2009, pp. 2451-2456.

- Glinicki, M., Zielinski, M., "Air void system in concrete containing circulating fluidized bed combustion fly ash", *Material and Structures*, Vol. 41, 2008, pp. 681-687.

- Golightly, D, Cheng, C., Sun, P., Weavers, L., Walker, H., Taerakul, P., Wolfe, W., "Gaseous Mercury Release during Steam Curing of Aerated Concretes That Contain Fly Ash and Activated Carbon Sorbent", Energy and Fuels, Vol. 22, 2008, pp. 3089-3095.

- Gong, Z., Yuan, C., Ke, Z., Yuan, X., "Energy futures and urban air pollution: challenges for China and the United States", *National Academies Press*, 2007, ISBN0309111404, 366 pages.

- GRACE, "The foam index test: a rapid indicator of relative AEA demand technical bulletin", technical bulletin, 2002, www.graceconstruction.com.

- Hale, W., Freyne, S., D. Bush Jr.,T., W. Russell, B., " Properties of concrete mixtures containing slag cement and fly ash for use in transportation structures*", Construction and Building Materials, Vol.* 22, 2008, pp. 1990–2000.

- Haque, M. N., Kayyali, O. A., "Strength and porosity of hardened cement -- fly ash pastes in hot environment", *ACI Materials Journal*, Vol. 86, 1989, pp.128-34.

- Headwaters Sources, "Fly ash: the modern pozzolan improving concrete performance enhancing our environment``, http://www.flyash.com/data/upimages/press/HWR_brochure_flyash.pdf, 2009, pp. 1-9.

- Hearn, N., Hooton, R.D., "Sample mass and dimension effects on mercury intrusion porosimetry results", *Cement and Concrete Research*, Vol. 22, 1992, pp. 970– 980.

- Herman, J., Yajun, J., "Effects of densified silica fume on microstructure and compressive strength of blended cement pastes", *Cement and Concrete Research*, Vol. 33, 2003, pp. 1543–1548.

- Hill, R., Zhang, Z., Shaw, B., "A fly ash carbon treatment for producing a marketable product from activated carbon contaminated fly ash", *World of Coal Ash Conference*, 2009, Lexington, USA, 10 p.

- Hill, R. L., Sarkar, S., Rathbone, R. F., Hower, J. C., "An examination of fly ash carbon and interactions with air entraining agent", *Cement and Concrete Research*, Vol. 27, 1997, pp. 193-204.

- Hoffmann, J., Brown, J., "Preliminary cost estimate of activated carbon injection for controlling mercury emissions from an un-scrubbed 500 mw coal-fired power plant", final report, US Department of Energy, 2003, 50p.

- Hover, K.C., Phares, R.J., "Impact of concrete placing method on air content, air-void system parameters, and freeze-thaw durability", *Transportation Research Record ,* Vol. 1532, 1996, pp. 1-8.

- Hsieh, Y., Tsai, M., "Physical and chemical analyses of unburned carbon from oil-fired fly ash", *Carbon,* Vol. 41, 2003, pp. 2317-2324.

- Idorn, G.M., and Thaolow, N., "Effectiveness of research on fly ash in concrete", *Cement and Concrete Research,* Vol. 15, 1985, pp. 535-544.

- Ilavsky, J., Berndt, C., Karthikeyan, J., "Mercury intrusion prosimetry of plasma sprayed ceramic", *Journal of Materials Science*, Vol. 32, 1997, pp. 3925-3932.

- "Image Processing and Analysis in Java", Accessed September 15th 2011, http://rsbweb.nih.gov/ij/.

- Jana, D., "Sample preparation techniques in petrographic examinations of construction materials", Proceeding of the 28th conference of Cement Microscopy, Colorado, USA, 2006, 48 p.

- Kaufmann, J., Loser, R., Leemann, A., "Analysis of cement-bonded materials by multi-cycle mercury intrusion and nitrogen sorption", *Journal of Colloid and Interface Science*, Vol. 336, 2009, pp. 730-737.

- Khan, M. I., Lynsdale, C. J. Waldron, P., "Porosity and strength of PFA/SF/OPC ternary blended paste", *Cement and Concrete Research*, Vol. 30, 2000, pp. 1225–1229.

- Klieger, P., Hanson, J. A., "Freezing and Thawing Tests of Lightweight Aggregate Concrete," *ACI JOURNAL, Proceedings,* V. 57, 1961, pp. 779-796.

- Klieger, P., Lamond, J., "Significance of tests and properties of concrete and concrete-making materials", *ASTM International*, 1994, 623 p.

- Kulaots, I., Hsu, A., Hurt, R. H., Suuberg, E. M., "Adsorption of surfactants on unburnt carbon in fly ash and development of a standardized foam index test", *Cement and Concrete Research*, Vol. 33, 2003, pp. 2091–2099.

- Kulaots, I., Gao, Y. M., Hurt, R. H. and Suuberg, E. M., "The role of polar surface and mesoporosity in adsorption of organics by fly ash carbon", *ACS Division of Fuel Chemistry*, Vol. 43, 1998, pp. 980-984.

- Kumar, B., Tike, G.K., Nanda, P.K., "Evaluation of properties of high-volume fly-ash concrete for pavements", *Journal of Materials in Civil Engineering*, 2007, Vol. 19, pp. 906-911.

- Kumar, R., Bhattacharjee, B., "Study on some factors affecting the results in the use of MIP method in concrete research", *Cement and Concrete Research*, Vol. 33, 2003a, pp. 417-424.

- Kumar, R., Bhattacharje, B., "Porosity, pore size distribution and in situ strength of concrete", *Cement and Concrete Research*, Vol. 33, 2003b, pp. 155–164.

- Kunhanandan Nambiar, E.K., Ramamurthy, K., "Air Void Characterisation of Foam Concrete", *Cement and Concrete Research,* Vol. 37, No. 2, 2007, pp. 221-230.

- Kwon, S. H., "Threshold selection based on cluster analysis", *Pattern Recognition Letters*, Vol. 25, 2004, pp. 1045–1050.

- Lamond, J., "Significance of tests and properties of concrete and concrete making materials", *ASTM International*, 2006, 664 p.

- Landreth, R., Nilson,. X., Liu, X., Tang, Z., Overholt, A., Brickett, L., "Mercury reduction performance of concrete friendly C-PAC sorbent", *World of Coal Ash Conference*, 2007, Kentucky, USA, 9 p.

- Lange, D., Jenning, H., Shah, S., "Image Analysis Techniques for Characterization of Pore Structure of Cement Based Materials", *Cement and Concrete Research*, Vol. 24, 1994, pp. 841-853.

- Larrimore, L., Berry, M., Been, D., Renfroe, S., Chang, R., "Effect of bromine addition on fly ash use in concrete", *Proceedings of the Power Plant Air Pollutant Control "Mega" Symposium*, Baltimore, MD, August 25-28, 2008.

- Laskar, A.I. Talukdar, S., "Rheological behaviour of high performance concrete with mineral admixtures and their blending", *Construction and Building Materials*, Vol. 22, 2008, pp. 2345–2354.

- Laskar, A. I., Kumar, R, Bhattacharje, B., "Some aspects of evaluation of concrete through

- mercury intrusion porosimetry", *Cement and Concrete Research*, Vol. 27, 1997, pp. 93-105.

- Laurencot, J., Pleau, R., Pigeon, M., "The microscopical determination of air voids characteristics in hardened concrete development of an automatic system using image analysis techniques applied to micro computers", *Proceedings of the 14th International Conference of Cement Microscopy*, Costa Mesa, USA, 1992. pp. 259–73.

- Lawrence, L., Dam. T., Thomas, M., "Evaluation of methods for characterizing air-void systems in Wisconsin paving concrete", *Transportation Materials Research Center*, Michigan Technological University, USA, 2002, 9 p.

- Lee, C. Y., Lee, H. K., Lee, K. M., "Strength and microstructural characteristics of chemically activated fly ash–cement systems", *Cement and Concrete Research*, Vol. 33, 2003, pp. 425–431.

- Liu, R., Durham, S, Rens, K., "Effects of post-mercury-control fly ash on fresh and hardened concrete properties", *Construction and Building Materials*, Vol. 25, 2011, pp. 3283-3290.

- Lockert, C.A., Zhow, Q., Zhang, Y., Nelson, S., "Further progress toward concrete-friendly Mercury sorbents", *Air Quality V Symposium*, 2005, September 21, Washington, DC, 13 p.

- Lomboy G., Wang K., "Effects of strength, permeability, and air void parameters on freezing-thawing resistance of concrete with and without air entrainment", *Journal of ASTM International*, Vol. 6, No. 10, 2009 Report number JA1102454, 14 p.

- Malhotra, V. M., "Durability of concrete incorporating high-volume of low-calcium (ASTM Class F) fly ash", *Cement and Concrete Composites*, Vol. 12, 1990, pp. 271-277.

- Marsh H., F. Rodriguez-Reinoso, Activated carbon, UK, Elsevier, 1st ed., 2006, chapter 6.

- Miranda, J.M., Ferna´ndez-Jime´nez A., Gonza´lez, J. A., Palomo, A., "Corrosion resistance in activated fly ash mortars", *Cement and Concrete Research*, Vol. 35, 2005, pp. 1210– 1217.

- "M. K. Instruments", Accessed September 15th 2011, http://www.mkinstruments.co.in/concretetesting.html.

- Mohammed, B, Fang, O. C., "Mechanical and durability properties of concretes containing paper-mill residuals and fly ash", *Construction and Building Materials*, Vol. 25, 2011, pp. 717-725.

- Montgomery , D. G., Hughes, D. C., Williams. R. I. T., "Fly ash in concrete - a microstructure study", *Cement and Concrete Research*, Vol. 11, Issue 4, 1981, pp. 591-603.

- Mulenga, D. M., Stark, J, Nobst, P., "Thaumasite formation in concrete and mortars containing fly ash", *Cement and Concrete Composites*, Vol. 25, 2003, pp. 907-912.

- Naik, T. R., "Sustainability of cement and concrete industries", Global Construction: Ultimate Concrete Opportunities, July 2005, Dundee, Scotland, pp. 141-150.

- Naik, T., Singh, S., M. Hossain, M. "Properties of high performance concrete systems incorporating large amounts of high-lime fly ash", *Construction and Building Materials*, Vol. 9, No. 4, 1995, pp. 195-204.

- Nemati, K., e-mail message to author, December 15th 2010.

- Nelson, S., Landreth, R., Zhou, Q., Miller, J., "Accumulated power-plant mercury-removal experience with brominated PAC injection", *Combined Power Plant Air Pollutant Control Mega Symposium*, Washington, DC, Aug. 30 – Sept. 2, 2004.

- Neville, AM. "Properties of Concret"e, Fourth Edition, Longman & John Wiley, Nondon, 1995.

- "Nikon Microscopy", Accessed September 15th 2011, http://www.microscopyu.com/articles/digitalimaging/dxm1200.

- Nkinamubanzi, P. C., Bilodeau, A., Jolicoeur, C., and Golden, D. M., "Air entraining admixture for use with fly ashes having high carbon contents", *Proceeding of Seventh CANMET/ACI international conference on superplasticizers and other chemical admixtures in concrete*, SP-217-36, 2003, pp. 543-572.

- Osbaeck, B., Smidth, F. L., "The Influence of Air Content By Assessing The Pozzolanic Activity of Fly Ash By Strength Testing", *Cement and Concrete Research*, Vol. 15, 1985, pp. 53-64.

- Pade, C., Jakobsen, U., Elsen, J., "A new automatic analysis system for analyzing the air void system in hardened concrete", *Proceeding of th 24th international conference on cement microscopy*, California, 2002, pp. 204-213.

- Pala, M., O¨ zbay, E., O¨ ztas, A., Ishak Yuce, M., "Appraisal of long-term effects of fly ash and silica fume on compressive strength of concrete by neural networks", *Construction and Building Materials*, Vol. 21, 2007, pp. 384–394.

- Parande, A., Stalin, K.,Thangarajan, R., KArthikeyan, M., "Utilization of agroresidual waste in effective blending in Portland cement", *International Research Scholarly Network*, Vol. 2011, 2011, 12 p.

- Parrott, L. J., "Water absorption in cover concrete", *Materials and Structures*, Vol. 25, 1992, pp. 284-292.

- Patil, S. G., Bhattacharjee, B., "Size and volume relationship of pore for construction materials", *Journal of Material in Civil Engineering*, ASCE, Vol. 20, 2008, pp. 410-418.

- Pederson, K. H., Jenson, A. D., Rasmussen, M. S., Johansen, K., "A review of the interference of carbon containing fly ash with air entrainment in concrete", *Progress in Energy and Combustion Science*, Vol. 34, 2008, pp. 135-154.

- Perlite Info, Accessed October 21th 2011, http://www.perlite.info/hbk/0032701.html.

- Peterson, K., Carlson, J., Sutter, L., Dam, T., "Methods for measuring optimization for image collected from contrast enhanced concrete surface for air void system characterization", *Materials Characterization*, Vol. 60, 2009, pp. 710-715.

- Pigeon, M., Provest, J., Simard, J., "Freeze thaw durability versus freezing rate", *ACI Materials Journal,* Vol. 82, 1985, pp. 682-602.

- Pigeon, M., Lachance, M., "Critical air void spacing factors for concrete submitted to slow freeze-thaw cycles", *ACI Materials Journal*, Vol. 78, 1981, pp. 282-291.

- Pistilli, M. "Air-void parameters developed by air-entraining admixtures, as influenced by soluble alkalies from fly ash and portland cement", *ACI Materials Journal*, Vol. 80, 1983, pp. 217-222.

- Pleau, R., Pigeon, M., Faure, R. M., Sedran, T., "Air voids in concrete: a study of the influence of superplasticizers by means of scanning electron microscopy and optical microscopy", ACI SP publication, Vol. 122, 1990, pp. 105-124.

- Pleau, R., Pigeon, M., Laurencot, J., "Some finding on the usefulness of image analysis for determining the characteristic of the air void system on hardened concrete", *Cement and Concrete Composites*, Vol. 2, 2001, pp. 237-246.

- Plowman, C., Cabrera, J. G., "The use of fly ash to improve the sulphate resistance of concrete", *Waste Management*, Vol. 16, 1996, pp. 145-149.

- Poon, C., Azhar, S., Anson, M., Wong, Y., "Comparison of the strength and durability performance of normal- and high-strength pozzolanic concretes at elevated temperatures", *Cement and Concrete Research*, Vol. 31, 2001, pp. 1291–1300.

- Poon, C., Lam, L., Wong, Y., "Study on high strength concrete prepared with large volumes of low calcium fly ash", *Cement And Concrete Research*, Vol. 30, 2000, pp. 447-455.

- Poonguzhali, A., Sheikh, H., Dayal, R, Khatak, H., "A review on degradation mechanism and life estimation of civil structures", Corrosion Reviews, Vol. 26, 2008, pp. 215-294.

- Powers, T. C., Copeland, L. E., Hayes, J. C., Mann, H. M., " Permeability of Portland cement paste", *Journal of American Concrete Institute,* Vol. 26, 1954, pp. 285-296.

- Powers, T. C., "The air requirement of forest resistance concrete", *Proceeding of the Highway Research Board*, Vol. 29, 1949, pp. 184-211.

- Ramezanianpour, A. A., Mahlohtra, V. M., "Effect of curing on the compressive strength, resistance to chloride-ion penetration and porosity of concretes incorporating slag, fly ash or silica fume", *Cement and Concrete Composites*, Vol. 17, 1995, pp. 125-133.

- Roberts, L.R., Scali, M.J., "Factors affecting image analysis for measurement of air content in hardened concrete", *Proceedings of the International Conference on Cement Microscopy*, 1984, pp. 402-419.

- Sabir, B. B., Kouyiali, K., "Freeze-thaw durability of air-entrained CSF concrete", *Cement and Concrete Composites*, Vol. 13, 1991, pp. 203-208.

- Sahmaran, M., "Sodium sulphate attack on blended cements under different exposure conditions", *Advances in Cement Research*, Vol. 19, 2007, pp. 47–56.

- Sahu, S., Badger, N., Thaulow, N., Lee, R., "Determination of water-cement ratio of hardened concrete by scanning electron microscopy", *Cement and Concrete Composites*, Vol. 26, 2004, pp. 987-922.

- Sanjuan, M. A., Martilaty, R., "Influence of the age on air permeability of concrete", *Journal of material Science*, Vol. 30, 1995, pp. 5657-5662.

- Saricimen, H., Maslehuddin, M., Shammem, M., AlGhamdi, A., Barry, M., "Effect of curing and drying on strength and absorption of concretes containing fly ash and silica fume", *ACI Special Publication*, Vol. 192, 2000, pp. 103-118.

- Saricimen, H., Maslehuddin, M., A1-Mana, A., Eid, O., "Effect of Field and Laboratory Curing on the Durability Characteristics of Plain and Pozzolan Concretes", *Cement & Concrete Composites*, Vol. 14, 1992, pp.169-177.

- Schneider, U., Diederichs, U., "Detection of crack by mercury penetration measurement", *Fracture Mechanics of Concrete*, 1983, pp. 207– 222.

- Schutter, S. G., Audenaert, K., "Evaluation of water absorption of concrete as a measure for resistance against carbonation and chloride migration", *Materials and Structures*, Vol. 37, 2004, pp. 591-596.

- Schutter, G., "Advanced monitoring of cracked structures using video microscope and automated image analysis", *NDT and E International,* Vol. 35, 2002, pp. 209-212.

- Sengul, O., Tasdemir, C., Tasdemir, M., "Mechancail properties and rapid chloride permeability of concrete with ground fly ash", *ACI Material Journal*, Vol 102, 2005, pp. 414-421.

- Setzer, M. J., Auberg, R., "Freeze-thaw and deicing salt resistance of concrete testing by the CDF method: CDF resistance limit and evaluation of precision", *Materials and Structures*, Vol. 28, 1995, pp. 16-31.

- Shehata, M. Thomas, M., "The effect of fly ash composition on the expansion of concrete due to alkali-silica reaction", *Cement and Concrete Research*, Vol. 30, 2000, pp. 1063-1072.

- Shon, C., Sarkar, S., Dan G. Zollinger, P.E., " Testing the effectiveness of class C and class f fly ash in controlling expansion due to alkali-silica reaction using modified ASTM c 1260 test method", *Journal Of Materials In Civil Engineering*, Vol. 16, 2004, pp. 20-27.

- Siddique, R., Khatib, J.,"Abrassion resistance and mechanical properties of high-volume fly ash concrete", *Materials and Structure*, Vol. 43, 2010, pp. 709-718.

- Siddique, R, Prince, W., Kamali, S., "Influence of utilization of high-volumes of class f fly ash on the abrasion resistance of concrete", *Leonardo Electronic Journal of Practices and Technologies,* Vol. 6, 2007, pp. 13-28.

- Siddique, R., "Performance characteristics of high-volume Class F fly ash concrete ", *Cement and Concrete Research*, Vol. 34, 2004, pp. 487–493.

- Smith, I., "Cement and concrete – benefits and barriers in coal ash utilization", *International Energy Agency (IEA) Clean Coal Centre report CCC/94*, January 2005, 70 p.

- Soroushian, P., Elzafraney, M., Nossoni, A., "Specimen preparation and image processing and analysis techniques for automated quantification of concrete micro cracks and voids", *Cement and concrete Research*, Vol. 33, 2003, pp. 1949-1969.

- Sporel, F., Uebachs, S., and Brameshuber, W., "Investigations on the influence of fly ash on the formation and stability of artificially entrained air voids in concrete", *Materials and Structures*, Vol. 42, 2009, pp. 227-240.

- Stencel, J. M., Song, H. and Cangialosi, F., "Automated foam index test: quantifying air entraining agent addition and interactions with fly ash cement admixtures", *Cement and Concrete Research*, Vol. 39, 2009, pp. 362-370.

- Stroeven, P., Hu, J., Koleva, D. A., "Concrete porosimetry: Aspects of feasibility, reliability and economy", *Cement and Concrete Composites*, Vol. 32, 2010, pp. 291-299.

- Stutzaman, P., "Detoriation of Iowa highway concrete pavements: A petrogeraphic study", NISTIR 6399, National Institute Standard and Technology, 1999, 84 p.

- Suuberg, E., Hurt, R. H., Kulaots, I., Gao, Y. M., Smit, K., "Fundamental study of low NO_x combustion utilization*", Proceeding of advance coal based power and environmental systems*, NETL, USA, 1998, 22 p.

- Tolentino, E., Lameiras, F., Gomes, A., Silva, C., Vasconcelos, W., "Effects of high temperature on the residual performance of portland cement concretes", *Materials Research*, Vol. 5, 2002, pp. 5-11.

- Toumi, B., Resheidat, M., "A simple and low cost method for rapid assessment of air voids in hardened concrete", *Asian Journal of Civil Engineering*, Vol. 11, 2010, pp. 335-343.

- Turner-Fairbank Highway Research Center (TFHRC), "Coal fly ash-material description", http://www.tfhrc.gov/hnr20/recycle/waste/cfa51.htm, retrieved on August 17, 2009.

- "Universiti Teknologi Mara", Accessed September 15th 2011, http://fka.uitm.edu.my/facilities-/109.html?tmpl=component

- Winslow, D. N., Diamond, S., "A mercury porosimetry study of the evaluation of porosity in Portland cement", *Journal of Material*, Vol. 5, 1970, pp. 564–585.

- Xing, F., Dong, B., Li. Z., "The study of pore structure and its influence on material properties of cement-based piezoelectric ceramic composites", *Construction and Building Materials*, Vol. 23, No. 3, 2009, pp. 1374-1377.

- Xu, R." Hg absorbents in fly-ash: effect on fresh concrete properties", MEng report, CIVE 900, 2008, University of Alberta, 56 p.

- Yang, E.-H., Yang, Y., Li, V.C., "Use of high volumes of fly ash to improve ECC mechanical properties and material greenness", *ACI Materials Journal*, Vol. 104, 2007, pp. 620-628.

- Y¨ucel, K. T., "Effect of fly ashes on the rheological properties of fresh cement mortars", *International Journal of Thermophysics*, Vol. 26, 2006, pp. 425-431.

- Yun, K.K., Kim, D.H., Kim, K.J., "Effect of micro air void system on the permeability of latex modified concrete with ordinary Portland and very early strength cements", *Canadian Journal of Civil Engineering*, Vol. 34, 2007, pp. 895-901.

- Zain, M.F.M., Safiuddin, M. Yusof, K. M., "A study on the properties of freshly mixed high performance concrete", *Cement and Concrete Research*, Vol. 29, 1999, pp. 1427–1432.

- Zalocha, D., Kasperkieiwicz, J., "Estimation of the structure of air entrained concrete using a flatbed scanner", *Cement and Concrete Research*, Vol. 35, 2005, pp. 2041-2046.

- Zhang, Y, Nelson, S., "Development of a new method to replace the foam index test", *World of Coal Ash Conference*, 2007, Lexington, USA, 9 p.

- Zhang, Z., Ansari, F., "Fracture mechanics of air-entrained concrete subjected to compression", *Engineering Fracture Mechanics*, Vol. 73, 2006, pp.1913–1924.

- Zhang, S., Wang, K., "Investigation into the effects of materials and mixing procedures on air-void characteristics of fresh concrete using air void analyzer (AVA)", *Journal of ASTM International*, Vol. 3, 2006, pp. 1-15.

- Zhang, Z., Ansari, F., Vitillo, N., "Automated determination of entrained air void parameters in hardened concrete", *ACI Materials Journal*, Vol. 102, 2005, 42-48.

- Zhou, Q., Nelson, P., Nelson, B., Minkara, R., Borowski, B., Brickett, L., "Concrete and fly ashes from a full-scale concrete friendly C-PAC", *World of Coal Ash Conference*, 2007, Lexington, USA, 16 p.

APPENDIX #1

Series#1

Fresh properties										
Mix	Air void content (%)	Average of air void content (%)	Weight of concrete +container * (kg)	Slump (cm)	Fresh density (kg/m^3)	Average of fresh density (kg/m^3)	Standard deviation of fresh density	C.O.V. of fresh density (%)	Standard deviation of air void content	C.O.V. of air void content (%)
0F0P	2.7	3.3	21.34	1.2	2345.7	2349	6	0.3	0.49	15.1
	3.6		21.33		2344.3					
	3.5		21.41		2355.7					
10F0P	2.6	2.5	21.45	1.2	2361.4	2362	1	0.0	0.23	9.4
	2.2		21.46		2362.9					
	2.6		21.46		2362.9					
10F1P	2.5	2.8	21.54	1.3	2374.3	2367	12	0.5	0.29	10.2
	3		21.54		2374.3					
	3		21.39		2352.9					
10F2P	2.1	2.2	21.4	3	2354.3	2360	9	0.4	0.12	5.3
	2.1		21.41		2355.7					
	2.3		21.51		2370.0					
10F3P	1.8	1.9	21.53	4.5	2372.9	2362	10	0.4	0.10	5.3
	2		21.4		2354.3					
	1.9		21.43		2358.6					
10F4P	2.2	2.0	21.67	1.8	2392.9	2377	17	0.7	0.21	10.2
	1.8		21.43		2358.6					
	2.1		21.58		2380.0					
10F5P	1.5	1.7	21.41	4.1	2355.7	2360	4	0.2	0.15	9.2
	1.8		21.45		2361.4					
	1.7		21.47		2364.3					
20F0P	1.9	2.1	21.45	8	2361.4	2354	7	0.3	0.20	9.5
	2.1		21.37		2350.0					
	2.3		21.37		2350.0					
20F1P	1.9	1.8	21.35	5.5	2347.1	2338	21	0.9	0.12	6.3
	1.7		21.12		2314.3					
	1.9		21.39		2352.9					
20F2P	1.8	1.8	21.4	6.5	2354.3	2355	5	0.2	0.06	3.3
	1.7		21.44		2360.0					
	1.8		21.37		2350.0					

Mix	Air void content (%)	Average of air void content (%)	Weight of concrete +container (kg)	Slump (cm)	Fresh density	Average of fresh density (kg/m^3)	Standard deviation of fresh density	C.O.V. of fresh density (%)	Standard deviation of air void content	C.O.V. of air void content (%)
20F3P	-	1.8	21.25	6.7	2332.9	2330	3	0.1	0.07	4.0
	1.7		21.23		2330.0					
	1.8		21.21		2327.1					
20F4P	1.8	1.8	21.32	4	2342.9	2344	5	0.2	0.06	3.3
	1.7		21.37		2350.0					
	1.8		21.3		2340.0					
20F5P	2	1.9	21.25	4.5	2332.9	2330	8	0.3	0.12	6.0
	2		21.17		2321.4					
	1.8		21.28		2337.1					
30F0P	1.6	1.6	21.31	14	2341.4	2341	1	0.0	0.06	3.5
	1.7		21.3		2340.0					
	1.6		21.31		2341.4					
30F1P	1.7	1.8	21.26	12.5	2334.3	2331	5	0.2	0.12	6.3
	1.9		21.2		2325.7					
	1.9		21.25		2332.9					
30F2P	1.3	1.3	21.27	16	2335.7	2333	2	0.1	0.06	4.3
	1.3		21.24		2331.4					
	1.4		21.24		2331.4					
30F3P	1.4	1.4	21.23	15	2330.0	2332	3	0.1	0.00	0.0
	1.4		21.27		2335.7					
	1.4		21.24		2331.4					
30F4P	1.6	1.3	21.21	17	2327.1	2329	3	0.1	0.26	20.4
	1.1		21.25		2332.9					
	1.2		21.21		2327.1					
30F5P	1.6	1.6	21.24	15.5	2331.4	2330	4	0.2	0.06	3.7
	1.5		21.26		2334.3					
	1.6		21.2		2325.7					

* weight of container= 4.92 kg

	Compressive strength							
Mix	Load- 7 days (kN)	Compressive strength (MPa)	Load- 14 days (kN)	Compressive strength (MPa)	Load- 28 days (kN)	Compressive strength (MPa)	Load- 60 days (kN)	Compressive strength (MPa)
0F0P	295.5	37.6	310.5	39.6	336.0	42.8	333.5	42.5
	279.5	35.6	314.5	40.1	306.0	39.0	355.0	45.2
	278.5	35.5	320.0	40.8	316.0	40.3	352.5	44.9
average		36.2		40.1		40.7		44.2
10F0P	238.0	30.3	287.0	36.6	331.0	42.2	391.0	49.8
	270.5	34.5	320.0	40.8	304.0	38.7	404.5	51.5
	264.0	33.6	273.0	34.8	301.0	38.3	413.5	52.7
average		32.8		37.4		39.7		51.3
10F1P	242.5	30.9	295.5	37.6	318.5	40.6	380.0	48.4
	265.5	33.8	302.5	38.5	307.0	39.1	354.0	45.1
	237.0	30.2	311.0	39.6	295.5	37.6	370.5	47.2
average		31.6		38.6		39.1		46.9
10F2P	220.5	28.1	269.5	34.3	288.0	36.7	348.5	44.4
	209.5	26.7	263.0	33.5	292.5	37.3	352.0	44.8
	247.0	31.5	274.5	35.0	282.0	35.9	334.0	42.5
average		28.7		34.3		36.6		43.9
10F3P	258.0	32.9	265.5	33.8	337.5	43.0	400	51.0
	243.0	31.0	286.0	36.4	325.5	41.5	360.5	45.9
	261.0	33.2	282.0	35.9	302.0	38.5	427.5	54.5
average		32.4		35.4		41.0		45.9
10F4P	255.4	32.5	269.0	34.3	319.5	40.7	422	53.8
	265.5	33.8	297.0	37.8	328.0	41.8	320	40.8
	276.5	35.2	266.5	33.9	292.5	37.3	383	48.8
average		33.9		35.4		39.9		44.8
10F5P	264.5	33.7	248.0	31.6	316.0	40.3	394	50.2
	234.0	29.8	267.5	34.1	307.0	39.1	354.5	45.2
	252.5	32.2	257.0	32.7	295.5	37.6	365.5	46.6
average		31.9		32.8		39.0		45.9
20F0P	195.0	24.8	238.0	30.3	298.5	38.0	308	39.2
	187.5	23.9	236.0	30.1	259.0	33.0	342.5	43.6
	206.5	26.3	227.0	28.9	301.0	38.3	309.5	39.4
average		25.0		29.8		36.5		40.8
20F1P	214.5	27.3	254.5	32.4	281.0	35.8	349	44.5
	203.0	25.9	219.0	27.9	263.5	33.6	357.0	45.5
	200.0	25.5	228.5	29.1	275.5	35.1	309.0	39.4
average		26.2		29.8		34.8		43.1

Compressive strength							
Mix	Load- 7 days (kN)	Compressive strength (MPa)	Load-14 days (kN)	Compressive strength (MPa)	Load-28 days (kN)	Compressive strength (MPa)	Load-60 days (kN)	Compressive strength (MPa)
20F2P	184.5	23.5	229.5	29.2	283.3	36.1	-	-
	172.0	21.9	248.0	31.6	261.8	33.3	-	-
	175.5	22.4	226.0	28.8	289.7	36.9	-	-
average		22.6		29.9		35.4		41.5
20F3P	192.0	24.5	218.5	27.8	299.5	38.2	322.0	41.0
	177.5	22.6	234.5	29.9	248.0	31.6	324.0	41.3
	166.0	21.1	238.5	30.4	287.0	36.6	342.0	43.6
average		22.7		29.4		35.4		42.0
20F4P	200.0	25.5	220.5	28.1	284.0	36.2	324.5	41.3
	217.5	27.7	243.5	31.0	291.5	37.1	307.0	39.1
	219.0	27.9	241.0	30.7	292.5	37.3	332.0	42.3
average		27.0		29.9		36.9		40.9
20F5P	194.0	24.7	242.5	30.9	280.0	35.7	352.0	44.8
	196.5	25.0	209.0	26.6	274.5	35.0	341.0	43.4
	184.0	23.4	240.0	30.6	273.0	34.8	328.5	41.8
average		24.4		29.4		35.1		43.4
30F0P	166.0	21.1	210.5	26.8	263.5	33.6	287.5	36.6
	163.5	20.8	210.0	26.8	272.5	34.7	283.0	36.1
	146.0	18.6	208.5	26.6	261.5	33.3	305.0	38.9
average		20.2		26.7		33.9		37.2
30F1P	185.0	23.6	204.5	26.1	260.0	33.1	261.0	33.2
	183.0	23.3	221.5	28.2	267.5	34.1	308.0	39.2
	164.0	20.9	220.0	28.0	255.5	32.5	302.5	38.5
average		22.6		27.4		33.2		37.0
30F2P	190.0	24.2	229.5	29.2	238.0	30.3	294.0	37.5
	195.0	24.8	225.5	28.7	227.0	28.9	280.5	35.7
	192.0	24.5	213.5	27.2	226.0	28.8	320.0	40.8
average		24.5		28.4		29.3		38.0
30F3P	172.5	22.0	223.0	28.4	190.5	24.3	310.0	39.5
	169.5	21.6	227.5	29.0	241.0	30.7	327.5	41.7
	180.0	22.9	229.5	29.2	262.0	33.4	338.5	43.1
average		22.2		28.9		32.0		39.5
30F4P	108.0	13.8	144.5	18.4	179.5	22.9	241.0	30.7
	103.5	13.2	150.0	19.1	181.0	23.1	248.0	31.6
	112.5	14.3	156.5	19.9	183.0	23.3	227.0	28.9
average		13.8		19.2		23.1		30.4
30F5P	174.5	22.2	198.5	25.3	212.5	27.1	287.5	36.6
	174.5	22.2	193.0	24.6	214.0	27.3	295.0	37.6
	150.5	19.2	200.5	25.5	214.0	27.3	310.0	39.5
average		21.2		25.1		27.2		39.5

Mix	Compressive strength							
	7 days		14 days		28 days		60 days	
	Standard deviation	C.O.V. (%)	Standard deviation	C.O.V. (%)	Standard deviation	C.O.V. (%)	Standard deviation	C.O.V. (%)
0F0P	1.2	3.4	0.6	1.5	1.9	4.8	1.5	3.4
10F0P	2.2	6.7	3.1	8.2	2.1	5.3	1.4	2.8
10F1P	1.9	6.1	1.0	2.6	1.5	3.7	1.7	3.6
10F2P	2.5	8.5	0.7	2.1	0.7	1.8	1.2	2.8
10F3P	1.2	3.8	1.4	3.9	2.3	5.6	4.3	9.3
10F4P	1.3	4.0	2.2	6.1	2.4	5.9	6.6	14.6
10F5P	2.0	6.1	1.2	3.8	1.3	3.4	2.6	5.7
20F0P	1.2	4.9	0.7	2.5	3.0	8.2	2.5	6.1
20F1P	1.0	3.7	2.3	7.9	1.1	3.3	3.3	7.6
20F2P	0.8	3.6	1.5	5.0	1.9	5.3		
20F3P	1.7	7.3	1.3	4.6	3.4	9.7	1.4	3.3

Mix	Compressive strength							
	7 days		14 days		28 days		60 days	
	Standard deviation	C.O.V. (%)	Standard deviation	C.O.V. (%)	Standard deviation	C.O.V. (%)	Standard deviation	C.O.V. (%)
20F4P	1.3	5.0	1.6	5.4	0.6	1.6	1.6	4.0
20F5P	0.8	3.5	2.4	8.1	0.5	1.3	1.5	3.5
30F0P	1.4	6.9	0.1	0.5	0.7	2.2	1.5	4.0
30F1P	1.5	6.5	1.2	4.4	0.8	2.3	3.3	8.8
30F2P	0.3	1.3	1.1	3.7	0.8	2.9	2.6	6.7
30F3P	0.7	3.1	0.4	1.5	4.7	14.6	1.8	4.6
30F4P	0.6	4.2	0.8	4.0	0.2	1.0	1.4	4.5
30F5P	1.8	8.3	0.5	2.0	0.1	0.4	1.5	3.7

	ASTM C642- 7 days													
MIX	absorption after immersion (%)	standard deviation	absorption after immersion and boiling (%)	standard deviation	bulk density, dry (Mg/m³)	standard deviation	bulk density after immersion (Mg/m³)	standard deviation	bulk density after immersion and boiling (Mg/m³)	standard deviation	apparent density (Mg/m³)	standard deviation	volume of permeable voids (%)	standard deviation
0F0P	5.00		2.77		2.24		2.35		2.30		2.39		6.20	
	4.97	0.10	3.17	0.22	2.22	0.01	2.33	0.01	2.29	0.00	2.39	0.00	7.04	0.47
	5.16		2.79		2.24		2.35		2.30		2.39		6.24	
average	5.04		2.78		2.23		2.35		2.30		2.39		6.22	
10F0P	4.82		2.63		2.25		2.36		2.31		2.39		5.90	
	4.92	0.21	2.61	0.09	2.24	0.01	2.35	0.00	2.30	0.00	2.38	0.00	5.84	0.19
	5.21		2.77		2.24		2.35		2.30		2.38		6.19	
average	4.87		2.67		2.24		2.35		2.30		2.38		5.98	
10F1P	4.75		2.51		2.23		2.34		2.29		2.37		5.60	
	4.76	0.25	2.47	0.14	2.23	0.01	2.34	0.01	2.29	0.01	2.36	0.00	5.52	0.28
	4.32		2.26		2.25		2.35		2.30		2.37		5.08	
average	4.75		2.41		2.24		2.34		2.29		2.37		5.56	
10F2P	4.77		2.83		2.26		2.37		2.32		2.41		6.38	
	4.91	0.07	2.97	0.07	2.26	0.00	2.37	0.01	2.33	0.01	2.43	0.01	6.72	0.18
	4.81		2.87		2.26		2.36		2.32		2.41		6.47	
average	4.83		2.89		2.26		2.37		2.32		2.42		6.52	
10F3P	4.35		2.37		2.27		2.37		2.32		2.40		5.38	
	4.66	0.19	2.63	0.14	2.27	0.00	2.37	0.00	2.33	0.00	2.41	0.01	5.96	0.30
	4.70		2.58		2.26		2.37		2.32		2.40		5.83	
average	4.57		2.60		2.27		2.37		2.32		2.40		5.89	
10F4P	4.29		1.91		2.27		2.37		2.32		2.38		4.34	
	4.45	0.16	1.96	0.07	2.27	0.00	2.37	0.00	2.32	0.00	2.38	0.00	4.46	0.16
	4.60		2.05		2.27		2.37		2.32		2.38		4.66	
average	4.45		1.97		2.27		2.37		2.32		2.38		4.49	
10F5P	4.90		3.01		2.27		2.38		2.33		2.43		6.81	
	4.67	0.12	2.88	0.07	2.26	0.00	2.37	0.01	2.33	0.00	2.42	0.01	6.53	0.17
	4.73		2.88		2.26		2.37		2.32		2.42		6.50	
average	4.76		2.92		2.26		2.37		2.33		2.42		6.51	
20F0P	4.72		3.35		2.25		2.36		2.32		2.43		7.53	
	4.72	0.10	3.35	0.09	2.25	0.00	2.36	0.00	2.33	0.00	2.44	0.01	7.56	0.20
	4.89		3.51		2.25		2.36		2.33		2.44		7.89	
average	4.78		3.40		2.25		2.36		2.33		2.44		7.54	

MIX	absorption after immersion (%)	standard deviation	absorption after immersion and boiling (%)	standard deviation	bulk density, dry (Mg/m³)	standard deviation	bulk density after immersion (Mg/m³)	standard deviation	bulk density after immersion and boiling (Mg/m³)	standard deviation	apparent density (Mg/m³)	standard deviation	volume of permeable voids (%)	standard deviation
							ASTM C642- 7 days							
20F1P	5.13		3.56		2.23		2.35		2.31		2.42		7.94	
	5.07	0.03	3.59	0.06	2.23	0.00	2.35	0.00	2.31	0.00	2.43	0.01	8.02	0.15
	5.09		3.68		2.24		2.35		2.32		2.44		8.23	
average	5.10		3.61		2.23		2.35		2.31		2.43		8.06	
20F2P	5.69		3.76		2.21		2.34		2.30		2.41		8.31	
	5.55	0.10	3.54	0.11	2.22	0.01	2.35	0.01	2.30	0.01	2.41	0.01	7.88	0.22
	5.50		3.58		2.23		2.36		2.31		2.43		8.00	
average	5.58		3.63		2.22		2.35		2.30		2.42		8.06	
20F3P	6.64		4.23		2.20		2.35		2.29		2.43		9.31	
	6.50	0.09	4.21	0.02	2.21	0.01	2.36	0.01	2.31	0.01	2.44	0.01	9.32	0.06
	6.66		4.19		2.20		2.34		2.29		2.42		9.21	
average	6.60		4.21		2.20		2.35		2.30		2.43		9.28	
20F4P	5.04		2.85		2.24		2.35		2.30		2.39		6.38	
	4.75	0.24	2.70	0.14	2.24	0.00	2.35	0.01	2.30	0.01	2.38	0.01	6.04	0.32
	5.21		2.97		2.25		2.36		2.31		2.41		6.68	
average	5.00		2.84		2.24		2.35		2.30		2.39		6.36	
20F5P	4.74		3.19		2.22		2.33		2.29		2.39		7.08	
	4.39	0.21	2.89	0.16	2.23	0.01	2.33	0.00	2.30	0.00	2.39	0.00	6.45	0.34
	4.76		3.12		2.23		2.33		2.30		2.39		6.96	
average	4.63		3.07		2.23		2.33		2.29		2.39		6.83	
30F0P	4.69		3.18		2.22		2.32		2.29		2.39		7.06	
	4.89	0.20	3.35	0.12	2.22	0.00	2.33	0.00	2.29	0.00	2.40	0.01	7.44	0.27
	4.49		3.11		2.22		2.32		2.29		2.38		6.91	
average	4.69		3.22		2.22		2.32		2.29		2.39		7.14	
30F1P	4.15		2.88		2.24		2.33		2.30		2.39		6.45	
	4.14	0.14	2.92	0.72	2.24	0.04	2.33	0.04	2.30	0.02	2.39	0.00	6.53	1.56
	4.38		1.65		2.31		2.41		2.34		2.40		3.79	
average	4.15		2.48		2.26		2.36		2.32		2.39		5.59	
30F2P	4.61		3.23		2.21		2.32		2.29		2.38		7.14	
	4.17	0.23	2.87	0.18	2.24	0.01	2.33	0.01	2.30	0.01	2.39	0.00	6.44	0.37
	4.52		3.15		2.22		2.32		2.29		2.39		7.00	
average	4.44		3.08		2.23		2.32		2.29		2.39		6.86	
30F3P	4.80		1.93		2.23		2.34		2.27		2.33		4.30	
	4.94	0.09	2.02	0.04	2.22	0.00	2.33	0.00	2.27	0.00	2.33	0.00	4.48	0.09
	4.97		1.98		2.22		2.33		2.27		2.33		4.41	
average	4.90		1.98		2.22		2.33		2.27		2.33		4.39	

MIX	absorption after immersion (%)	standard deviation	absorption after immersion and boiling (%)	standard deviation	bulk density, dry (Mg/m³)	standard deviation	bulk density after immersion (Mg/m³)	standard deviation	bulk density after immersion and boiling (Mg/m³)	standard deviation	apparent density (Mg/m³)	standard deviation	volume of permeable voids (%)	standard deviation
							ASTM C642- 7 days							
30F4P	6.81		4.67		2.19		2.34		2.29		2.44		10.22	
	6.85	0.05	4.73	0.03	2.17	0.01	2.32	0.01	2.28	0.01	2.42	0.01	10.28	0.05
	6.90		4.68		2.18		2.33		2.28		2.42		10.18	
average	6.85		4.70		2.18		2.33		2.28		2.43		10.23	
30F5P	6.77		3.96		2.17		2.32		2.26		2.38		8.60	
	6.58	0.15	3.89	0.05	2.18	0.01	2.33	0.00	2.27	0.00	2.38	0.00	8.49	0.09
	6.89		3.99		2.17		2.32		2.26		2.38		8.67	
average	6.75		3.95		2.18		2.32		2.26		2.38		8.59	

	ASTM C642- 14 days													
MIX	absorption after immersion (%)	standard deviation	absorption after immersion and boiling (%)	standard deviation	bulk density, dry (Mg/m³)	standard deviation	bulk density after immersion (Mg/m³)	standard deviation	bulk density after immersion and boiling(Mg/m³)	standard deviation	apparent density (Mg/m³)	standard deviation	volume of permeable voids (Mg/m³)	standard deviation
0F0P	5.19		3.63		2.25		2.36		2.33		2.45		8.17	
	5.82	0.32	3.43	0.19	2.22	0.02	2.35	0.01	2.29	0.02	2.40	0.03	7.60	0.45
	5.56		3.26		2.23		2.36		2.31		2.41		7.28	
average	5.52		3.44		2.23		2.36		2.31		2.42		7.69	
10F0P	4.64		2.51		2.25		2.35		2.30		2.38		5.63	
	4.54	0.17	2.43	0.14	2.24	0.00	2.35	0.00	2.30	0.00	2.37	0.01	5.45	0.31
	4.86		2.70		2.24		2.35		2.30		2.39		6.05	
average	4.68		2.54		2.24		2.35		2.30		2.38		5.54	
10F1P	4.68		2.38		2.33		2.44		2.38		2.46		5.53	
	4.35	0.26	2.26	0.13	2.26	0.04	2.36	0.05	2.31	0.04	2.38	0.05	5.11	0.38
	4.18		2.11		2.26		2.35		2.31		2.37		4.77	
average	4.40		2.25		2.28		2.38		2.33		2.41		5.14	
10F2P	4.93		2.83		2.26		2.37		2.32		2.41		6.40	
	4.84	0.08	2.71	0.06	2.26	0.00	2.37	0.00	2.32	0.00	2.41	0.00	6.11	0.14
	4.78		2.78		2.26		2.37		2.32		2.41		6.28	
average	4.85		2.77		2.26		2.37		2.32		2.41		6.26	
10F3P	4.46		2.53		2.27		2.37		2.32		2.40		5.73	
	5.01	0.35	2.95	0.26	2.25	0.01	2.36	0.00	2.32	0.01	2.41	0.00	6.64	0.55
	4.37		2.49		2.27		2.37		2.33		2.41		5.65	
average	4.61		2.66		2.26		2.37		2.32		2.41		5.69	
10F4P	4.04		1.79		2.29		2.38		2.33		2.39		4.10	
	4.33	0.14	2.01	0.11	2.27	0.01	2.37	0.01	2.32	0.01	2.38	0.00	4.55	0.23
	4.23		1.95		2.28		2.38		2.32		2.39		4.44	
average	4.20		1.92		2.28		2.38		2.32		2.38		4.37	
10F5P	4.18		2.62		2.29		2.38		2.35		2.43		5.98	
	4.31	0.15	2.72	0.05	2.28	0.01	2.37	0.01	2.34	0.01	2.43	0.01	6.18	0.10
	4.48		2.69		2.27		2.37		2.33		2.42		6.10	
average	4.32		2.67		2.28		2.38		2.34		2.42		6.09	
20F0P	5.34		2.89		2.25		2.37		2.31		2.40		6.49	
	5.54	0.10	3.05	0.09	2.24	0.00	2.37	0.00	2.31	0.00	2.41	0.01	6.85	0.19
	5.46		3.02		2.25		2.37		2.32		2.41		6.80	
average	5.45		2.99		2.25		2.37		2.31		2.41		6.71	

MIX	absorption after immersion (%)	standard deviation	absorption after immersion and boiling (%)	standard deviation	bulk density, dry (Mg/m³)	standard deviation	bulk density after immersion (Mg/m³)	standard deviation	bulk density after immersion and boiling (Mg/m³)	standard deviation	apparent density (Mg/m³)	standard deviation	volume of permeable voids (%)	standard deviation
	4.59		2.39		2.28		2.39		2.34		2.42		5.45	
20F1P	4.44	0.09	2.35	0.06	2.28	0.01	2.39	0.01	2.34	0.01	2.41	0.01	5.36	0.14
	4.61		2.46		2.29		2.40		2.35		2.43		5.64	
average	4.55		2.40		2.29		2.39		2.34		2.42		5.48	
	4.84		2.93		2.21		2.31		2.27		2.36		6.46	
20F2P	4.68	0.13	2.86	0.13	2.22	0.01	2.33	0.01	2.29	0.01	2.37	0.01	6.35	0.28
	4.57		2.67		2.22		2.32		2.28		2.36		5.93	
average	4.70		2.82		2.22		2.32		2.28		2.36		6.25	
	4.77		2.63		2.25		2.35		2.30		2.39		5.89	
20F3P	4.80	0.21	2.60	0.13	2.25	0.01	2.35	0.00	2.31	0.00	2.39	0.00	5.85	0.29
	5.15		2.85		2.24		2.35		2.30		2.39		6.37	
average	4.91		2.69		2.24		2.35		2.30		2.39		5.87	
	4.74		2.10		2.25		2.36		2.30		2.36		4.74	
20F4P	4.49	0.13	2.05	0.05	2.26	0.00	2.36	0.00	2.30	0.00	2.37	0.00	4.62	0.10
	4.56		2.01		2.25		2.35		2.30		2.36		4.54	
average	4.60		2.06		2.25		2.36		2.30		2.36		4.63	
	4.65		2.35		2.24		2.35		2.29		2.37		5.27	
20F5P	4.49	0.08	2.23	0.06	2.25	0.00	2.35	0.00	2.30	0.00	2.37	0.00	5.03	0.12
	4.62		2.29		2.25		2.35		2.30		2.37		5.14	
average	4.57		2.29		2.25		2.35		2.30		2.37		5.15	
	5.97		3.33		2.23		2.36		2.30		2.40		7.40	
30F0P	5.76	0.11	3.22	0.07	2.22	0.01	2.34	0.01	2.29	0.01	2.39	0.01	7.13	0.18
	5.80		3.20		2.21		2.34		2.28		2.38		7.07	
average	5.78		3.25		2.22		2.35		2.29		2.39		7.10	
	6.06		3.48		2.21		2.34		2.29		2.39		7.68	
30F1P	6.04	0.50	3.25	0.12	2.23	0.01	2.36	0.01	2.30	0.01	2.40	0.01	7.25	0.22
	5.18		3.31		2.23		2.34		2.30		2.40		7.37	
average	6.05		3.35		2.22		2.35		2.30		2.40		7.43	
	4.44		2.20		2.22		2.32		2.27		2.33		4.89	
30F2P	4.61	0.12	2.08	0.06	2.21	0.00	2.32	0.00	2.26	0.01	2.32	0.01	4.61	0.15
	4.68		2.11		2.21		2.31		2.26		2.32		4.67	
average	4.58		2.13		2.21		2.32		2.26		2.32		4.73	
	4.02		2.02		2.24		2.33		2.28		2.34		4.51	
30F3P	4.32	0.15	2.00	0.04	2.22	0.01	2.31	0.01	2.26	0.01	2.32	0.01	4.44	0.07
	4.20		1.95		2.25		2.34		2.29		2.35		4.38	
average	4.18		1.99		2.23		2.33		2.28		2.34		4.44	

MIX	absorption after immersion (%)	standard deviation	absorption after immersion and boiling (%)	standard deviation	bulk density, dry (Mg/m³)	standard deviation	bulk density after immersion (Mg/m³)	standard deviation	bulk density after immersion and boiling (Mg/m³)	standard deviation	apparent density (Mg/m³)	standard deviation	volume of permeable voids (%)	standard deviation
							ASTM C642- 14 days							
30F4P	5.57		2.40		2.22		2.34		2.27		2.34		5.31	
	4.02	0.82	2.48	0.08	2.22	0.01	2.30	0.02	2.27	0.01	2.34	0.01	5.50	0.15
	4.30		2.55		2.20		2.29		2.25		2.33		5.61	
average	4.16		2.48		2.21		2.31		2.26		2.34		5.47	
30F5P	4.55		2.38		2.24		2.34		2.29		2.36		5.31	
	4.73	0.09	2.51	0.07	2.26	0.02	2.37	0.02	2.32	0.02	2.40	0.02	5.69	0.20
	4.66		2.42		2.23		2.33		2.28		2.36		5.40	
average	4.65		2.44		2.24		2.35		2.30		2.37		5.47	

MIX	Absorption after immersion (%)	standard deviation	absorption after immersion and boiling (%)	standard deviation	bulk density, dry (Mg/m³)	standard deviation	bulk density after immersion (Mg/m³)	standard deviation	bulk density after immersion and boiling (Mg/m³)	standard deviation	apparent density (Mg/m³)	standard deviation	volume of permeable voids (%)	standard deviation
								ASTM C642- 28 days						
0F0P	4.92		2.82		2.25		2.36		2.31		2.40		6.35	
	4.79	0.10	3.02	0.46	2.25	0.00	2.36	0.00	2.32	0.01	2.42	0.02	6.79	1.02
	4.98		3.70		2.24		2.36		2.33		2.45		8.30	
average	4.90		3.18		2.25		2.36		2.32		2.42		6.57	
10F0P	4.81		3.61		2.24		2.35		2.32		2.44		8.09	
	3.80	0.58	2.48	0.65	2.28	0.02	2.37	0.01	2.34	0.01	2.42	0.02	5.66	1.41
	3.81		2.49		2.27		2.36		2.33		2.41		5.66	
average	3.81		2.49		2.26		2.36		2.33		2.42		5.66	
10F1P	4.66		3.49		2.24		2.34		2.31		2.42		7.81	
	3.95	0.36		4.00	2.64	0.23	2.75	0.23	2.55	0.13	2.41	0.01		9.79
	4.23		3.14		2.25		2.34		2.32		2.42		7.07	
average	4.28		3.32		2.38		2.34		2.39		2.42		7.07	
10F2P	4.32		2.17		2.28		2.37		2.32		2.39		4.94	
		3.61	2.30	0.07	2.27	0.01	2.23	0.08	2.32	0.00	2.39	0.00	5.22	0.14
	4.48		2.22		2.27		2.37		2.32		2.39		5.04	
average	4.40		2.23		2.27		2.32		2.32		2.39		5.22	
10F3P	4.09		2.09		2.27		2.37		2.32		2.39		4.74	
	4.57	0.25	2.47	0.23	2.26	0.01	2.37	0.00	2.32	0.00	2.40	0.01	5.61	0.50
	4.22		2.08		2.28		2.37		2.33		2.39		4.73	
average	4.29		2.08		2.27		2.37		2.32		2.39		5.61	
10F4P	4.19		2.92		2.25		2.35		2.32		2.41		6.58	
	3.93	0.13	2.74	0.21	2.24	0.01	2.33	0.01	2.30	0.01	2.38	0.01	6.13	0.45
	4.11		3.16		2.23		2.32		2.30		2.40		7.04	
average	4.08		2.94		2.24		2.33		2.31		2.40		6.59	
10F5P	4.18		2.32		2.28		2.37		2.33		2.40		5.27	
	4.09	0.17	2.34	0.02	2.23	0.02	2.32	0.03	2.28	0.02	2.35	0.03	5.22	0.05
	3.85		2.30		2.25		2.33		2.30		2.37		5.17	
average	4.04		2.32		2.25		2.34		2.30		2.38		5.22	
20F0P	4.53		2.36		2.26		2.36		2.31		2.39		5.34	
	4.04	0.25	2.06	0.15	2.27	0.01	2.37	0.01	2.32	0.01	2.39	0.00	4.70	0.33
	4.37		2.28		2.26		2.36		2.31		2.38		5.15	
average	4.31		2.24		2.26		2.36		2.31		2.38		5.06	
20F1P	5.15		3.16		2.24		2.36		2.31		2.41		7.08	
	5.44	0.15	3.27	0.06	2.23	0.01	2.35	0.00	2.30	0.01	2.40	0.00	7.29	0.12
	5.26		3.26		2.23		2.35		2.31		2.41		7.28	
average	5.35		3.23		2.24		2.35		2.31		2.41		7.22	

MIX	Absorption after immersion (%)	standard deviation	absorption after immersion and boiling (%)	standard deviation	bulk density, dry (Mg/m³)	standard deviation	bulk density after immersion (Mg/m³)	standard deviation	bulk density after immersion and boiling (Mg/m³)	standard deviation	apparent density (Mg/m³)	standard deviation	volume of permeable voids (%)	standard deviation
						ASTM C642- 28 days								
20F2P	5.67	0.42	3.41	0.36	2.21	0.01	2.34	0.00	2.29	0.00	2.39	0.01	7.53	0.77
	6.39		3.90		2.20		2.34		2.28		2.40		8.58	
	6.41		4.11		2.20		2.34		2.29		2.42		9.04	
average	6.40		4.01		2.20		2.34		2.29		2.40		7.53	
20F3P	3.89	0.19	1.99	0.23	2.25	0.02	2.34	0.02	2.29	0.02	2.35	0.02	4.47	0.47
	4.23		2.29		2.24		2.34		2.30		2.37		5.14	
	3.90		1.85		2.28		2.37		2.33		2.38		4.23	
average	4.01		2.04		2.26		2.35		2.31		2.37		5.14	
20F4P	4.19	0.19	2.17	0.10	2.25	0.01	2.34	0.00	2.29	0.00	2.36	0.00	4.88	0.21
	4.47		2.33		2.24		2.34		2.30		2.37		5.23	
	4.12		2.15		2.25		2.35		2.30		2.37		4.86	
average	4.26		2.22		2.25		2.34		2.30		2.37		4.87	
20F5P	3.90	0.25	1.77	0.14	2.25	0.01	2.34	0.01	2.29	0.01	2.35	0.01	3.99	0.29
	4.40		2.05		2.23		2.33		2.28		2.34		4.57	
	4.17		1.88		2.23		2.33		2.28		2.33		4.20	
average	4.16		1.90		2.24		2.33		2.28		2.34		4.10	
30F0P	3.97	0.06	1.98	0.03	2.22	0.00	2.31	0.00	2.27	0.00	2.32	0.00	4.39	0.06
	4.04		2.00		2.22		2.31		2.26		2.32		4.45	
	4.08		1.95		2.22		2.31		2.26		2.32		4.33	
average	4.03		1.98		2.22		2.31		2.26		2.32		4.36	
30F1P	3.91	0.20	1.86	0.12	2.25	0.01	2.33	0.01	2.29	0.01	2.34	0.01	4.18	0.26
	4.30		2.11		2.22		2.32		2.27		2.33		4.69	
	4.02		1.96		2.23		2.32		2.27		2.33		4.38	
average	4.08		1.98		2.23		2.32		2.28		2.34		4.28	
30F2P	4.97	0.28	2.50	0.07	2.23	0.00	2.34	0.00	2.29	0.00	2.36	0.00	5.58	0.15
	4.91		2.52		2.23		2.34		2.29		2.36		5.61	
	4.46		2.39		2.24		2.34		2.29		2.36		5.35	
average	4.94		2.47		2.23		2.34		2.29		2.36		5.51	
30F3P	5.11	0.08	2.77	0.10	2.21	0.01	2.32	0.01	2.27	0.01	2.35	0.01	6.10	0.19
	5.00		2.61		2.22		2.34		2.28		2.36		5.81	
	4.96		2.58		2.22		2.33		2.28		2.36		5.74	
average	5.02		2.65		2.22		2.33		2.28		2.36		5.89	

MIX	Absorption after immersion (%)	standard deviation	absorption after immersion and boiling (%)	standard deviation	bulk density, dry (Mg/m^3)	standard deviation	bulk density after immersion (Mg/m^3)	standard deviation	bulk density after immersion and boiling (Mg/m^3)	standard deviation	apparent density (Mg/m^3)	standard deviation	volume of permeable voids (%)	standard deviation
							ASTM C642- 28 days							
	5.18		2.77		2.20		2.32		2.26		2.35		6.10	
30F4P	5.37	0.18	2.77	0.11	2.19	0.01	2.31	0.01	2.25	0.01	2.33	0.01	6.06	0.24
	5.54		2.97		2.19		2.31		2.26		2.34		6.50	
average	5.36		2.83		2.19		2.31		2.26		2.34		6.22	
	5.39		2.54		2.21		2.33		2.26		2.34		5.60	
30F5P	4.87	0.35	2.60	0.06	2.21	0.01	2.32	0.00	2.27	0.01	2.35	0.01	5.75	0.13
	4.73		2.47		2.22		2.33		2.28		2.35		5.49	
average	5.00		2.54		2.21		2.32		2.27		2.35		5.62	

MIX	Absorption after immersion (%)	standard deviation	absorption after immersion and boiling (Mg/m³)	standard deviation	bulk density, dry (Mg/m³)	standard deviation	bulk density after immersion (Mg/m³)	standard deviation	bulk density after immersion and boiling (Mg/m³)	standard deviation	apparent density (Mg/m³)	standard deviation	volume of permeable voids (%)	standard deviation
									ASTM C642- 60 days					
0F0P	4.78		2.56		2.24		2.35		2.30		2.38		5.74	
	5.07	0.20	2.65	0.90	2.24	0.01	2.35	0.01	2.30	0.03	2.38	0.06	5.94	2.06
	5.17		4.17		2.26		2.37		2.35		2.49		9.40	
average	5.01		2.60		2.25		2.36		2.32		2.42		5.84	
10F0P	5.17		1.95		2.34		2.46		2.39		2.46		4.58	
	5.08	0.05	2.02	0.03	2.21	0.07	2.33	0.07	2.26	0.07	2.32	0.07	4.46	0.09
	5.16		1.96		2.25		2.36		2.29		2.35		4.41	
average	5.14		1.98		2.27		2.38		2.31		2.37		4.48	
10F1P	4.37		1.56		2.24		2.33		2.27		2.32		3.48	
	3.67	0.35	1.31	0.13	2.27	0.02	2.35	0.01	2.30	0.01	2.34	0.01	2.97	0.27
	3.95		1.37		2.26		2.35		2.29		2.33		3.09	
average	4.00		1.41		2.25		2.34		2.29		2.33		3.18	
10F2P	4.67		2.84		2.26		2.37		2.33		2.42		6.43	
	4.89	0.18	2.79	0.11	2.27	0.01	2.38	0.01	2.33	0.00	2.42	0.00	6.33	0.22
	5.03		2.99		2.26		2.37		2.32		2.42		6.75	
average	4.86		2.87		2.26		2.37		2.33		2.42		6.38	
10F3P	4.82		2.62		2.24		2.35		2.30		2.38		5.86	
	3.69	1.10	1.52	1.08	2.27	0.02	2.35	0.02	2.31	0.02	2.35	0.05	3.45	2.41
	2.62		0.46		2.26		2.32		2.27		2.28		1.04	
average	3.71		2.07		2.26		2.34		2.29		2.34		3.45	
10F4P	3.22		1.47		2.28		2.35		2.31		2.35		3.35	
	3.33	0.16	1.73	0.17	2.29	0.01	2.36	0.01	2.33	0.01	2.38	0.01	3.96	0.39
	3.01		1.42		2.29		2.35		2.32		2.36		3.25	
average	3.18		1.54		2.28		2.36		2.32		2.37		3.52	
10F5P	3.38		1.56		2.28		2.36		2.32		2.37		3.56	
	3.52	0.08	1.57	0.01	2.27	0.01	2.35	0.01	2.31	0.01	2.36	0.01	3.57	0.01
	3.52		1.57		2.27		2.35		2.31		2.36		3.57	
average	3.47		1.57		2.28		2.36		2.31		2.36		3.57	
20F0P	3.38		0.82		2.29		2.36		2.30		2.33		1.87	
	5.20	1.07	2.54	1.02	2.25	0.02	2.37	0.00	2.31	0.00	2.38	0.03	5.72	2.27
	5.27		2.62		2.24		2.36		2.30		2.38		5.87	
average	5.24		2.58		2.26		2.36		2.30		2.37		5.80	

MIX	Absorption after immersion (%)	standard deviation	absorption after immersion and boiling (%)	standard deviation	bulk density, dry (Mg/m³)	standard deviation	bulk density after immersion (Mg/m³)	standard deviation	bulk density after immersion and boiling (Mg/m³)	standard deviation	apparent density (Mg/m³)	standard deviation	volume of permeable voids (%)	standard deviation
							ASTM C642- 60 days							
20F1P	3.30		1.68		2.28		2.36		2.32		2.37		3.84	
	3.31	0.04	1.67	0.01	2.28	0.01	2.35	0.01	2.31	0.01	2.37	0.01	3.80	0.02
	3.24		1.67		2.30		2.37		2.33		2.39		3.84	
average	3.28		1.67		2.28		2.36		2.32		2.37		3.83	
20F2P	3.12		1.63		2.28		2.35		2.31		2.36		3.72	
	3.55	0.22	1.92	0.14	2.27	0.01	2.35	0.01	2.31	0.01	2.37	0.01	4.35	0.32
	3.44		1.75		2.29		2.37		2.33		2.38		4.00	
average	3.37		1.77		2.28		2.35		2.32		2.37		4.02	
20F3P	3.55		1.83		2.27		2.35		2.31		2.37		4.15	
	3.46	0.05	1.76	0.05	2.28	0.01	2.36	0.01	2.32	0.01	2.38	0.01	4.01	0.11
	3.45		1.86		2.27		2.35		2.31		2.37		4.22	
average	3.49		1.81		2.27		2.35		2.31		2.37		4.12	
20F4P	3.84		2.06		2.27		2.35		2.31		2.38		4.68	
	3.58	0.23	1.89	0.16	2.27	0.01	2.36	0.00	2.32	0.00	2.38	0.00	4.30	0.35
	4.03		2.22		2.26		2.35		2.31		2.38		5.01	
average	3.82		2.06		2.27		2.35		2.31		2.38		4.66	
20F5P	3.78		2.14		2.26		2.35		2.31		2.38		4.85	
	3.59	0.14	2.02	0.08	2.26	0.00	2.35	0.00	2.31	0.00	2.37	0.00	4.58	0.17
	3.87		2.16		2.26		2.35		2.31		2.38		4.88	
average	3.75		2.11		2.26		2.35		2.31		2.38		4.77	
30F0P	3.73		2.12		2.25		2.33		2.30		2.36		4.76	
	3.63	0.44	1.03	1.41	2.32	0.07	2.40	0.06	2.34	0.04	2.37	0.01	2.40	3.02
	4.44		3.84		2.19		2.28		2.27		2.39		8.39	
average	3.93		2.33		2.25		2.34		2.30		2.37		5.18	
30F1P	3.23		1.86		2.28		2.36		2.32		2.38		4.24	
	3.33	0.09	1.92	0.05	2.27	0.01	2.34	0.01	2.31	0.01	2.37	0.01	4.35	0.10
	3.42		1.96		2.27		2.35		2.31		2.37		4.44	
average	3.32		1.91		2.27		2.35		2.32		2.38		4.34	
30F2P	2.63		1.31		2.28		2.34		2.31		2.35		2.99	
	2.95	0.21	1.52	0.15	2.28	0.01	2.35	0.01	2.31	0.01	2.36	0.01	3.47	0.34
	2.55		1.23		2.30		2.36		2.33		2.36		2.82	
average	2.71		1.35		2.29		2.35		2.32		2.36		3.09	
30F3P	2.95		1.43		2.23		2.30		2.26		2.31		3.19	
	3.31	0.18	1.44	0.03	2.21	0.01	2.28	0.01	2.24	0.01	2.28	0.01	3.18	0.07
	3.13		1.39		2.22		2.28		2.25		2.29		3.07	
average	3.13		1.42		2.22		2.29		2.25		2.29		3.15	

MIX	Absorption after immersion (%)	standard deviation	absorption after immersion and boiling (%)	standard deviation	bulk density, dry (Mg/m^3)	standard deviation	bulk density after immersion (Mg/m^3)	standard deviation	bulk density after immersion and boiling (Mg/m^3)	standard deviation	apparent density (Mg/m^3)	standard deviation	volume of permeable voids (%)	standard deviation
							ASTM C642- 60 days							
30F4P	3.11	0.14	1.33	0.08	2.21	0.00	2.28	0.00	2.24	0.00	2.28	0.00	2.93	0.18
	3.31		1.44		2.21		2.29		2.24		2.28		3.18	
	3.05		1.27		2.22		2.29		2.25		2.29		2.83	
average	3.16		1.35		2.22		2.29		2.25		2.28		2.98	
30F5P	3.12	0.16	1.26	0.06	2.22	0.00	2.29	0.00	2.25	0.00	2.28	0.00	2.80	0.13
	2.87		1.15		2.23		2.29		2.25		2.28		2.56	
	2.82		1.17		2.23		2.29		2.25		2.28		2.60	
average	2.94		1.19		2.22		2.29		2.25		2.28		2.65	

APPENDIX #2

Series#2

Fresh properties							
Mix	Air void content (%)	Air void content-average (%)	Weight of concrete +container * (kg)	Slump (cm)	Fresh density (kg/m³)	Standard deviation of air void content	C.O.V. of air void content (%)
A20F0P	11	10.0	20.165	11	2177.9	1.41	14.1
	9						
	-						
A20F2P	8.5	8.5	20.205	15	2183.6	-	-
	-						
	-						
A20F5P	3.7	3.4	19.81	13	2127.1	0.25	7.3
	3.4						
	3.2						
A20F10P	2	2.1	19.79	6.5	2124.3	0.15	7.2
	2.3						
	2.1						

* weight of container- 4.92 kg

Compressive strength						
Mix	Load- 7 days (kN)	Compressive strength (MPa)	Load- 28 days (kN)	Compressive strength (MPa)	Load- 60 days (kN)	Compressive strength (MPa)
A20F0P	140.5	17.9	187.5	23.9	210.5	26.8
	114.0	14.5	168.0	21.4	209.5	26.7
	127.5	16.2	156.0	19.9	206.0	26.2
average		16.2		21.7		26.6
A20F2P	156.5	19.9	177.5	22.6	241.5	30.8
	133.0	16.9	190.0	24.2	244.0	31.1
	125.0	15.9	184.0	23.4	245.5	31.3
average		17.6		23.4		31.0
A20F5P	194.0	24.7	257.0	32.7	326.5	41.6
	203.5	25.9	335.5	42.7	324.5	41.3
	197.0	25.1	255.0	32.5	315.5	40.2
average		25.2		36.0		41.0
A20F10P	218.5	27.8	275.0	35.0	357.0	45.5
	214.0	27.3	311.5	39.7	330.0	42.0
	182.5	23.2	296.0	37.7	402.0	51.2
average		26.1		37.5		43.8

	compressive strength					
Mix	7 days		28 days		60 days	
	Standard deviation	C.O.V. (%)	Standard deviation	C.O.V. (%)	Standard deviation	C.O.V. (%)
A20F0P	1.69	10.4	2.03	9.3	0.30	1.1
A20F2P	2.09	11.8	0.80	3.4	0.26	0.8
A20F5P	0.62	2.4	5.85	16.2	0.75	1.8
A20F10P	2.50	9.5	2.33	6.2	4.63	10.6

Mix	absorption after immersion (%)	standard deviation	absorption after immersion and boiling (%)	standard deviation	bulk density, dry (Mg/m³)	standard deviation	bulk density after immersion (Mg/m³)	standard deviation	bulk density after immersion and boiling (Mg/m³)	standard deviation	apparent density (Mg/m³)	standard deviation	volume of permeable voids (%)	standard deviation
								ASTM C642- 7 days						
A20F0P	5.04		2.61		2.08		2.19		2.14		2.20		5.43	
	5.04	0.20	2.24	0.32	2.09	0.01	2.19	0.01	2.13	0.00	2.19	0.01	4.69	0.65
	5.38		2.89		2.07		2.18		2.13		2.20		5.97	
average	5.16		2.58		2.08		2.19		2.13		2.20		5.36	
A20F2P	5.53		3.15		2.05		2.17		2.12		2.19		6.47	
	5.69	0.09	3.22	0.17	2.05	0.01	2.17	0.01	2.12	0.00	2.20	0.00	6.61	0.34
	5.55		2.89		2.06		2.18		2.12		2.19		5.97	
average	3.13		1.42		2.22		2.29		2.25		2.29		3.15	
A20F5P	4.54		2.56		2.23		2.33		2.29		2.36		5.70	
	4.28	0.16	2.30	0.13	2.28	0.03	2.38	0.03	2.34	0.03	2.41	0.03	5.25	0.23
	4.58		2.46		2.23		2.34		2.29		2.36		5.49	
average	4.47		2.44		2.25		2.35		2.30		2.38		5.48	
A20F10P	4.62		2.54		2.23		2.34		2.29		2.37		5.67	
	4.48	0.12	2.51	0.06	2.24	0.01	2.34	0.01	2.30	0.01	2.38	0.01	5.63	0.13
	4.38		2.43		2.24		2.33		2.29		2.36		5.43	
average	4.49		2.49		2.24		2.34		2.29		2.37		5.58	

Mix	Absorption after immersion (%)	standard deviation	absorption after immersion and boiling (%)	standard deviation	bulk density, dry (Mg/m³)	standard deviation	bulk density after immersion (Mg/m³)	standard deviation	bulk density after immersion and boiling (Mg/m³)	standard deviation	apparent density (Mg/m³)	standard deviation	volume of permeable voids (%)	standard deviation
								ASTM C642- 28 days						
A20F0P	4.71		2.31		2.07		2.17		2.12		2.17		4.78	
	4.71	0.07	8.67	3.69	1.81	0.16	1.89	0.16	1.96	0.09	2.14	0.02	15.64 (is ignored)	0.09
	4.59		2.24		2.08		2.17		2.13		2.18		4.66	
average	4.67		2.27		1.98		2.08		2.07		2.17		4.72	
A20F2P	4.81		2.42		2.08		2.18		2.13		2.19		5.04	
	4.48	0.22	2.15	0.17	2.07	0.03	2.16	0.03	2.11	0.03	2.17	0.03	4.44	0.33
	4.40		2.12		2.12		2.21		2.17		2.22		4.50	
average	4.56		2.23		2.09		2.19		2.14		2.19		4.66	
A20F5P	3.79		1.97		2.24		2.32		2.28		2.34		4.40	
	3.72	0.24	1.87	0.05	2.25	0.01	2.33	0.00	2.29	0.01	2.34	0.01	4.19	0.11
	3.35		1.91		2.25		2.33		2.30		2.35		4.31	
average	3.62		1.92		2.24		2.33		2.29		2.35		4.30	
A20F10P	3.28		2.06		2.27		2.34		2.31		2.38		4.67	
	3.43	0.15	1.93	0.08	2.25	0.01	2.33	0.01	2.30	0.01	2.36	0.01	4.36	0.20
	3.59		1.91		2.25		2.33		2.29		2.35		4.29	
average	3.43		1.97		2.26		2.33		2.30		2.36		4.44	

Mix	Absorption after immersion (%)	standard deviation	absorption after immersion and boiling (%)	standard deviation	bulk density, dry (Mg/m^3)	standard deviation	bulk density after immersion (Mg/m^3)	standard deviation	bulk density after immersion and boiling (Mg/m^3)	standard deviation	apparent density (Mg/m^3)	standard deviation	volume of permeable voids (%)	standard deviation
							ASTM C642- 60 days							
A20F0P	4.20		2.20		2.10		2.18		2.14		2.20		4.62	
	4.21	0.01	2.25	0.05	2.10	0.00	2.18	0.00	2.14	0.00	2.20	0.00	4.72	0.11
	4.20		2.30		2.10		2.19		2.15		2.20		4.83	
average	4.20		2.25		2.10		2.18		2.14		2.20		4.72	
A20F2P	3.94		2.08		2.10		2.18		2.14		2.20		4.37	
	3.76	0.09	2.02	0.03	2.11	0.01	2.19	0.01	2.15	0.01	2.20	0.01	4.26	0.06
	3.88		2.05		2.11		2.20		2.16		2.21		4.33	
average	3.86		2.05		2.11		2.19		2.15		2.20		4.32	
A20F5P	2.92		1.79		2.25		2.31		2.29		2.34		4.03	
	3.14	0.29	1.98	0.19	2.23	0.02	2.30	0.01	2.28	0.01	2.34	0.01	4.42	0.40
	3.50		2.18		2.21		2.29		2.26		2.33		4.83	
average	3.19		1.98		2.23		2.30		2.28		2.34		4.43	
A20F10P	3.42		1.74		2.23		2.31		2.27		2.32		3.88	
	3.09	0.24	1.59	0.12	2.25	0.01	2.32	0.01	2.28	0.01	2.33	0.01	3.57	0.24
	2.95		1.50		2.26		2.33		2.29		2.34		3.40	
average	3.15		1.61		2.25		2.32		2.28		2.33		3.62	

APPENDIX #3

Series#3

Mix	Fresh properties							
	Air void content %	Air void content-average (%)	weight of concrete +container * (kg)	slump (cm)	Fresh density (kg/m^3)	Average of fresh density (kg/m^3)	Standard deviation of air void content	C.O.V. of air void content (%)
A0F-G	9	8.7	20.48	8	2222.9	2223	0.29	3.3
	8.5		20.48		2222.9			
	8.5		20.48		2222.9			
A10F-G	12	12.0	19.66	14	2105.7	2106	0.00	0.0
	12		19.66		2105.7			
	12		19.66		2105.7			
A20F-G	13	13.0	19.54	17	2088.6	2089	0.00	0.0
	13		19.54		2088.6			
	13		19.54		2088.6			
A30F-G	9.7	9.8	20	18	2154.3	2154	0.153	1.6
	9.8		20		2154.3			
	10		20		2154.3			
A40F-G	11.7	11.3	19.62	19	2100.0	2100	0.32	2.8
	11.1		19.62		2100.0			
	11.2		19.62		2100.0			
A50F-G	11.8	11.8	19.5	20	2082.9	2083	0.15	1.3
	11.7		19.5		2082.9			
	12		19.5		2082.9			
A60F-G	9.7	9.7	19.89	22	2138.6	2139	0.10	1.03
	9.8		19.89		2138.6			
	9.6		19.89		2138.6			
A70F-G	10	10.1	19.56	16	2091.4	2091	0.12	1.1
	10.2		19.56		2091.4			
	10		19.56		2091.4			
A80F-G	9.1	9.1	19.62	18	2100.0	2100	0.07	0.8
	9		19.62		2100.0			
			19.62		2100.0			

* weight of container= 4.92 kg

	Compressive strength							
Mix	Load- 3 days (kN)	Strength (MPa)	Load- 14 days (kN)	Strength (MPa)	Load- 28 days (kN)	Strength (MPa)	Load- 60 days (kN)	Strength (MPa)
A0F-G	151.0	19.2	221.6	28.2	230.5	29.4	248.8	31.7
	149.0	19.0	197.6	25.2	261.9	33.4	234.5	29.9
	152.0	19.4	193.1	24.6	236.9	30.2	233.0	29.7
average		19.2		26.0		31.0		30.4
A10F-G	95.0	12.1	131.7	16.8	164.9	21.0	167.2	21.3
	86.5	11.0	136.8	17.4	151.0	19.2	170.5	21.7
	90.5	11.5	139.9	17.8	148.9	19.0	190.7	24.3
average		11.5		17.3		19.7		22.4
A20F-G	87.7	11.2	119.0	15.2	138.0	17.6	178.3	22.7
	84.3	10.7	118.0	15.0	152.3	19.4	166.5	21.2
	83.0	10.6	124.0	15.8	136.3	17.4	167.8	21.4
average		10.8		15.3		18.1		21.8
A30F-G	71.3	9.1	116.0	14.8	151.8	19.3	191.1	24.3
	57.7	7.4	114.4	14.6	152.2	19.4	186.3	23.7
	66.4	8.5	115.5	14.7	162.7	20.7	192.5	24.5
average		8.3		14.7		19.8		24.2
A40F-G	36.7	4.7	80.3	10.2	117.7	15.0	152.7	19.5
	32.9	4.2	82.3	10.5	127.8	16.3	135.6	17.3
	34.2	4.4	84.2	10.7	119.1	15.2	145.5	18.5
average		4.4		10.5		15.5		18.4
A50F-G	38.5	4.9	61.9	7.9	84.7	10.8	118.6	15.1
	33.0	4.2	61.1	7.8	88.2	11.2	102.8	13.1
	28.8	3.7	67.8	8.6	94.1	12.0	115.6	14.7
average		4.3		8.1		11.3		14.3
A60F-G	38.1	4.9	60.7	7.7	83.1	10.6	104	13.2
	36.5	4.6	61.5	7.8	87.0	11.1	117.2	14.9
	40.2	5.1	59.3	7.6	90.2	11.5	110.9	14.1
average		4.9		7.7		11.1		14.1
A70F-G	22.1	2.8	44.8	5.7	71.2	9.1	103.9	13.2
	21.8	2.8	42.5	5.4	68.4	8.7	99.6	12.7
	22.7	2.9	43.3	5.5	75.4	9.6	102	13.0
average		2.8		5.5		9.1		13.0
A80F-G	8.4	1.1	34.3	4.4	40.8	5.2	70.1	8.9
	9.5	1.2	35.3	4.5	42.1	5.4	74.3	9.5
	10.2	1.3	35.0	4.5	40.7	5.2	78.3	10.0
average		1.2		4.4		5.2		9.5

Mix	Compressive strength							
	3 days		14 days		28 days		60 days	
	Standard deviation	C.O.V. (%)	Standard deviation	C.O.V. (%)	Standard deviation	C.O.V. (%)	Standard deviation	C.O.V. (%)
A0F-G	0.19	1.01	1.95	7.51	2.11	6.83	1.11	3.65
A10F-G	0.54	4.69	0.53	3.04	1.11	5.61	1.62	7.22
A20F-G	0.31	2.86	0.41	2.67	1.12	6.18	0.82	3.79
A30F-G	0.88	10.58	0.10	0.71	0.79	3.97	0.41	1.71
A40F-G	0.25	5.58	0.25	2.37	0.70	4.50	1.09	5.94
A50F-G	0.62	14.55	0.47	5.75	0.61	5.34	1.07	7.47
A60F-G	0.24	4.85	0.14	1.84	0.45	4.10	0.84	5.96
A70F-G	0.06	2.06	0.15	2.68	0.45	4.92	0.27	2.12
A80F-G	0.12	9.82	0.07	1.47	0.10	1.90	0.52	5.52

Mix	Absorption after immersion (%)	standard deviation	absorption after immersion and boiling (%)	standard deviation	bulk density, dry (Mg/m³)	standard deviation	after immersion	standard deviation	bulk density after immersion and boiling (Mg/m³)	standard deviation	apparent density (Mg/m³)	standard deviation	volume of permeable voids (%)	standard deviation
									ASTM C642- 3 days					
A0F-G	5.34		3.02		2.13		2.14		2.19		2.27		6.43	
	5.21	0.15	2.89	0.12	2.13	0.01	2.24	0.06	2.19	0.01	2.27	0.00	6.16	0.23
	5.04		2.79		2.14		2.25		2.20		2.28		5.98	
average	5.19		2.91		2.13		2.21		2.19		2.27		6.20	
A10F-G	6.62		4.30		2.01		2.15		2.10		2.20		8.65	
	6.49	0.10	4.23	0.03	2.02	0.00	2.15	0.01	2.10	0.00	2.21	0.00	8.53	0.06
	6.69		4.25		2.02		2.16		2.11		2.21		8.60	
average	6.55		4.26		2.02		2.15		2.10		2.21		8.59	
A20F-G	6.40		4.18		1.98		2.11		2.07		2.16		8.29	
	6.60	0.10	4.28	0.09	1.98	0.01	2.11	0.01	2.06	0.01	2.16	0.02	8.47	0.21
	6.47		4.36		2.00		2.13		2.08		2.19		8.71	
average	6.50		4.27		1.99		2.11		2.07		2.17		8.38	
A30F-G	6.93		4.92		2.02		2.15		2.11		2.24		9.92	
	6.80	0.09	4.79	0.07	2.03	0.01	2.16	0.01	2.12	0.01	2.24	0.01	9.71	0.11
	6.75		4.84		2.03		2.16		2.13		2.25		9.82	
average	6.83		4.85		2.02		2.16		2.12		2.24		9.82	
A40F-G	7.27		5.21		1.98		2.12		2.08		2.20		10.30	
	7.09	0.11	4.97	0.13	1.99	0.01	2.13	0.01	2.09	0.00	2.21	0.00	9.89	0.22
	7.08		5.02		1.99		2.13		2.09		2.21		9.96	
average	7.15		4.99		1.98		2.13		2.08		2.21		9.93	
A50F-G	6.71		3.52		1.98		2.12		2.05		2.13		6.98	
	6.92	0.12	3.67	0.09	1.98	0.01	2.11	0.01	2.05	0.01	2.13	0.01	7.25	0.16
	6.89		3.69		1.97		2.10		2.04		2.12		7.26	
average	6.84		3.63		1.98		2.11		2.05		2.13		7.16	
A60F-G	6.26		4.52		2.03		2.16		2.12		2.24		9.18	
	6.41	0.11	4.76	0.17	2.02	0.01	2.14	0.01	2.11	0.01	2.23	0.01	9.60	0.29
	6.47		4.85		2.01		2.14		2.11		2.23		9.73	
average	6.38		4.71		2.02		2.15		2.11		2.23		9.66	
A70F-G	7.57		5.60		1.91		2.06		2.02		2.14		10.72	
	7.25	3.98	5.34	0.22	1.91	0.01	2.05	0.09	2.01	0.01	2.13	0.01	10.20	0.39
	14.30		5.16		1.93		2.20		2.03		2.14		9.95	
average	9.70		5.36		1.92		2.10		2.02		2.14		10.46	
A80F-G	7.43		5.37		1.93		2.07		2.03		2.15		10.33	
	7.23	0.16	5.24	0.07	1.93	0.00	2.07	0.00	2.03	0.00	2.14	0.00	10.09	0.13
	7.54		5.34		1.93		2.07		2.03		2.15		10.29	
average	7.40		5.31		1.93		2.07		2.03		2.15		10.24	

Mix	Absorption after immersion (%)	standard deviation	absorption after immersion and boiling (%)	standard deviation	bulk density, dry (Mg/m³)	standard deviation	after immersion (Mg/m³)	standard deviation	immersion and boiling (Mg/m³)	standard deviation	apparent density (Mg/m³)	standard deviation	volume of permeable voids (%)	standard deviation
ASTM C642- 14 days														
A0F-G	5.34		1.83		2.14		2.25		2.18		2.23		3.92	
	5.07	0.14	1.71	0.06	2.14	0.01	2.25	0.01	2.18	0.01	2.22	0.01	3.67	0.13
	5.24		1.78		2.15		2.26		2.19		2.24		3.83	
average	5.22		1.78		2.14		2.26		2.18		2.23		3.81	
A10F-G	6.30		3.82		2.01		2.14		2.09		2.18		7.69	
	5.92	0.21	3.52	0.15	2.01	0.01	2.13	0.01	2.09	0.01	2.17	0.01	7.10	0.29
	5.94		3.72		2.00		2.12		2.07		2.16		7.44	
average	6.05		3.69		2.01		2.13		2.08		2.17		7.39	
A20F-G	6.04		3.62		1.97		2.08		2.04		2.12		7.12	
	6.08	0.05	3.66	0.04	1.97	0.00	2.08	0.00	2.04	0.00	2.12	0.00	7.19	0.07
	6.14		3.70		1.96		2.08		2.03		2.11		7.26	
average	6.08		3.66		1.96		2.08		2.04		2.12		7.19	
A30F-G	5.86		3.65		2.04		2.16		2.12		2.21		7.47	
	5.57	0.17	3.63	0.02	2.04	0.01	2.16	0.01	2.12	0.01	2.21	0.01	7.42	0.03
	5.55		3.61		2.05		2.17		2.13		2.22		7.40	
average	5.66		3.63		2.05		2.16		2.12		2.21		7.43	
A40F-G	6.25		3.49		1.98		2.10		2.05		2.13		6.91	
	5.97	0.36	3.36	0.23	2.00	0.01	2.12	0.01	2.06	0.01	2.14	0.01	6.71	0.42
	6.68		3.82		1.97		2.10		2.04		2.13		7.51	
average	6.30		3.56		1.98		2.11		2.05		2.13		7.21	
A50F-G	4.96		4.03		1.97		2.07		2.05		2.14		7.94	
	5.98	0.53	4.31	0.14	1.97	0.01	2.08	0.01	2.05	0.01	2.15	0.01	8.48	0.27
	5.72		4.13		1.98		2.10		2.07		2.16		8.19	
average	5.55		4.16		1.97		2.08		2.06		2.15		8.21	
A60F-G	6.34		4.82		2.02		2.15		2.12		2.24		9.74	
	6.00	0.20	4.58	0.15	2.04	0.01	2.16	0.01	2.13	0.01	2.25	0.01	9.33	0.24
	5.98		4.56		2.05		2.17		2.14		2.26		9.32	
average	6.11		4.65		2.04		2.16		2.13		2.25		9.46	
A70F-G	7.67		5.83		2.06		2.22		2.18		2.35		12.04	
	10.77	3.59	5.48	0.29	1.94	0.07	2.15	0.11	2.05	0.08	2.17	0.10	10.64	0.95
	3.60		5.26		1.94		2.01		2.05		2.16		10.22	
average	7.35		5.52		1.98		2.13		2.09		2.23		10.96	
A80F-G	7.37		5.33		1.96		2.10		2.06		2.18		10.42	
	12.30	2.88	10.15	2.86	1.87	0.05	2.10	0.00	2.06	0.00	2.31	0.08	19.01	5.10
	7.27		5.08		1.96		2.10		2.06		2.17		9.94	
average	8.98		6.85		1.93		2.10		2.06		2.22		13.13	

Mix	Absorption after immersion (%)	standard deviation	absorption after immersion and boiling (%)	standard deviation	bulk density, dry (Mg/m³)	standard deviation	bulk density after immersion (Mg/m³)	standard deviation	bulk density after immersion and boiling (Mg/m³)	standard deviation	apparent density (Mg/m³)	standard deviation	volume of permeable voids (%)	standard deviation
							ASTM C642- 28 days							
A0F-G	5.24		3.17		2.11		2.22		2.18		2.26		6.70	
	5.32	0.16	3.31	0.10	2.28	0.10	2.40	0.10	2.35	0.10	2.46	0.11	7.53	0.42
	5.55		3.37		2.11		2.23		2.18		2.27		7.12	
average	5.37		3.28		2.17		2.28		2.24		2.33		7.11	
A10F-G	5.99		3.19		2.04		2.16		2.10		2.18		6.50	
	6.04	0.53	3.63	0.84	2.01	0.01	2.14	0.01	2.09	0.01	2.17	0.03	7.31	1.66
	6.94		4.82		2.01		2.15		2.11		2.23		9.69	
average	6.49		4.22		2.02		2.15		2.10		2.19		8.50	
A20F-G	6.39		4.21		1.90		2.03		1.98		2.07		8.01	
	6.34	0.04	4.05	0.08	1.92	0.01	2.04	0.01	1.99	0.01	2.08	0.01	7.77	0.14
	6.31		4.16		1.92		2.04		2.00		2.09		8.00	
average	6.35		4.19		1.91		2.04		1.99		2.08		8.00	
A30F-G	6.28		7.86		1.91		2.03		2.06		2.25		15.01	
	6.52	0.22	4.52	1.89	2.03	0.07	2.17	0.08	2.13	0.03	2.24	0.01	9.20	3.30
	6.72		4.66		2.02		2.15		2.11		2.22		9.39	
average	6.50		5.68		1.99		2.12		2.10		2.24		9.20	
A40F-G	8.00		4.47		1.99		2.15		2.08		2.18		8.89	
	7.29	0.71	4.57	0.05	1.98	0.01	2.12	0.02	2.07	0.01	2.18	0.01	9.04	0.11
	6.57		4.48		1.97		2.10		2.06		2.16		8.84	
average	7.29		4.48		1.98		2.12		2.07		2.17		9.04	
A50F-G	6.70		4.64		1.96		2.09		2.05		2.16		9.10	
	6.50	0.10	4.49	0.07	1.97	0.01	2.10	0.00	2.06	0.00	2.17	0.00	8.87	0.12
	6.60		4.57		1.97		2.10		2.06		2.16		9.00	
average	6.60		4.57		1.97		2.10		2.06		2.16		8.99	
A60F-G	4.27		2.72		2.00		2.09		2.06		2.12		5.44	
	4.36	0.05	2.84	0.07	2.02	0.01	2.11	0.01	2.08	0.01	2.14	0.01	5.74	0.17
	4.32		2.84		2.02		2.11		2.08		2.14		5.74	
average	4.32		2.80		2.01		2.10		2.07		2.13		5.64	
A70F-G	5.06		3.62		1.96		2.06		2.03		2.11		7.11	
	4.93	0.15	3.37	0.18	2.01	0.03	2.11	0.02	2.08	0.02	2.15	0.02	6.77	0.27
	5.23		3.72		1.97		2.07		2.04		2.12		7.30	
average	5.07		3.57		1.98		2.08		2.05		2.13		7.06	
A80F-G	6.63		4.43		1.96		2.09		2.05		2.15		8.70	
	6.71	0.19	4.51	0.09	1.95	0.01	2.08	0.00	2.04	0.00	2.14	0.00	8.81	0.15
	6.34		4.33		1.97		2.09		2.05		2.15		8.51	
average	6.53		4.42		1.96		2.09		2.05		2.15		8.67	

Mix	Absorption after immersion (%)	standard deviation	absorption after immersion and boiling (%)	standard deviation	bulk density, dry (Mg/m³)	standard deviation	bulk density after immersion (Mg/m³)	standard deviation	bulk density after immersion and boiling (Mg/m³)	standard deviation	apparent density (Mg/m³)	standard deviation	volume of permeable voids (Mg/m³)	standard deviation
	ASTM C642- 60 days													
A0F-G	5.60	0.02	4.16	0.15	2.09	0.01	2.20	0.01	2.17	0.01	2.28	0.01	8.67	0.30
	5.62		3.87		2.10		2.22		2.18		2.28		8.12	
	5.64		4.11		2.10		2.22		2.18		2.30		8.62	
average	5.62		4.01		2.09		2.21		2.18		2.29		8.40	
A10F-G	3.38	0.89	1.89	0.75	-0.24	1.30	-0.24	1.36	-0.24	1.34	-0.23	1.38	-0.44	3.96
	4.89		3.18		2.01		2.11		2.07		2.15		6.39	
	4.95		3.20		2.01		2.11		2.07		2.15		6.43	
average	4.92		3.19		2.01		2.11		2.07		2.15		6.41	
A20F-G	4.90	0.04	2.66	0.04	1.98	0.01	2.08	0.01	2.03	0.01	2.09	0.01	5.28	0.07
	4.83		2.73		1.96		2.06		2.02		2.07		5.35	
	4.90		2.74		1.97		2.07		2.03		2.09		5.41	
average	4.88		2.71		1.97		2.07		2.03		2.08		5.34	
A30F-G	4.09	0.07	2.62	0.03	2.04	0.00	2.13	0.00	2.10	0.00	2.16	0.00	5.35	0.07
	4.21		2.67		2.05		2.13		2.10		2.17		5.47	
	4.22		2.62		2.05		2.13		2.10		2.16		5.36	
average	4.17		2.63		2.05		2.13		2.10		2.16		5.41	
A40F-G	4.18	0.66	2.62	0.18	2.05	0.01	2.13	0.03	2.10	0.02	2.16	0.02	5.36	0.38
	3.76		2.30		2.04		2.12		2.09		2.14		4.70	
	2.88		2.32		2.02		2.08		2.07		2.12		4.70	
average	3.61		2.46		2.04		2.11		2.09		2.14		4.92	
A50F-G	4.59	0.18	2.50	0.05	1.99	0.01	2.09	0.02	2.04	0.01	2.10	0.02	4.99	0.13
	4.29		2.41		1.97		2.06		2.02		2.07		4.77	
	4.60		2.50		2.00		2.09		2.05		2.10		5.00	
average	4.49		2.47		1.99		2.08		2.04		2.09		4.92	
A60F-G	3.98	0.21	2.40	0.11	2.06	0.01	2.14	0.01	2.11	0.01	2.16	0.01	4.94	0.24
	4.35		2.61		2.06		2.15		2.12		2.18		5.38	
	4.33		2.58		2.07		2.16		2.12		2.19		5.34	
average	4.22		2.53		2.06		2.15		2.12		2.18		5.22	
A70F-G	5.29	1.73	3.62	1.73	2.01	0.03	2.12	0.01	2.09	0.01	2.17	0.05	7.28	3.48
	1.83		0.15		2.08		2.11		2.08		2.08		0.32	
	3.55		1.84		2.06		2.13		2.10		2.14		3.78	
average	3.56		1.87		2.05		2.12		2.09		2.13		3.79	
A80F-G	4.38	0.07	1.84	1.02	2.04	0.04	2.13	0.04	2.08	0.02	2.12	0.00	3.75	1.99
	4.51		2.98		1.99		2.08		2.05		2.12		5.94	
	4.50		0.95		2.07		2.17		2.09		2.11		1.97	
average	4.46		1.92		2.03		2.13		2.07		2.12		3.88	

University of Alberta

CHARACTERISTICS OF CONCRETE CONTAINING FLY ASH WITH Hg-ADSORBENT

by

Mehrdad Mahoutian

A thesis submitted to the Faculty of Graduate Studies and Research

in partial fulfillment of the requirements for the degree of

Master of Science in Civil Engineering

in

Structural Engineering

Department of Civil and Environmental Engineering

©Mehrdad Mahoutian

Fall 2011

Edmonton, Alberta